

ELECTRONIC CONDUCTION IN LIQUID TRANSITION METALS
AND THEIR ALLOYS.

Submitted for the Degree of
Doctor of Philosophy,
University of Leicester, 1976.

Barry Charles Dupree.

UMI Number: U419006

All rights reserved

INFORMATION TO ALL USERS

The quality of this reproduction is dependent upon the quality of the copy submitted.

In the unlikely event that the author did not send a complete manuscript and there are missing pages, these will be noted. Also, if material had to be removed, a note will indicate the deletion.



UMI U419006

Published by ProQuest LLC 2015. Copyright in the Dissertation held by the Author.
Microform Edition © ProQuest LLC.

All rights reserved. This work is protected against
unauthorized copying under Title 17, United States Code.



ProQuest LLC
789 East Eisenhower Parkway
P.O. Box 1346
Ann Arbor, MI 48106-1346



THESIS
516324
14.12.76

x753016450

I am very pleased to thank all those who provided help and encouragement during the work for this thesis, in particular my supervisor, Professor J.E. Enderby and also Professor J.B. Van Zytveld, Dr. J. Hennessy, Dr. R.A. Howe, Mr. V.T. Ngyen, and Mr. S. Taylor. I am grateful for the help of my mother in typing the thesis and the patient assistance of my wife. My thanks are also due to the Science Research Council for their support and members of the Physics Department of this University for their advice.

ABSTRACT

Apparatus has been developed to perform measurements of the thermoelectric power and resistivity of liquid metals at high temperatures of the order of 1500°C. Measurements have been performed on the transition metals, iron, cobalt, nickel and palladium in the liquid state, together with some measurements on these metals in the solid state and on liquid alloys of nickel with cobalt and palladium with silver. In most cases the results obtained are in agreement with other experimental data, where available.

If use is made of a single site resonant scattering model (the only theory for liquid transition metals for which a number of quantitative calculations of resistivity and thermoelectric power have been reported), approximate expressions can be derived which give the resistivity of liquid nickel - cobalt

alloys in terms of the resistivities of the pure components. It is also possible to express the thermoelectric power of the alloy in terms of the thermoelectric powers and resistivities of the pure components and the resistivity of the alloy. The predictions of these expressions have been compared with the experimental data; the comparison indicates that the theory does not account for the observed transport properties of liquid nickel-cobalt alloys. The conclusion is therefore drawn that by implication the theory is not applicable, in its present form, to pure liquid transition metals.

CONTENTS

	Page No.
Chapter 1. <u>Introduction.</u>	
i) Phenomenological Description.	1
ii) Microscopic Theories.	4
iii) The Pseudopotential.	10
iv) Application to Real Liquid Metals.	14
Chapter 2. <u>Transition Metal Theories.</u>	
i) Early Work.	18
ii) The 'Bristol' Theory.	24
iii) An Alternative Theory.	29
iv) The d electron Contribution.	30
v) Experiments Undertaken.	31
Chapter 3. <u>Measurement of the Thermoelectric <u>Power.</u></u>	
i) Introduction.	33
ii) Muffle Furnace.	34
iii) Vacuum and Argon System.	38
iv) The Carriage.	40
v) Filling the Crucible.	48
vi) Signal Measurement and Experimental Procedure.	49
vii) Errors in the Measurement.	52
viii) Sample Details.	57

	Page No.
Chapter 4. <u>Measurement of the Resistivity.</u>	
i) Introduction.	60
ii) The Furnace.	60
iii) The Specimen.	64
iv) Measurement Circuitry.	70
v) Errors.	75
Chapter 5. <u>Experimental Results.</u>	
i) Thermoelectric Power of Pure Transition Metals.	78
ii) Thermoelectric Power of Transition Metal Alloys.	92
iii) Resistivity.	102
Chapter 6. <u>Comparison of Theoretical and Experimental Values of Resistivity and Thermoelectric Power.</u>	
i) Pure Metals.	108
ii) Transition Metal - Transition Metal Alloys.	108
iii) Silver-Palladium.	124
Chapter 7. <u>Conclusion.</u>	130
References.	135

i) Phenomenological Description.

When a material is subjected to an electric field, the magnitude of the resulting electric current is related to the value of the field by the electrical conductivity of the material. Similarly when a temperature gradient is imposed on a material the thermal conductivity of the material governs the magnitude of the resulting heat flow.

There is another bulk property of a material, related to those above, known as the absolute thermoelectric power. This is manifested in three phenomena:-

Thomson Effect: When an electric current flows through a metal in which a temperature gradient exists reversible heat, independent of the normal Joule heating is emitted or absorbed depending on the relative direction of the current flow and temperature gradient. If there is a current (density j Amps/ m^2) in the x direction say and a temperature gradient dT/dx the reversible heat generated per unit volume in unit time is given by

$$-\mu j \frac{dT}{dx}$$

This is known as the Thomson heat and μ is known as the Thomson coefficient.

Peltier Effect: If an electric current flows across a junction between two dissimilar metals then the normal Joule heating (proportional to the square of

the current) will occur in both materials, but at the junction further heat will be emitted or absorbed depending on the current direction. The Peltier coefficient (Π_{12}) is defined as the reversible heat generated per unit charge passed across the junction, the current flowing from metal 1 to metal 2.

Seebeck Effect: If junctions between wires of two dissimilar metals are formed as in figure 1 - 1 with the junctions held at different temperatures T_A , T_B as shown then the resultant e.m.f. in the circuit (ΔV_{12}) is known as the Seebeck e.m.f. The absolute thermoelectric powers of the two materials are then related by the equation

$$\frac{\Delta V_{12}}{\Delta T} = S_1 - S_2 \quad 1.1$$

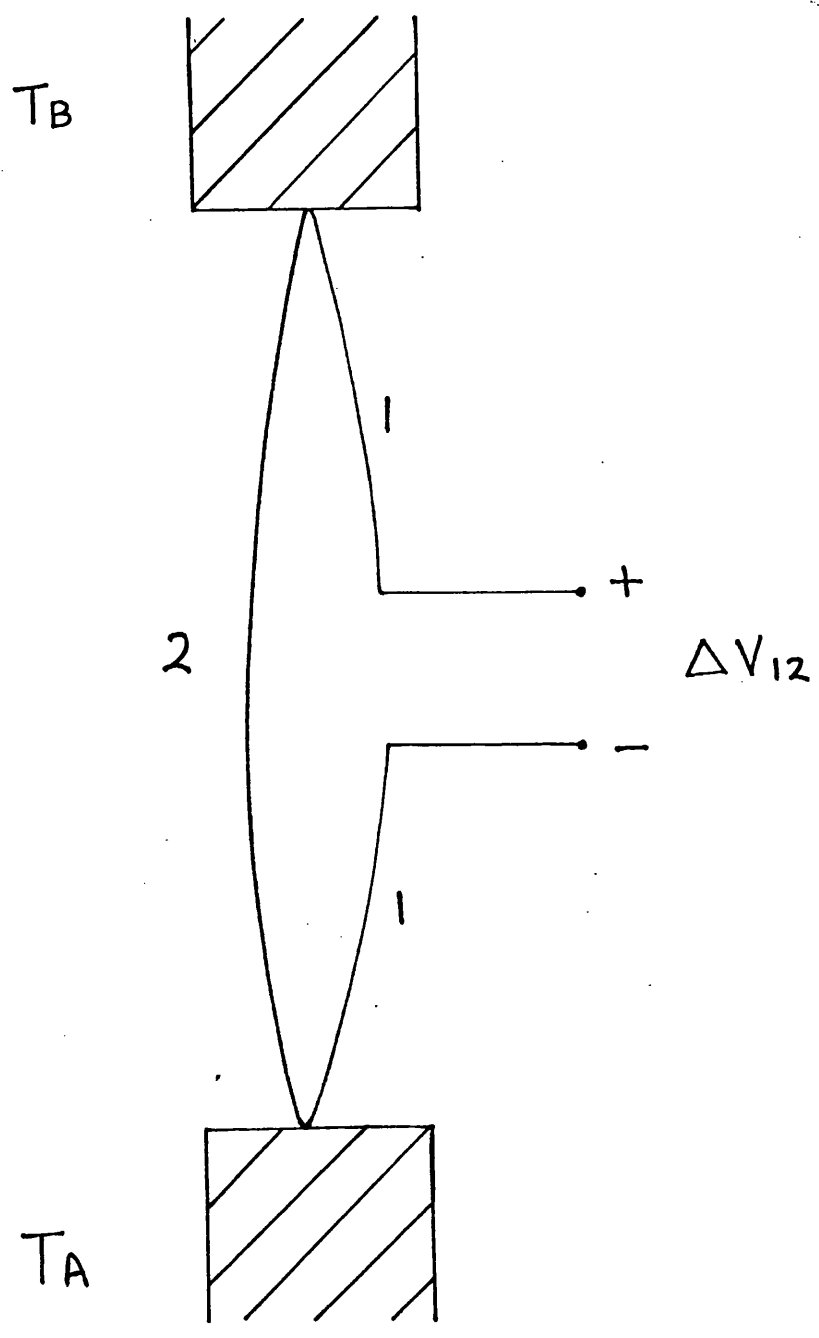
Where S_1 is the absolute thermoelectric power of material 1.

Lord Kelvin, by the application of reversible thermodynamics was able to obtain the following relationships between the above coefficients.

$$\frac{\Pi_{12}}{T} = S_1 - S_2$$

$$\mu = -T \frac{dS}{dT}$$

These are consequently known as the Thomson relations. However, such analysis is not entirely rigorous because of the neglect of the irreversible phenomena (thermal conduction and Joule heating)



$$T_B = T_A + \Delta T$$

The Seebeck Effect

Figure 1-1

associated with any thermoelectric experiment. These relations were tested experimentally and later derived by the full application of irreversible thermodynamics. (Callen, 1948; Ziman, 1960).

Particularly with liquid samples and at high temperatures it is often most accurate and convenient to determine the absolute thermoelectric power for a given sample in an indirect manner. One or several successive applications of the Seebeck effect allow the absolute thermoelectric power of any given sample to be related quantitatively to that of any standard material. The values for standard materials as a function of temperature may of course be obtained by direct experimental determination of the Thomson coefficient but since materials in the superconducting state do not exhibit thermoelectric effects and their absolute thermoelectric power is zero, they provide a convenient standard. The absolute thermoelectric powers of a range of suitable reference materials may then be obtained throughout the temperature range of experimental interest by the use of the Seebeck effect alone. Values for a number of commonly used reference materials have been obtained by these methods and compared for consistency (Cusack and Kendall, 1958; Bradley, 1962).

ii) Microscopic Theories.

The first attempt to explain the above phenomena on a microscopic basis was a classical theory (Drude, 1900). It assumed that in a metal the atoms were

in an ionized state, providing a large concentration of electrons free to move randomly about the volume of the metal as in a classical gas and suffering collisions with the array (spatially ordered in the solid state) of positive ions. The presence of an electrical or thermal gradient is supposed to cause a nett drift of electrons, between their randomizing collisions, giving rise to electrical or thermal conduction respectively.

In the simplest model, by the application of Newton's laws of motion to the movement of the electrons Drude obtained for the electrical conductivity (σ):

$$\sigma = \frac{ne^2\tau}{m}$$

Where n is the number of electrons per unit volume,
 e is the electronic charge,
 m is the electronic mass,
and 2τ is the time between collisions.

In reality the electrons do not all have the same velocity and attempts were made to allow for this in a classical theory by the application of Maxwell-Boltzmann statistics. This classical theory, in spite of providing reasonable values for the electrical and thermal conductivity of metals at room temperature and some agreement with the experimental law of Wiedemann and Franz, gave an

excessive value for the electronic contribution to the specific heat of metals.

The application of quantum mechanics and the realization that electrons are fermions and as such subject to Fermi-Dirac statistics provided reasonable agreement here as well.

Thus we now have for the conductivity:

$$\sigma = \frac{ne^2\tau(E_F)}{m} \quad 1.2$$

Where $\tau(E_F)$ is now the relaxation time evaluated at the Fermi energy since only electrons with energies close to the maximum of the Fermi distribution are scattered. This is because the energy change in any collision is very small due to the relative masses of electrons and ions.

The distribution of the energies of the electrons in a metal is clearly affected by the presence of external forces (electric field, temperature gradient etc.). The steady state distribution function, $f(\underline{k})$, in the presence of say, an electric field is effectively related to that in the absence of external forces (the equilibrium distribution function) by the Boltzmann equation. Applying Fermi-Dirac statistics to the electrons in a metal gives for the equilibrium distribution function:

$$f_0(\mathbf{k}) = 1/\exp((E - E_F)/k_b T) \quad 1.3$$

Where E_F is the Fermi energy and k_b is Boltmann's constant.

Using the Boltzmann transport equation to discuss a metal subject to an external temperature gradient and electric field (in the x direction say)

$$\text{i.e. } -\mathbf{v} \cdot \nabla f - \frac{1}{\hbar} \mathbf{F} \cdot \nabla_{\mathbf{k}} f + \frac{\partial f}{\partial t}_{\text{coll.}} = 0 \quad 1.4$$

Where $\nabla_{\mathbf{k}}$ is the grad. operator in reciprocal space, \mathbf{F} is the electric field, \hbar is Planck's constant $/2\pi$, \mathbf{v} is the electron velocity and the second term represents the rate of change of the distribution function due to the randomizing collisions suffered by the electrons.

and making the assumption that there is one dominant scattering mechanism tending, upon the cessation of the external forces, to return the distribution to its equilibrium value exponentially with time constant τ (the relaxation time) it can be shown that (Mott and Jones, 1936):-

$$\sigma(E) = \frac{2e^2}{(2\pi)^3 \hbar^2} \int \left(\frac{\partial E}{\partial k_x} \right)^2 \tau(\underline{k}) \left| \frac{ds}{\nabla_{\underline{k}} \cdot \underline{E}} \right| \quad 1.5$$

$$\text{with } \frac{1}{\tau} = \int (1 - \cos\theta) P(\underline{k}\underline{k}') ds \quad 1.6$$

and also

$$S = \frac{-\pi^2 k_b^2 T}{3e} \left[\frac{\partial}{\partial E} \log \sigma(E) \right]_{E=E_F} \quad 1.7$$

Where s is the surface of the Fermi distribution in reciprocal space and $\sigma(E)$ represents the value that the conductivity of the metal would have if the energy at the surface of the Fermi distribution were E . Thus $\sigma(E_F)$ is the actual calculated conductivity of the metal. S is the absolute thermoelectric power of the metal.

The derivation of the above equations assumes that:-

$$kT \ll E_F ; \frac{d^2 T}{dx^2} \text{ and } \left(\frac{dT}{dx} \right)^2 \text{ are negligible;}$$

the calculation of the actual conductivity, $\sigma(E_F)$, also requiring that $\frac{df_0}{dE}$ is negligible except at $E = E_F$.

Equation 1.5 reduces to 1.2 in the case of a spherical Fermi distribution in reciprocal space (when τ becomes independent of direction) and for free electrons when

$$E = \frac{\hbar^2 k^2}{2m}$$

In equation 1.6 $P(\underline{k}\underline{k}')$ is the probability of the scattering of an electron with wave vector \underline{k} to another state of wave vector \underline{k}' (known to be empty) of the same energy. Due to the relative masses of electrons and the ionic scattering centres, the energy change at a collision is very small. θ is the angle between \underline{k} and \underline{k}' and $|\underline{k}'| = |\underline{k}| = k$.

$P(\underline{k}\underline{k}')$ can be evaluated for scattering off some small potential v (such as that resulting from a perturbation of a regular crystal lattice) by means of time dependent perturbation theory giving:

$$P(\underline{k}\underline{k}')ds = \frac{V}{4\pi^2\hbar} \left| V_{\underline{k}\underline{k}'} \right|^2 \frac{ds}{\partial E / \partial k_n} \quad 1.8$$

Where V is the volume of the metal, k_n is a vector in reciprocal space normal to the surface s of the Fermi distribution, $V_{\underline{k}\underline{k}'}$ is the matrix element of v between the states of wave vector \underline{k} and \underline{k}'

$$V_{\underline{k}\underline{k}'} = \int \Psi_{\underline{k}'}^* v \Psi_{\underline{k}} d\underline{r}$$

iii) The Pseudopotential.

In 1961 the concept of the pseudopotential was applied to liquid metals (Ziman, 1961; Bradley, Faber, Wilson and Ziman, 1962). The liquid is pictured as an assembly of ions with an attractive coulomb potential due to their electrostatic charge, but this is screened by the electron gas in which the ions are immersed. The electrons filling the core states of the ions interact via the Pauli exclusion principle with the conduction electrons - the wave functions for the conduction electrons must be orthogonal to those of the core states of the ions. It is believed (Cohen and Heine, 1961) that these effects cancel most of the strongly attractive bare ionic potential leaving only a relatively weak 'pseudopotential'. This is known as the cancellation theorem.

This weak pseudopotential is then used to calculate the scattering of the electrons in the gas. The electrons are described by wave functions which, far from the ion core, are of the form:

$$\Psi_{\underline{k}} = \frac{1}{\sqrt{V}} e^{i\underline{k} \cdot \underline{r}} \quad \text{i.e. plane waves.}$$

Since it has been found difficult (Wiser, 1966) to calculate the pseudopotential sufficiently accurately, a convenient approach is to formulate

in real space a model, with one or more parameters fixed by reference to various experimental data, of the unscreened form of this potential $u_b(\underline{r})$ with Fourier components $u_b(\underline{K})$. The effect of screening by the electron gas can then be allowed for by means of a dielectric function $\epsilon(\underline{K})$ (Faber, 1972) giving $u(\underline{K})$, the Fourier components of the screened ion model potential:

$$u(\underline{K}) = \frac{u_b(\underline{K})}{\epsilon(\underline{K})}$$

This is reasonable in a metal since the conduction electron gas has a high density and kinetic energy. Thus the potential at any given point \underline{r} is

$$U(\underline{r}) = \sum_{\underline{R}_i} u(\underline{r} - \underline{R}_i)$$

Where \underline{R}_i is the position vector of the i^{th} ion core.

This is the weak potential from which the scattering of the plane wave states of the conduction electrons is considered, giving for the matrix element:

$$\begin{aligned} V_{\underline{k}\underline{k}'} &= v^{-1} \int e^{-i\underline{k}' \cdot \underline{r}} \sum_{\underline{R}_i} u(\underline{r} - \underline{R}_i) e^{i\underline{k} \cdot \underline{r}} d\underline{r} \\ &= u(\underline{K}) N^{-1} \sum_{\underline{R}_i} e^{i\underline{K} \cdot \underline{R}_i} \end{aligned} \quad 1.9$$

where $\underline{K} = \underline{k} - \underline{k}'$

$$\text{and } u(\underline{K}) = NV^{-1} \int e^{i\underline{K} \cdot \underline{r}} u(\underline{r}) d\underline{r} \quad 1.10$$

It is $|v_{\underline{k}\underline{k}'}|^2$ which is needed in equation 1.8 and this is given by:

$$|v_{\underline{k}\underline{k}'}|^2 = \frac{1}{N} |u(\underline{K})|^2 a(\underline{K}) \quad 1.11$$

where $a(\underline{K})$ is given by:

$$a(\underline{K}) = \frac{1}{N} \left| \sum_{\underline{R}_i} e^{i\underline{K} \cdot \underline{R}_i} \right|^2 \quad 1.12$$

$a(\underline{K})$ is the static structure factor or interference function and can be evaluated from X-ray or Neutron diffraction experiments (Egelstaff, 1967).

Thus combining the above formulae and applying to the scattering of the electrons of the free electron gas (where the probability $P(\underline{k}\underline{k}')$ is a function only of $\underline{K} = |\underline{k} - \underline{k}'|$ and not of the initial state) by the pseudopotential gives for the resistivity:

$$\rho = \frac{1}{\sigma(E_F)} = \frac{6\pi^2}{he^2} \frac{1}{v_F^2} \frac{V}{N} \int_0^{\frac{1}{2}} \left[|u(\underline{K})|^2 a(\underline{K}) \right] \frac{4(\frac{K}{2k_F})^3 d(\frac{K}{2k_F})}{(2k_F)} \quad 1.13$$

Where v_F is the velocity corresponding to the surface of the Fermi distribution.

The theory outlined above can be generalised to include liquid alloys; there are then different pseudopotentials for each type of ion present and account must be taken of the relative spatial distribution of the various ionic species. The

resistivity is still given by equation 1.13 and the thermoelectric power by equation 1.7 from equation 1.13, but the term in brackets in equation 1.13 must be modified (Faber and Ziman, 1965). In the particular case of a binary liquid alloy with an atomic concentration c of type A atoms with associated pseudopotential $u_A(K)$ and an atomic concentration $(1 - c)$ of atoms of type B with associated pseudopotential $u_B(K)$ the bracketed term becomes:

$$|u_A(K)|^2 [c(1-c) + c^2 a_{AA}] + |u_B(K)|^2 [c(1-c) + (1-c)^2 a_{BB}] + 2u_A(K) u_B(K) c(1-c)(a_{AB} - 1) \quad 1.14$$

Where a_{AA} , a_{BB} , a_{AB} , are the three partial structure factors. $a_{\alpha\beta}$ is related to $g_{\alpha\beta}$ the probability of finding an ion of type α in unit volume at a radius r from an ion of type β

$$a_{\alpha\beta}(K) = 1 + \frac{N}{V} \int_0^{\infty} (g_{\alpha\beta}(r) - 1) \frac{\sin Kr}{K} 4\pi r dr \quad 1.15$$

where α, β are dummy suffices.

These partial structure factors can in some suitable cases be determined from three neutron diffraction experiments in which the scattering length of one of the constituents is varied by means of isotopic enrichment and substitution. This is not always feasible but in some cases where the ionic species are sufficiently similar a substitutional

model (implying $a_{AA} = a_{AB} = a_{BB} = a$) can be used.

iv) Application to Real Liquid Metals.

Using the basic formulae for the resistivity and thermoelectric power it has been possible to explain, qualitatively at least, the majority of experimental results for liquid normal metals - that is metals that are not transition, rare earth, or actinide metals - and their mutual alloys.

The nature of the integral in equation 1.13 accounts for the increase in the magnitude of the electrical resistivity with increasing values of the Fermi energy (and hence k_F) resulting from the higher valence of some metals (Ziman, 1972). In the particular case of sodium (with a low resistivity corresponding to an electronic mean free path of many interatomic spacings), where the pseudopotential is very weak and this nearly free electron model would seem most applicable, the calculated resistivity can agree closely with the experimental value, but is very dependent on the exact value of the pseudopotential. In the calculation by Wiser (Wiser, 1966) the estimated error in the pseudopotential used was sufficient to alter the calculated resistivity by a factor of two. Similarly, although the formulae predict a positive temperature coefficient of resistivity for metals of valency 1, 3 and 4, even in the apparently suitable case of sodium it was found (Greenfield, 1966) that the prediction of the magnitude of this coefficient

is not certain. This is primarily because of the uncertain effects of thermal expansion on the pseudopotential (Ziman, 1967). The prediction of the thermoelectric power of the alkali metals generally gives results within 15 to 20 per cent of the experimental values (e.g. Sundstrom, 1965) but some energy dependence of the pseudopotential is implied at least in the case of potassium (Ziman, 1967).

The formulae also allow for a negative temperature coefficient of resistivity in the divalent metals and alloys of such a composition that, as in the divalent metals, the Fermi wave vector has a value in the region of the first peak of the total structure factor for the substance. It has been postulated (Bradley et al, 1962) that this is due to a negative temperature coefficient of the structure factor in this region of reciprocal space. However, it has been shown by neutron diffraction experiments (Wingfield and Enderby, 1968) that, at least in the case of liquid zinc, the change in the structure factor is not as large as would be required and it would appear that the effects on the pseudopotential of thermal expansion are of major importance.

In the case of the heavy polyvalent metals, such as mercury, thallium and lead, where the electronic mean free path is only of the order of a few interionic spacings and so it might well be expected that a nearly free electron model was inappropriate, calculations using an ordinary

pseudopotential of the type mentioned above give resistivity values consistently low, about 50 to 80 per cent of the experimental ones. (Ziman, 1967). Predictions for the thermoelectric power are in error by as much as a factor of four. Improvement can however be obtained by using an energy (i.e. k) dependent pseudopotential (Evans, Greenwood, Lloyd and Ziman, 1969 and Evans, 1970). This energy dependence is taken to be due to the presence of a narrow 'd' like band near the bottom of the conduction band. Described in terms of the theory of partial wave analysis, this d like band produces a significant shift of the 3rd ($d, \ell=2$) partial wave.

Applications of the basic formulae to the lower alkaline earths, calcium, strontium and barium do not (by a factor of two or worse, deteriorating as one descends the periodic table) correctly predict their resistivity although the calculated values for magnesium are somewhat closer, the discrepancy of course depending on the exact form of the structure factor and pseudopotential used. (Van Zytveld, Enderby and Collings, 1972). This, together with the qualitatively similar pattern in the results for the thermoelectric powers, has been interpreted (Van Zytveld, Enderby and Collings, 1973) as due to an increasing energy dependence of the pseudopotential, caused by the approach of a narrow unfilled band having d-electron character towards the Fermi level (from above) with increasing atomic number.

Calculations using such energy dependent pseudopotentials have been reported (Cubiotti, Giuliano, Ruggeri and Stancanelli, 1975) yielding values for the resistivity within 10 per cent of the experimental values. Calculations have also been reported (Ratti and Evans, 1973) however, using the method of partial wave analysis to describe the scattering of electrons from the ionic potentials, giving resistivities differing by up to 36 per cent from the experimental values. These calculations are similar to some used for transition metals and are mentioned in Chapter 2.

Applications of this theory with ordinary pseudopotentials to the cases of the noble metals lead to values for the resistivity which are several times too large (Ziman, 1967), again due to a narrow d like band with a large density of electron states but here it lies not far below the Fermi level. Similarly, for the transition metals where a narrow d band overlaps the Fermi energy the use of a weak local pseudopotential is not appropriate. It is the presence of the d band in transition and some other metals which gives rise to the major differences between these and 'simple' liquid metals. Some more suitable ideas for these cases are mentioned in Chapter 2.

i) Early Work.

A theoretical description of the electronic structure of transition metals was given in 1936 by Mott (Mott and Jones, 1936). The band structure is pictured (as in figure 2-1) as consisting of a broad free electron conduction band ('s' band) and a 'd' band which is narrow due, in the tight binding model, to the small overlap between the d orbitals centred on adjacent ions. This narrow band accommodates substantially those electrons (about 10 per atom) which in an isolated atom would be in discrete d states; consequently the band in transition metals has a large density of electron states. The presence of this high narrow band is indicated by X-ray and optical spectra (Skinner and Johnston, 1937; Beeman and Friedman, 1939 and Friedman and Beeman, 1940). The two bands overlap and the Fermi energy lies within the range of the d band.

This band structure, with a large density of electron states at the Fermi energy, is consistent with certain experimental observations such as the high electronic specific heat of palladium and the low conductivity of transition metals (Mott and Jones, 1936). The latter is explained as follows: due to the high and narrow nature of the d band the electrons concerned have an effective mass large with respect

Density of Electron States in a Transition Metal

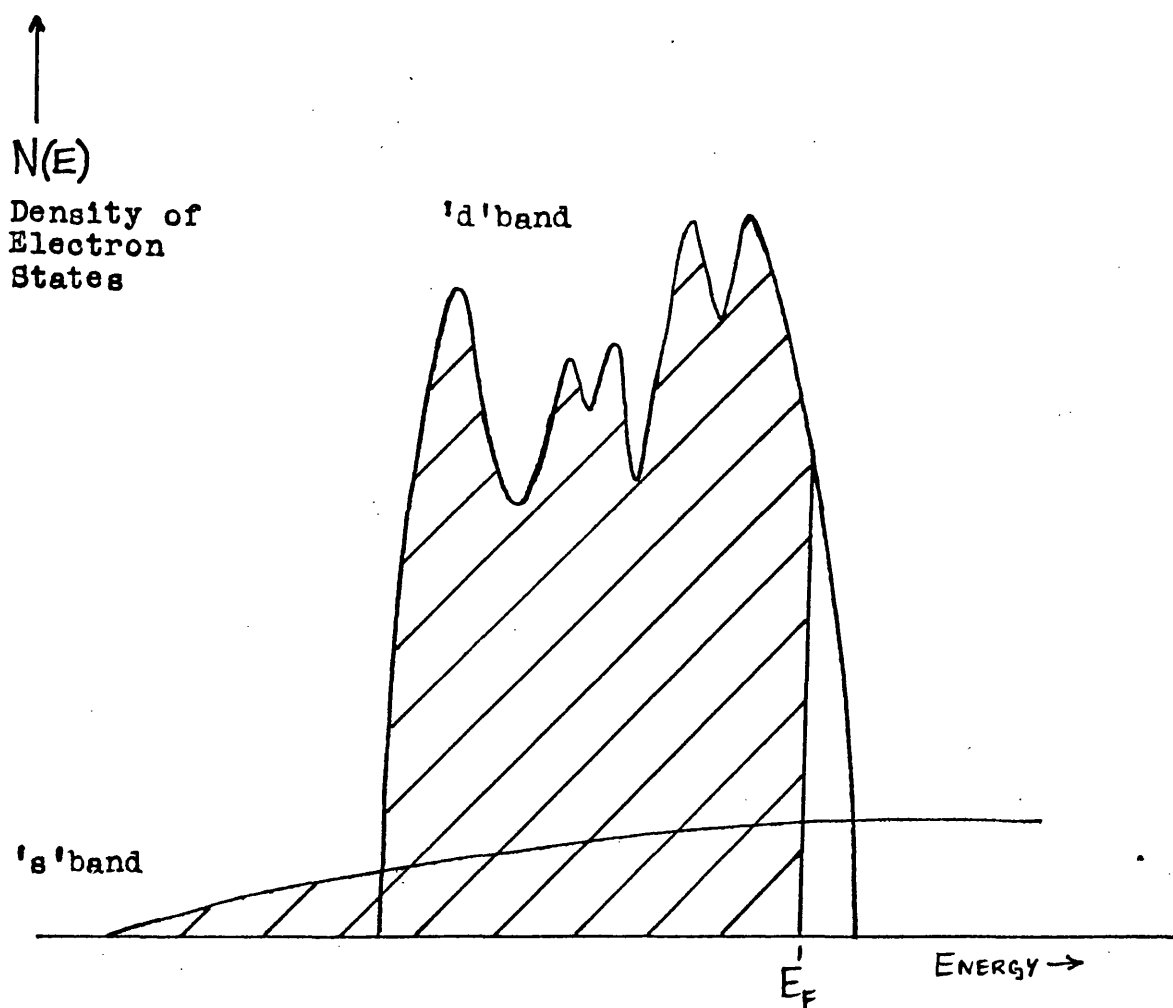


Figure 2-1

to that of the electrons in the nearly free s band. This means that the d electrons will be relatively unresponsive to an applied electric field so that the s electrons carry the bulk of the current.

By the golden rule (c.f. equation 1.8) the probability ($\frac{1}{\tau_{z-z'}}$) of transitions from one state (z) to another (z') is directly related to the density of final states; so it is considerably more probable that an s electron near the Fermi surface will be scattered into a vacant d state than into a vacant s state.

$$\frac{1}{\tau_{s-d}} \gg \frac{1}{\tau_{s-s}}$$

Thus the conductivity is much lower than it would be in the absence of the d band. As an approximation, neglecting the s-s transitions gives for the probability of a s electron being scattered:

$$\frac{1}{\tau_s} \approx \frac{1}{\tau_{s-d}} = \left[N_d(E) \right]_{E=E_F}$$

Where $N_d(E)$ is the density of electron states in the d band. In principle, in conjunction with equation 1.5, this gives $\sigma(E)$, but the actual conductivity for transition metals at high temperatures is given by:

$$\sigma = \left[\sigma(E) \right]_{E=E_F} + \frac{\pi^2 (k_b T)^2}{6} \left[\frac{d^2 \sigma(E)}{dE^2} \right]_{E=E_F} + \dots \quad 2.1$$

The second term provides a correction for the significant variation in $\sigma(E)$ caused by the rapid variation of $N_d(E)$ within a range $k_b T$ at the Fermi energy. This is used to explain the decrease in the temperature coefficient of resistivity of solid palladium and platinum with increase in temperature (Mott and Jones, 1936).

The variation in the thermoelectric powers of the transition metals, including the large negative values for palladium and nickel, can also be allowed for. The form of equation 1.7 together with the discussion above concerning σ indicates that the thermoelectric power is directly dependent on the energy derivative of the density of d states at the Fermi energy. The position of the Fermi energy with respect to the d band will vary from metal to metal; when in the position shown in figure 2-1 a large negative thermoelectric power is predicted. Should the Fermi energy lie near a stationary point of the density of states versus energy curve (such as a peak shown in figure 2-1) then the thermoelectric power will be small in magnitude.

The above model applies both to the liquid and

solid state and has been used to discuss the properties of transition metal alloys, in particular the concentration dependence of the thermoelectric power and resistivity of solid silver-palladium alloys (Mott and Jones, 1936; Taylor and Coles, 1956 and Coles and Taylor, 1962). Originally a rigid band structure was assumed with a common s band, a palladium d band similar in character to that shown in figure 2-1 and a silver d band well below the Fermi energy and near the bottom of the conduction band. On the addition of silver to palladium it was imagined that the holes in the palladium d band were gradually filled up. The magnetic susceptibility indicated that the d band was just full at a silver concentration of approximately 55 atomic per cent implying that in pure palladium there are 0.55 holes per atom in the d band. At silver concentrations less than 55 atomic per cent the s-d transitions mentioned above still occur but at larger silver concentrations they cannot take place since the d band is full. This leads to a reasonable qualitative picture of the variation of the resistivity of silver - palladium with concentration (Mott and Jones, 1936). Quantitative agreement between experiment and calculated values was later obtained, though for palladium-rich alloys it was necessary to consider contributions to the conductivity from the holes in the d band (Coles and Taylor, 1962).

The upward movement of the Fermi energy with respect to the d band upon the addition of silver to palladium means that $\frac{d}{dE} (N_d(E))$ becomes more negative and an increase of the large negative thermoelectric power with concentration is predicted until, at the composition containing approximately 55 atomic per cent silver, the d band is filled and the magnitude of the thermoelectric power is expected to drop to a value comparable with that of pure silver. The results for the solid alloy shown in figure 5-16 show this general behaviour. A measure of quantitative agreement has been obtained (Kimura and Shimizu, 1964) and conduction by d band holes is considered significant. However, observations of the de Haas - van Alphen effect in palladium at low temperatures (Vuillemin and Priestley, 1965) indicated that there were in fact only 0.36 's' electrons per atom (and thus only 0.36 holes per atom in the d band) but the hypothesis (Dugdale and Guénault, 1966) of a linear shift of the common s band with respect to the d band - the shift being linear with atomic concentration - enabled the theory to remain consistent with experiment.

The full situation is not of course described by the crude assumptions mentioned above, for example as stated, there is evidence that particularly at high palladium concentrations there is appreciable conduction due to the holes in the d band. Also, photoemission experiments on solid silver-palladium alloys

(Norris and Myers, 1971) and theoretical calculations using a coherent potential approximation (Stocks, Williams and Faulkner, 1973) indicate that the band structure is not as simple as that described.

ii) The 'Bristol' Theory.

An explanation of the resistivity and thermoelectric power of liquid transition metals has been given (Evans, Greenwood and Lloyd, 1971) which uses features of the theory for simple metals given in Chapter 1. During electronic conduction, electrons in a nearly free s band carry most of the current but are scattered from the ionic potentials. The scattering is considered to be caused by virtual bound d states. It is known (Friedel, 1969) that in alloys containing a small concentration of a transition metal in a simple metal there exist such virtual bound states. These correspond to the d levels of isolated transition metal atoms - when such atoms are added to a simple metal, due to the overlap of ionic potentials, the d level lies above the mean interstitial potential of the alloy. In general the d level lies within the conduction band of the host and becomes broadened and somewhat shifted by (s-d) hybridization. This gives rise to an extended state in which an electron is not truly bound to the impurity atom, but does remain localized in the region of the impurity. The combination of the attractive potential well centred on the ion and the 'centrifugal potential' of the appropriate radial part of the Schroedinger equation provides a barrier

separating the virtual bound state from the conduction electron gas, but through which the electrons may tunnel; the probability of this process giving the width of the resonance.

The model generally assumes potentials, centred on each ion, which are spherically symmetric out to some radius r_m ; the potential in the interstitial regions outside these spheres being taken as constant throughout the sample. Such spherically symmetric 'muffin tin' potentials have been calculated in some cases, e.g. for solid iron (Wood, 1962).

The scattering of the conduction electrons is then considered in terms of partial wave analysis. The scattering amplitude for the elastic scattering of an electron by a single potential well from a state \underline{k} to a state \underline{k}' through an angle θ is given by (Schiff, 1955):

$$f(\theta) = \frac{1}{k} \sum_{l=0}^{\infty} (2l+1) \exp(i\eta_l(E)) \sin \eta_l(E) P_l(\cos\theta) \quad 2.2$$

Where l is the angular momentum quantum number

$\eta_l(E)$ is the phase shift of the l^{th} partial wave
 $P_l(\cos\theta)$ is the l^{th} Legendre Polynomial.

For a real metal it would be better to calculate the T matrix (Ziman, 1967) whose elements give the exact probability of scattering from the state \underline{k} to \underline{k}' .

However, this is approximated to first order by the t matrix for scattering from a single atomic site, the appropriate elements of this matrix being

equivalent to the scattering amplitude given above (Ziman, 1964).

In transition metals, due to the resonance of the conduction electrons with the d like virtual bound states, the phase shift at the Fermi energy for the $\mathcal{L}=2$ partial wave has a much larger magnitude (and generally varies more rapidly with energy) than the phase shifts for partial waves of other angular momenta. Thus the t matrix element is itself approximated by:

$$t_{\underline{k}\underline{k}'} = \frac{-2\pi\hbar^3}{m(2mE)^{1/2}} \frac{5}{\Omega} \sin\eta_2(E_F) \exp(i\eta_2(E_F)) P_2(\cos\theta) \quad 2.3$$

where Ω is the atomic volume and substituting this for the pseudopotential matrix elements in the theory given in Chapter 1 gives for the resistivity of a liquid transition metal:

$$\rho = \frac{600\pi^3\hbar^3}{mE_F k_F^2 \Omega e^2} \sin^2\eta_2(E_F) \int_0^\pi x^3 a(q) \left[P_2(\cos\theta) \right]^2 dx \quad 2.4$$

Since the integral is dominated by the contribution from the region $\theta \approx \pi$, the expression for the resistivity reduces to:

$$\rho = \frac{30\pi^3\hbar^3}{mE_F k_F^2 \Omega e^2} a(2k_F) \sin^2\eta_2(E_F) \quad 2.5$$

and using equation 1.7, which is derived only to first order in $k_b T/E_F$ but should be sufficiently accurate for the degree of approximation involved in calculations such as these, gives for the thermoelectric power:

$$S = \frac{\pi^2 k_b^2 T}{3|e|} \left[\frac{-2}{E_F} + \frac{1}{a} \frac{da}{dE} + 2 \cot \eta_2(E_F) \frac{d\eta_2(E_F)}{dE} \right] \quad 2.6$$

For noble metals it is necessary to include other (s,p) phase shifts which gives for the resistivity:

$$\rho = \frac{24\pi^3 n^3}{m E_F k_F^2 \Omega e^2} \int_0^1 x^3 a(q) \left| \sum_{l=0}^{\infty} (2l+1) \sin \eta_l(E_F) \exp(i\eta_l(E_F)) P_l(\cos \theta) \right|^2 dx \quad 2.7$$

Calculations based on equations such as these have yielded values of the correct order of magnitude for the resistivity and thermoelectric power of liquid noble and transition metals; the values rarely differing from experiment by more than a factor of two. (Evans et al, 1971; Dreirach, 1971 and Brown, 1973). A significant difficulty has been to establish suitable numerical values for k_F and E_F . The Fermi wave vector is frequently derived by the usual free electron formula

$$k_F = \left(\frac{3\pi^2 Z_{\text{eff.}}}{\Omega} \right)^{1/3} \quad 2.8$$

from an 'effective valence' Z_{eff} , representing the number of nearly free electrons present in the metal per atom. This has been variously estimated for nickel for example as 1, 2, 0.46 (Evans et al, 1971; Dreirach, Evans, Guntherodt and Kunzi, 1972 and Brown, 1973). Attempts have been made to evaluate this quantity for palladium theoretically and from neutron diffraction experiments (Brown, 1976). Since, for the transition metals, the d phase shift varies rapidly with energy near E_F high precision is desirable in the estimate of the Fermi energy. This has not been obtained with certainty. A method normally used (Dreirach, 1971) is to calculate the position of the bottom of the conduction band in the solid from the solid s-wave phase shifts (Ziman, 1967b), use the position of the Fermi energy in the solid (estimated from optical data pertaining to the solid state) to obtain the width of the band in the solid and then to approximate the band as a nearly free electron band with one effective mass m^* . This same effective mass is then used to calculate the width of a nearly free band at the appropriate liquid density, the bottom of the band being calculated in the same way as for the solid but using the s-wave phase shifts for the liquid (which do not vary rapidly with energy).

Calculations have also been reported (Dreirach et al, 1972) of the resistivity of certain liquid

noble and transition metal—non-transition metal alloys, using formulae similar to those above but including appropriate t matrix elements for both types of ion present in the alloy (Chapter 1 (iii) and 6 (ii)).

These calculations do reproduce the general form of the variation of resistivity with concentration for the alloy systems investigated.

iii) An Alternative Theory.

Mott, however, maintains a fundamental objection to the above formalism insisting that for pure liquid transition metals there are two significant mean free paths to be considered - a short one of the order of one interatomic spacing at high temperatures for the d like electrons and a longer one for the nearly free electrons (having a typical value of several interatomic spacings) (Mott, 1972).

With a separate short mean free path for the d electrons Mott argues that the resonance described in the theory above cannot build up. The likelihood of a resonance of the type mentioned developing varies as the ratio of the coupling between the s and d orbitals on one atom and the coupling between d orbitals on adjacent atoms. Since the latter is a steep inverse function of the inter-transition metal atom spacing, it is accepted that the resonance type approximation is tenable for alloys containing a significant concentration of a non-transition metal.

In terms of the ideas advanced by Mott, the resistivity of the liquid does not depend on the structure factor, thus implying a small temperature dependence of the resistivity of the liquid. It also implies that the theory for the liquid is substantially the same as for the solid at high temperature so the change in the resistivity of a transition metal upon melting is predicted to be a small fraction of the solid resistivity near the melting point. This is in accord with the experimental observations (Wilson, 1965; Table 5-D) although for palladium the liquid resistivity is nearly one and a half times the solid value, which is similar to the situation in the case of copper.

Specific detailed calculations for liquid transition metals have not been performed, but the correct order of magnitude is predicted for the resistivity of a liquid transition metal.

iv) The d electron Contribution.

Model calculations have been reported (ten Bosch and Bennemann, 1975) which indicate that for a pure liquid transition metal the contribution of the d electrons to the electrical conductivity could be as large as that of the s electrons rather than the small correction mentioned above (Chapter 2 (i)) for the case of solid palladium-rich silver-palladium alloys.

Upon melting, the spatial ionic disorder will cause an increase in the scattering of the s electrons and thus a decrease in their contribution to the conductivity, whereas the d electron contribution is presumed to be less sensitive to melting due to the localization of these electrons on ionic sites. The results show that the d electron contribution to the liquid conductivity reaches a maximum when the model d band is half filled. In the cases for which this contribution is significant it will decrease the relative change of resistivity on melting.

For alloys containing a non-transition metal the calculations indicate that the relative contribution of the d electrons decreases rapidly with increasing concentration of the non-transition metal.

v) Experiments Undertaken.

The experiments reported in this thesis were initiated in order to provide further experimental data relevant to the above discussion. It was felt desirable to re-determine the thermoelectric power for liquid cobalt and nickel (Howe and Enderby, 1973) using a completely different technique; the thermoelectric powers of liquid iron and palladium were not known although calculations were reported (Evans et al, 1971 and Brown, 1973). The resistivity of pure liquid palladium had been measured (Vatolin, Esin and Dubinin, 1967) but the value reported was high, giving palladium a relative change in resistivity upon melting $(\frac{\Delta\rho}{\rho})_{\text{Melt.}}$ several times larger than

the highest value observed for any other transition metal (Faber, 1972) - a check was therefore made on the liquid value. It was decided to examine an inter-transition metal ("TT") binary alloy and a transition metal — non-transition metal ("TN") one. For the "TT" case nickel-cobalt was chosen because it most closely fulfilled the conditions for the application of the semi-quantitative test, described in Chapter 6, of the resonance approximation. For the "TN" case silver-palladium was chosen because the well known properties of the solid alloy and pure components facilitated comparison of the liquid and solid state properties. In summary the following measurements were undertaken:

Thermoelectric Power:-

Liquid Ni, Co, Fe, Pd.

Solid Ni, Co, Fe.

Liquid Ni-Co alloys 10,22,45,70 atomic % Co.

Solid Ni-Co alloy 45 atomic % Co.

Liquid Pd-Ag alloys 24,38,49,59,74,85 atomic %Ag.

Resistivity:-

Liquid Fe, Ni, Co, Pd.

Liquid Ni-Co alloy 18 atomic % Co.

CHAPTER 3. MEASUREMENT OF THE THERMOELECTRIC POWER.

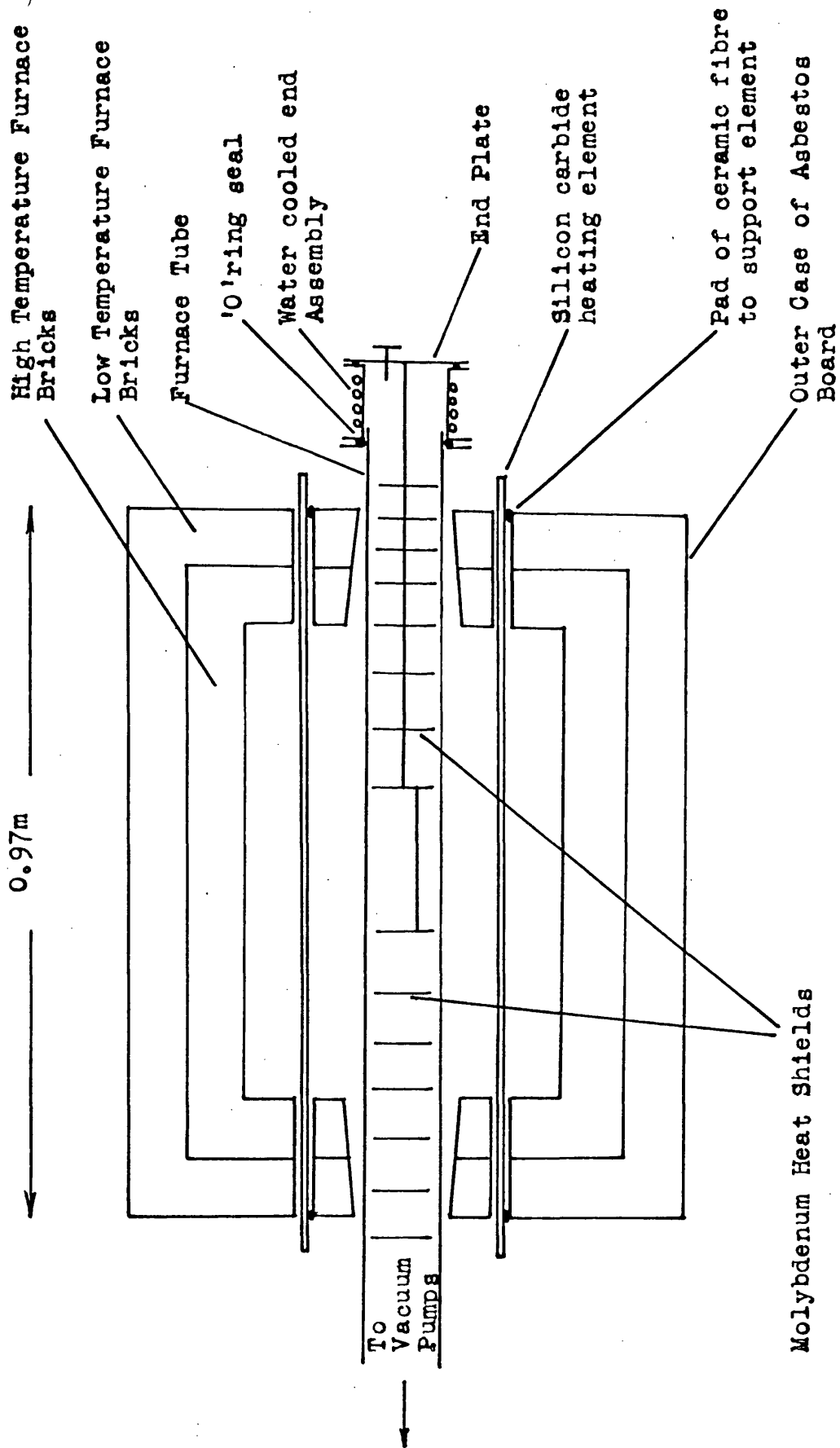
i) Introduction.

The principal difficulties encountered in measuring the electronic transport coefficients of the liquid transition metals are the containment of, and the provision of electrical contacts to these highly corrosive and volatile materials. The absolute thermoelectric powers were determined using the Seebeck effect with the contacts to the liquid achieved by dipping wires of the reference material into the liquid for very short periods, thus minimising contamination of the sample. Pure tungsten was used as the reference material or "counter electrode" since past experience and inspection of the available data (Hansen, 1958) indicated that of the available metals, this would suffer the least corrosion by the liquid samples. Similar experience dictated the use of crucibles of pure (99.7%) high density recrystallised alumina (supplied by Thermal Syndicate Ltd.). The metals investigated all had high melting points (up to 1552°C) so a large rectangular 'muffle' furnace was constructed capable of reaching temperatures of the order of 1500°C - uniform to within a few degrees over a region two or three times the size of the sample. The sample was placed in the centre of this region surrounded by a horizontal large

bore (nominally 89mm.) high purity alumina tube ("Purox" tube supplied by Morgan Refractories Ltd.). Arrangements were made to evacuate this tube, or to fill it with argon gas to prevent oxidation of the sample and apparatus or evaporation of the sample itself.

ii) Muffle Furnace.

The muffle furnace was constructed as shown in figure 3-1 with two types of furnace bricks, high temperature bricks for their refractory properties (G-33 supplied by A.P. Green Fire Brick Co.) and lower temperature bricks (G-28 - A.P. Green) with greater thermal insulating properties at lower temperatures. The inner surfaces of the high temperature bricks were coated with alumina cement (C.101 supplied by Thermal Syndicate Ltd.) which was also used to fill any small gaps between the high temperature bricks. The furnace was heated by eight horizontal $\frac{5}{8}$ inch diameter silicon carbide heating rods (Crystolon Hot Rods supplied by Morganite Electroheat Ltd.) supported at each end by pads of ceramic fibre. The heating rods were connected in series and supplied with electric power of up to 440 volts and up to 30 Amps D.C. obtained from the normal mains via a three phase, phase angle fired, half controlled thyristor and rectifier bridge circuit. The power to the furnace was controlled via the thyristor bridge by a two-loop servo circuit



Muffle Furnace

Figure 3-1

which adjusted the power input to such a value as was needed to reach and then hold the required temperature. Feedback for this temperature control loop was, as shown in figure 3-2, from one of the thermocouples (Platinum versus Platinum/13% Rhodium) mounted in the top of the furnace with their junctions near to the furnace tube in the uniform temperature region. The temperature demand control was calibrated in terms of temperature by means of a series of test experiments in which the general accuracy of the thermocouples was checked using an optical pyrometer. The second servo loop was used to set a maximum current level which could not be exceeded in supplying power to the furnace.

The manufacturers specified that during the heating or cooling of the furnace the rate of change of temperature to which the furnace tube was subjected should not exceed 100°C/hr . Therefore a programmer (type J.A.06 supplied by Eurotherm Ltd.) was connected to the main controller, as in figure 3-2, allowing the operator to set a given rate of change of temperature which continued until the desired temperature was achieved. The programmer functioned by injecting a slowly decreasing ramp voltage in series aiding with the feedback thermocouple of the main controller.

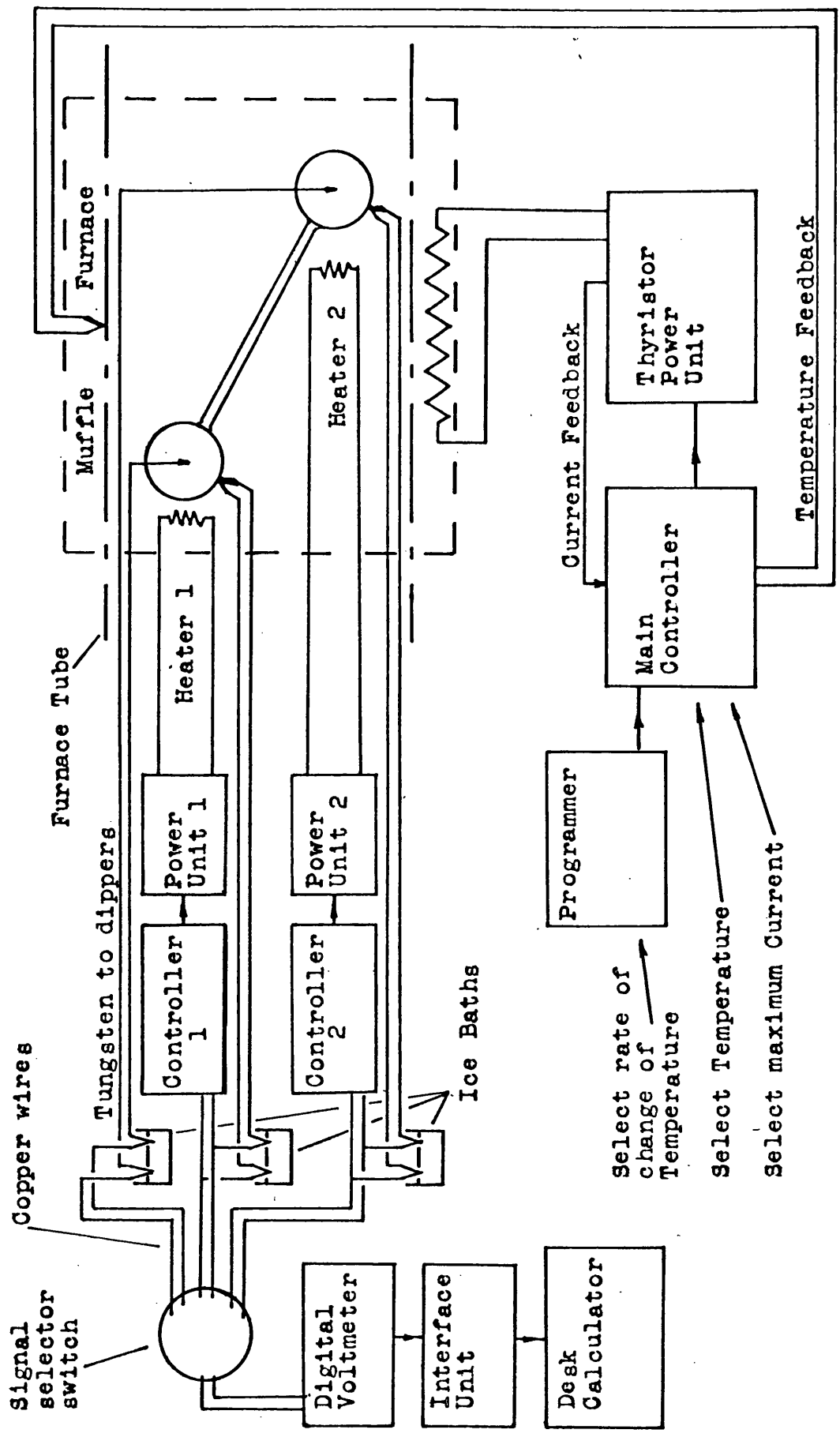


Figure 3-2 Temperature Control and Signal Measurement Arrangements

iii) Vacuum and Argon System.

The arrangements for the evacuation of the furnace tube are shown in figure 3-3. Pressures of the order of 10^{-5} torr, as measured on a Penning guage in the position shown, could be attained at 1500°C . During heating up, outgassing from the tube and other internal surfaces caused the vacuum to deteriorate although it was seldom worse than 10^{-4} torr. The control unit of the Penning guage was connected via a switch unit to the programmer in such a manner that should the vacuum deteriorate as far as 2×10^{-4} torr, the programmer would change from a temperature upwards condition to a temperature downwards one, only reverting to the upwards mode if the vacuum improved to better than 5×10^{-5} torr. The furnace tube was sealed at either end to water cooled concentric brass coupling parts by means of greased neoprene 'O' rings. This was adequate as the temperature at the ends of the tube did not exceed 80°C due to heat conduction to the water cooled end assemblies.

When required during the course of an experiment the furnace tube was filled to a pressure of a few centimetres of mercury above atmospheric pressure with argon obtained via a pressure regulator from a high pressure storage cylinder. To allow for the thermal expansion of this gas as a result of the heating up of the furnace a mercury filled

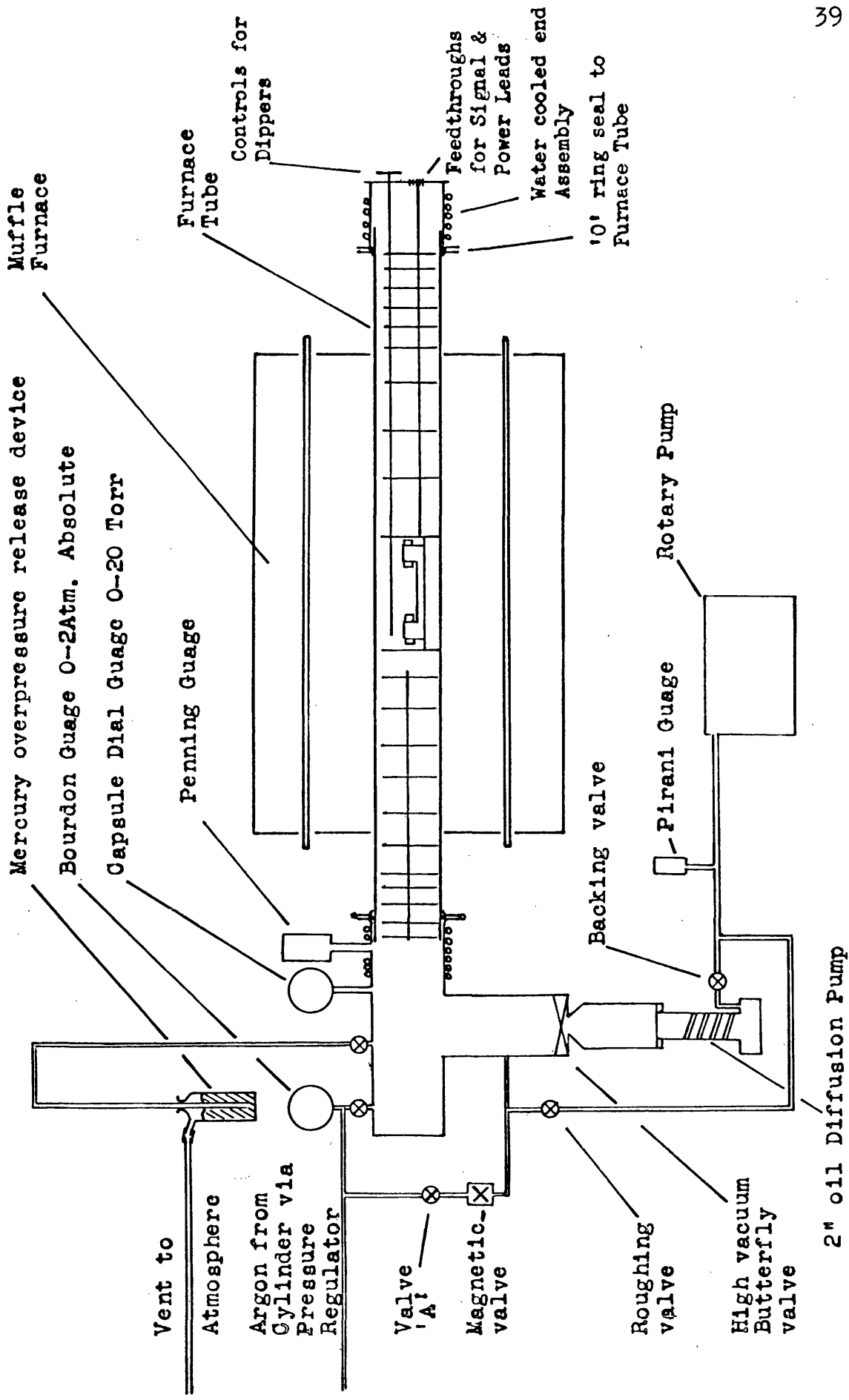


Figure 3-3

non-return overpressure release device was connected to the system. This allowed some argon to escape if the internal pressure rose to more than 100 mm. of mercury above that of the atmosphere. Guages covering the ranges 0 - 20 torr and 0 - 2 atmospheres absolute were used to monitor the gas pressure in the system.

In order to safeguard the sample and its supports etc. an arrangement was made employing an electromagnetic valve normally held shut but which opened, filling the furnace tube with argon gas, should the mains supply fail causing the vacuum pumps to stop. This safety arrangement was put into a state of readiness by opening the valve 'A' shown in figure 3-3. As an additional safety feature the mains supply was fed to the bridge circuit via a latching contactor which opened once the supply had failed and did not re-connect even if the supply was restored. The contactor could also be opened by a vacuum switch controlled by the signals from the Penning guage. Thus, if the vacuum failed for any reason, power to the furnace was cut off. This latter arrangement could be overridden when it was desired to fill the chamber with argon.

iv) The Carriage.

The crucibles used to contain the samples were supplied in the form of 'pipe-boats' as shown

in figure 3-4. A typical sample solidified after experiment and with its crucible removed is shown in figure 3-5.

The crucible was supported on a carriage (figure 3-6) constructed primarily of molybdenum sheet and high purity alumina plate. The carriage was correctly positioned in the furnace tube by molybdenum rods attached to the brass end plate sealing off the end of the furnace tube. These rods also supported the disc heat shields necessary to prevent excessive heat loss down the long axis of the furnace tube. This entire assembly is shown in figure 3-7. The essential features of the carriage are illustrated in figure 3-8. As indicated, the thermocouples passed through holes drilled in the molybdenum heat sinks and abutted against the bowls of the crucible itself. Thus the thermocouple junction was in good thermal contact with the end of the sample in a region of uniform temperature due to the presence of the surrounding heat sink. The thinnest practicable thermocouple wires were used together with thermocouple insulators and sheaths of the smallest possible cross section in order to keep the heat losses from the tip as low as possible. The closed end alumina sheaths covering each thermocouple and its insulators protected the thermocouple wires from attack by vapour from the sample or any other source.

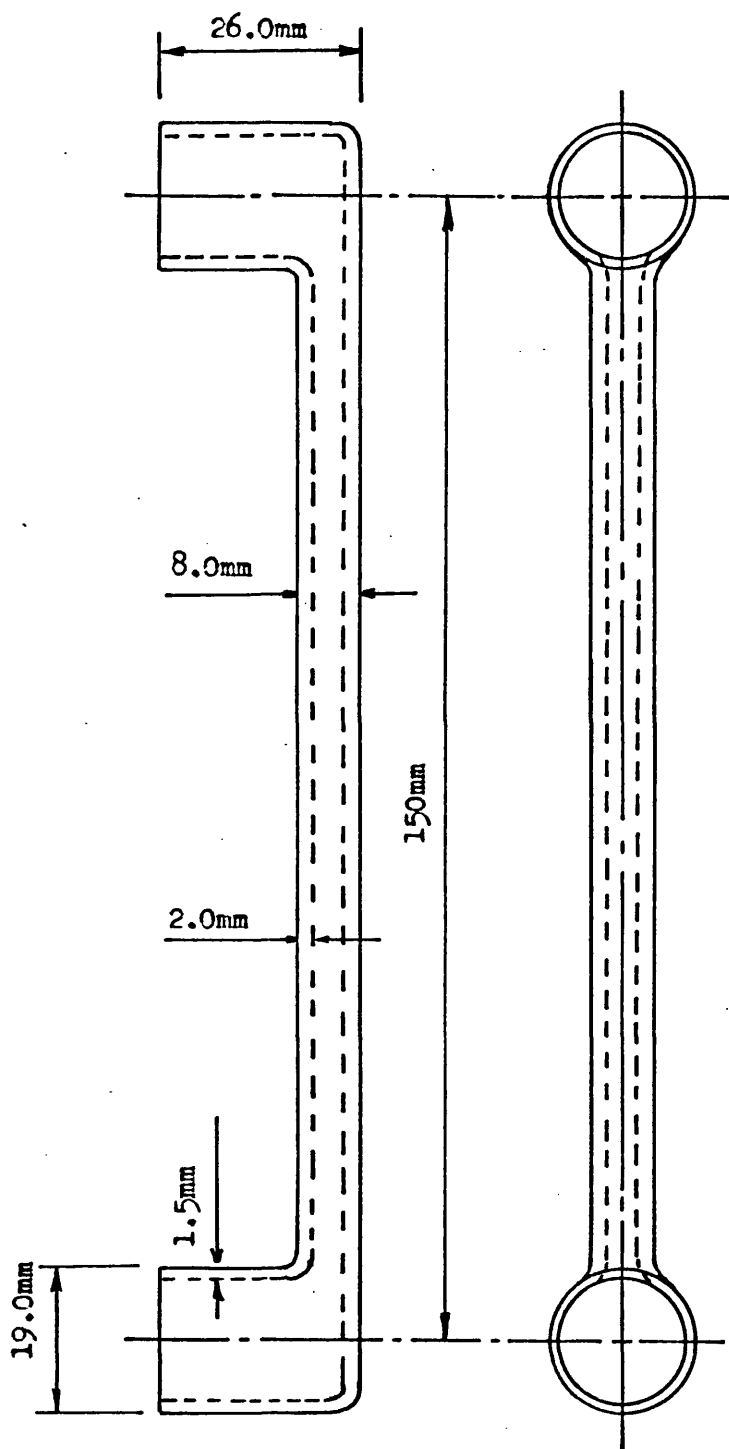


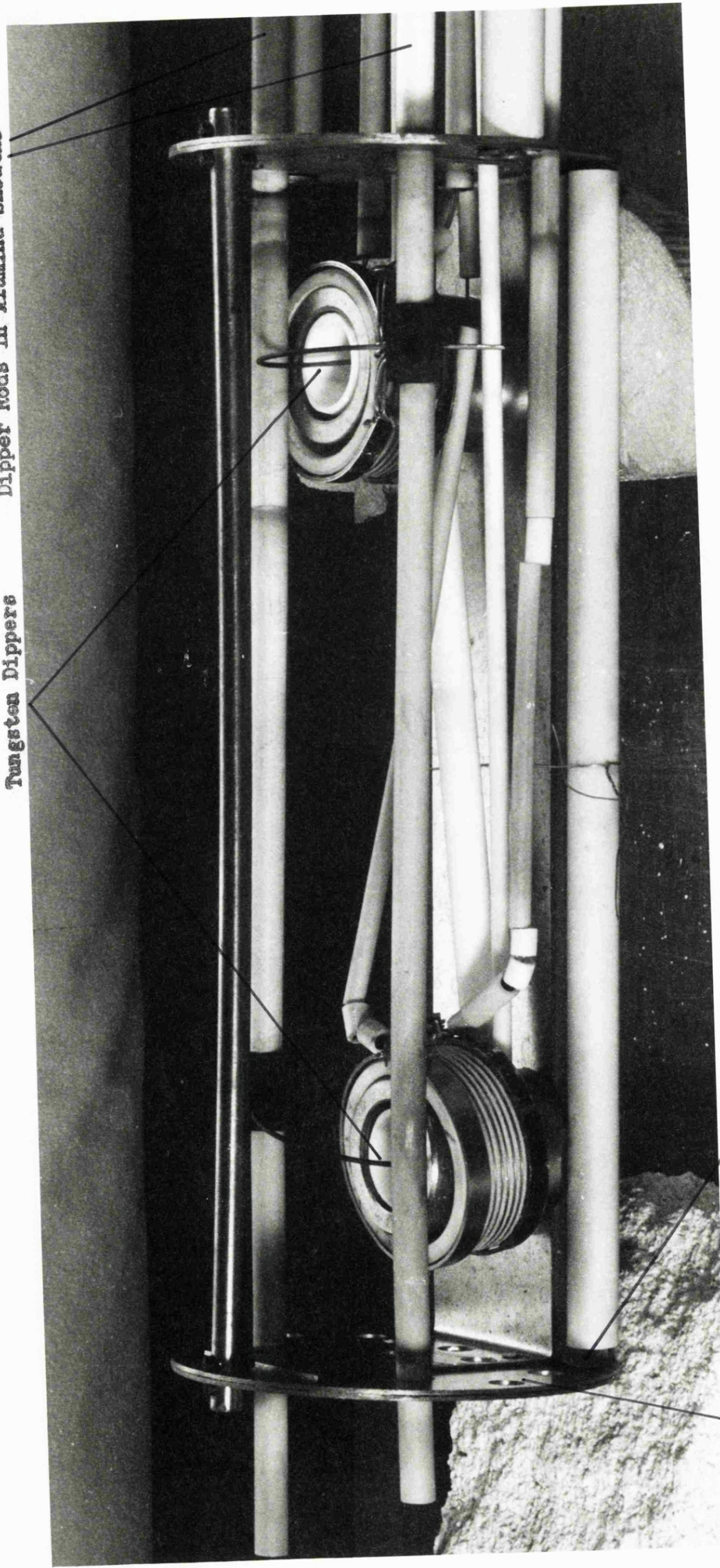
Figure 3-4 The Crucible



Figure 3-5 A Typical Sample After Use

Dipper Rods in Alumina Sheaths

Tungsten Dippers



Alumina Plate

Molybdenum Sheet

The Carriage

Figure 3-6

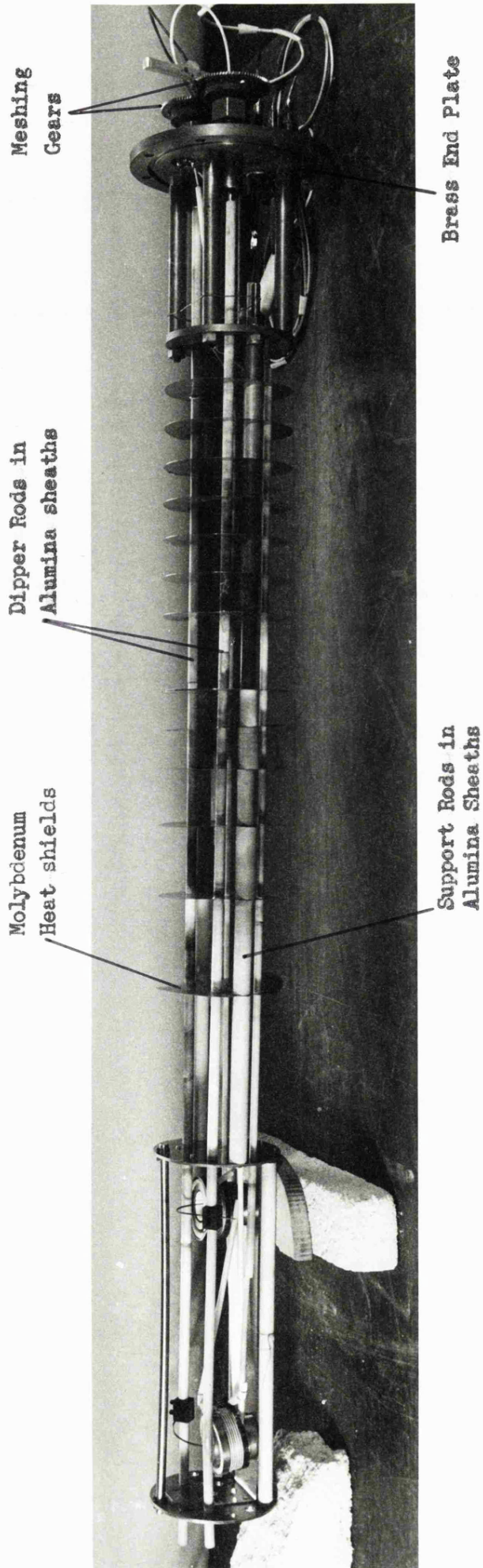


Figure 3-7 The Carriage Assembly

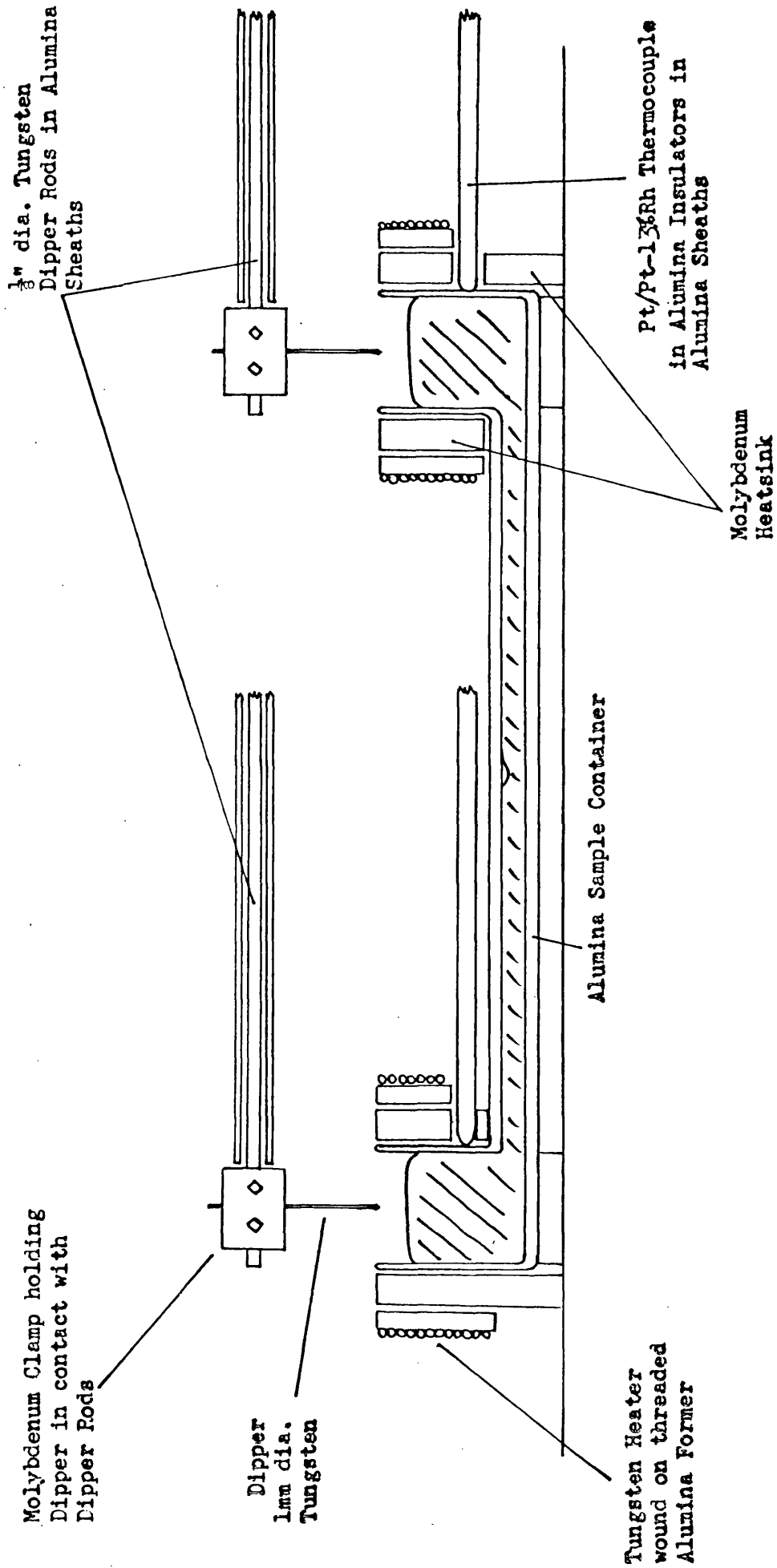


Figure 3-8

Schematic diagram of Carriage Operation

This arrangement was found to be satisfactory although there were some initial difficulties due to the use of heatsinks of inadequate size, heater wires of inadequate surface area and experiment temperatures much too far (120°C or more) above the temperature of the muffle furnace. These faults (which caused excessive element temperatures and large temperature gradients in the region of the sample) were all corrected in the apparatus used for the measurements reported in this thesis.

The tungsten counter electrode wires or 'dippers' are shown in figure 3-6 and figure 3-8. When required, the ends were dipped into the liquid surfaces by rotating the dipper rods. The two meshing gears (shown in figure 3-7) affixed to the outer ends of the tungsten rods ensured that the dippers moved down in synchronism, the ends touching the liquid surfaces simultaneously.

Power for the small difference heaters was derived, via 5 to 1 power transformers for matching the impedances, from mains supplied single phase thyristor power units driven by temperature controllers (type O40 from Eurotherm Ltd.). The feedback for each of these controllers was obtained from the appropriate thermocouple as shown in figure 3-2. These controllers sensed and allowed for not only the difference between the desired and actual temperatures but also the time derivative

and integral of this difference. This enabled the desired temperatures to be achieved speedily. It was thus possible to set and maintain the temperatures at either end of the crucible constant to within 0.2°C . This was normally done with differences of up to $\pm 25^{\circ}\text{C}$; the mean of all temperatures over the course of an experiment being about 40°C above the muffle furnace temperature.

v) Filling the Crucible.

Prior to performing the actual measurements it was necessary to fill the crucible with liquid sample. Solid pieces of the sample were placed in both bowls of the crucible before the carriage was inserted in the furnace tube. With the carriage in place the tube was evacuated and the furnace heated to above the melting point or appropriate liquidus temperature. Argon was then applied to force some of the now liquid sample along the interconnecting tube of the crucible, the two parts meeting and joining near the centre. In the cases of samples with high vapour pressures - i.e. greater than about 10^{-2} torr at the experiment temperature - it was necessary to fill the system with argon during most of the heating process to avoid excessive loss of sample by vaporization. It was then only necessary to evacuate the system to a pressure of about 10 torr for ten minutes before and after melting to ensure filling of the crucible as described.

vi) Signal Measurement and Experimental Procedure.

All signal leads came out through the end plate via various types of feedthrough. The subsequent circuitry is shown in figure 3-2. Ice baths were used to eliminate spurious thermoelectric e.m.f.s wherever it was necessary to make junctions between different metals and to provide a reference temperature for the temperature measurement thermocouples. The various signals for the digital voltmeter (which had an accuracy of ± 1 microvolt) could be selected by means of the switch shown and also reversed in polarity to allow for errors in the zero setting of the voltmeter. The temperature measurement using the thermocouples was straight forward, the measured voltages being interpreted in terms of temperature using the British Standard Tables (B.S. 1826: 1952).

The measurement of the Seebeck e.m.f. for the sample circuit was more difficult since due to the short dipping period the readings of the digital voltmeter had to be recorded very quickly. This was achieved by interconnecting (as shown in figure 3-2) the digital voltmeter and a programmable desk calculator (Wang 600). The digital voltmeter sampled and displayed the voltage at its input every 0.1 second. This information was passed to the desk calculator where it could be stored for later examination. This storage process was

initiated as soon as contact between the dippers and the liquid sample was observed by the characteristic change in the digital voltmeter display. The calculator was also programmed to calculate and print the mean and standard deviation of each series of readings.

From early test experiments it was established that 3 to 4 seconds was an adequate contact period, further contact time giving no significant advantage. In these tests, during the first few tenths of a second after dipping the readings were unstable as the tip of the dipper approached thermal equilibrium with the surrounding liquid. There then followed a period of 70 to 80 seconds in which the reading was constant. After this there began a slow decline in the magnitude of the observed e.m.f. which was attributed to extensive attack and alloying of the dipper by the liquid sample. By the thermoelectric law of intermediate metals, the slight contamination of the dipper tip during the normal short contact period does not significantly affect the Seebeck e.m.f. This is because the contamination occurs only in a (small) region of uniform temperature.

The experimental procedure was as follows:

- (1) Once the sample was molten and the crucible filled as described above the temperatures of the bowl ends of the pipe boat were brought to their required values by means of the two difference heaters and their controllers.

(2) The apparatus was then left for about one hour to ensure complete thermal stability of the sample. Initial test experiments had shown that reproducible results could be obtained after about one quarter of this period had elapsed.

(3) The dippers were lowered until the tips just made contact with the liquid sample.

(4) The desk calculator was instructed to store the digital voltmeter readings.

(5) The dippers were removed after about four seconds.

(6) The desk calculator instructed to print out the mean and standard deviation of the readings.

(7) The measurement was repeated with the polarity of the signal reversed by the selector switch.

The entire process was then repeated for a number of temperature differences, the average of the two temperatures (the experiment temperature, $T_{\text{exp.}}$) always about 40°C above that of the muffle furnace ($T_{\text{muffle.}}$). A graph was then plotted of the Seebeck e.m.f. against the various temperature differences used, the slope giving the difference in the absolute thermoelectric powers of the sample and tungsten counter electrode as in equation 1.1 with figure 1-1. The values for the counter electrode were obtained from the work of Cusack and Kendall (Cusack and Kendall,

1958) noting the confirmation of these values provided by Bradley (Bradley, 1962). The values used are given in table 3-A and figure 3-9.

vii) Errors in the Measurement.

Although not designed to perform highly accurate experiments at temperatures as low as 1100°C, confidence in the overall satisfactory operation of the apparatus and in the thermoelectric purity of the tungsten was afforded by the first complete test experiment which was performed on pure liquid copper. This experiment yielded results in agreement with previously observed values within the experimental error of this measurement. Values are given in Table 3-B.

There are three sources of error in the method of measurement described here:-

(1) Uncertainty in the values used for the thermoelectric power of the counter electrode material, estimated at $\pm 1\mu\text{V}/^\circ\text{C}$. This is not included in any errors shown elsewhere in this thesis, since an error in these values gives rise to a systematic shift of all results.

(2) The statistical scatter in the points of the e.m.f. - temperature difference plot. This is due primarily to errors in the measured temperature difference since it was necessary to determine a small quantity as the difference of two large quantities.

The Absolute Thermoelectric Power of Tungsten (S_w)

Temp. ($^{\circ}$ K)	S_w (μ V/ $^{\circ}$ K)
273	0.13
300	1.07
400	4.44
500	7.53
600	10.29
700	12.66
800	14.65
900	16.28
1000	17.57
1100	18.53
1200	19.18
1300	19.53
1400	19.60
1600	18.97
1800	17.41
2000	15.05
2200	12.01
2400	8.39

Reference: -

Cusack and Kendall, 1958.

TABLE 3-A.

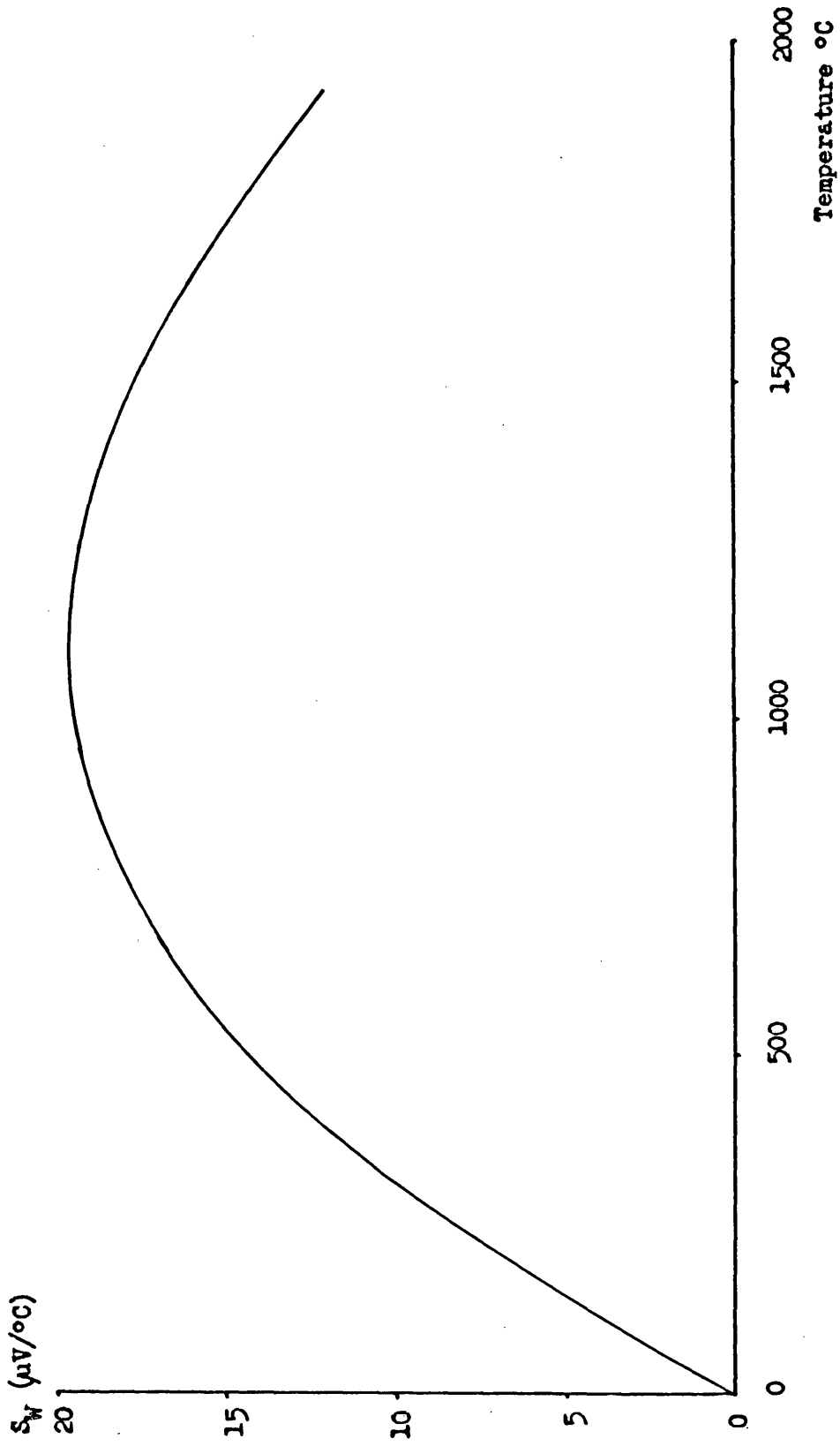


Figure 3-9 The Absolute Thermoelectric Power of Tungsten (S_M)

The Absolute Thermoelectric Power of Liquid Copper
at the melting point. (S_L).

	S_L ($\mu\text{V}/\text{C}$)	Counter Electrode
L	+16.1	Tungsten.
R&S	+17.7	Molybdenum.
RAH	+16.6	Molybdenum.
*	+16 \pm 1	Tungsten.

References:-

L	Lander, 1948
R&S	Ricker and Schaumann, 1966
RAH	Howe, 1967
*	Present Work.

TABLE 3-B.

each with their associated error. In comparison, the contribution resulting from inaccuracies in the measurement of the Seebeck e.m.f. was small, except in the case of some solid samples when difficulty was experienced in obtaining good contact between the dipper ends and the sample surfaces.

(3) There remained a small systematic inaccuracy due to the fact that the thermocouple junctions could not be in perfect thermal contact with the ends of the liquid sample. This was tolerated as a small and predictable phenomenon in preference to the unpredictable and large consequences of thermocouple contamination by sample vapour which would have occurred had the integrity of the thermocouple sheathing been compromised in attempts to improve still further the thermal contact.

In chapter 5 estimates of the combined effect of (2) and (3) are given for each measurement reported.

An estimate of the quantity of tungsten introduced during the course of each experiment was obtained by measurement of the loss from the dippers. In the cases of some of the more expensive palladium alloys the samples were re-used to form further alloys and the contamination was thus partially progressive.

Upper limits of the total level of contamination present in each sample after the measurement are given in Chapter 5. These levels produced no observable effects in the experimental results; a time dependence of the slope of the e.m.f. versus temperature difference graph would be expected.

viii) Sample Details.

The pure metals used in this work, with the exception of palladium, were obtained from Koch-Light Ltd. with a nominal initial purity of 99.998%. The palladium was supplied by Johnson Matthey Metals Ltd. with a purity of better than 99.9%. Typical batch purities reported by the manufacturer for this material were 99.95%.

The alloys used were prepared in a molybdenum wire furnace mounted in a stainless steel vacuum chamber. The constituents were each weighed on a chemical balance to an accuracy of ± 0.002 g and transferred to an alumina crucible in the furnace. After evacuation to 10^{-5} torr for several hours the chamber was filled with argon to a pressure of 1 atmosphere. The sample was heated to at least 100°C above the melting point of the highest melting component element i.e. to more than 100°C above the liquidus at any composition (Figure 3-10 and Hansen, 1958). This temperature was maintained for at least two hours to allow thorough mixing of the constituents before cooling to room temperature. Sophisticated stirring procedures were

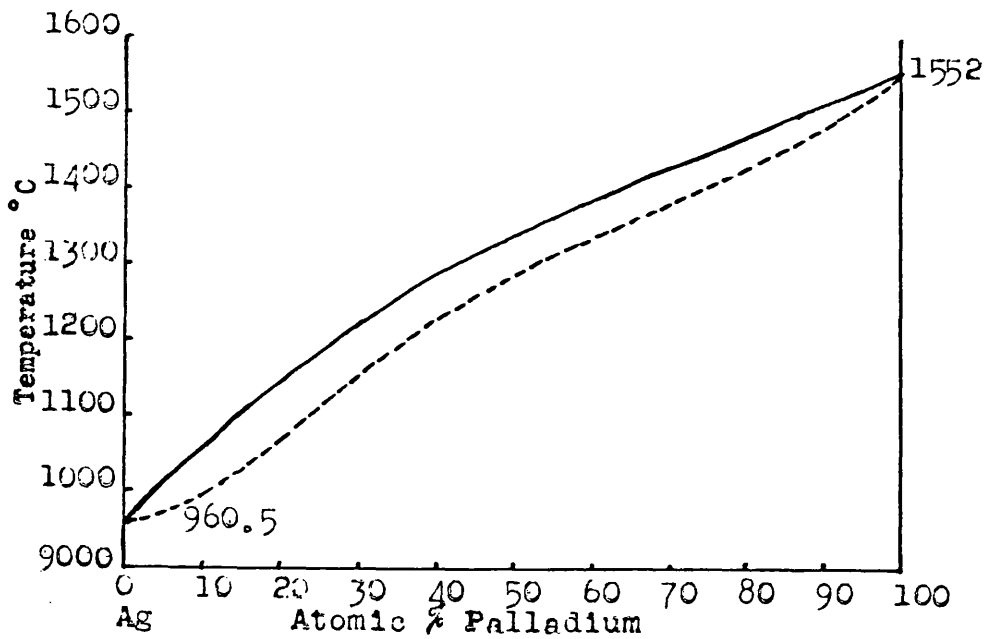
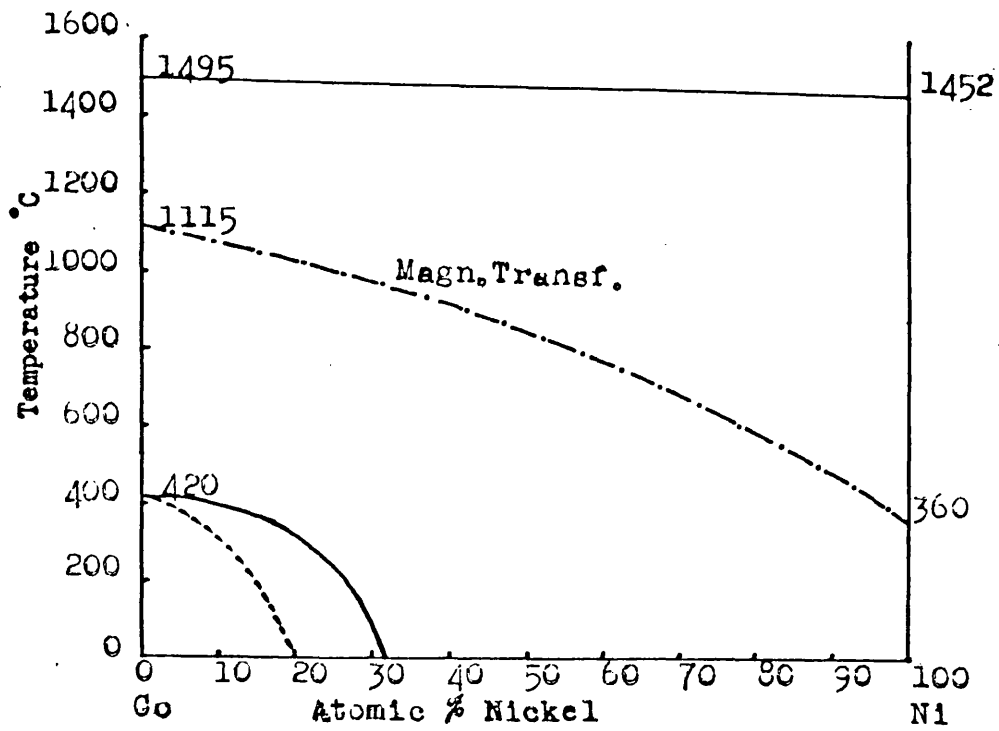


Figure 3-10 Phase Diagrams

not required due to the high temperature and miscibility of the components. To allow for any partial separation on cooling, the alloy ingot was cut into small pieces and suitably mixed before transfer to the thermoelectric power apparatus. No evidence of sample inhomogeneity was observed in the experimental results; the phenomena to be expected are a large zero error in the e.m.f. versus temperature difference graph and irreproducibility in the thermoelectric e.m.f. at each experimental point.

CHAPTER 4. MEASUREMENT OF THE RESISTIVITY.

i) Introduction.

The design and development was undertaken, in conjunction with Professor J. Van Zytveld, of apparatus to facilitate measurements of the resistivity of liquid transition metals.

The problems of contact and containment of the sample were identical to those encountered in the design of the thermoelectric power apparatus so the same materials were used. The resistivity was measured using a four point D.C. technique, the sample being contained in a cylindrical high grade alumina crucible. Electrical contact with the sample was obtained by drawing liquid up the four capillaries of a specially designed alumina probe to meet tungsten wires. The region of overlap was then frozen to prevent continuous corrosion of the tungsten.

A large electrically powered furnace was employed to heat the samples to the required temperatures. The crucible was supported in the hot zone of the furnace by a vertical closed end high purity alumina tube which could be evacuated or filled with an atmosphere of argon as required during the course of an experiment.

ii) The Furnace.

The construction of the furnace is shown in figure 4-1, and is a modification of a furnace which was available in the Physics Department of the

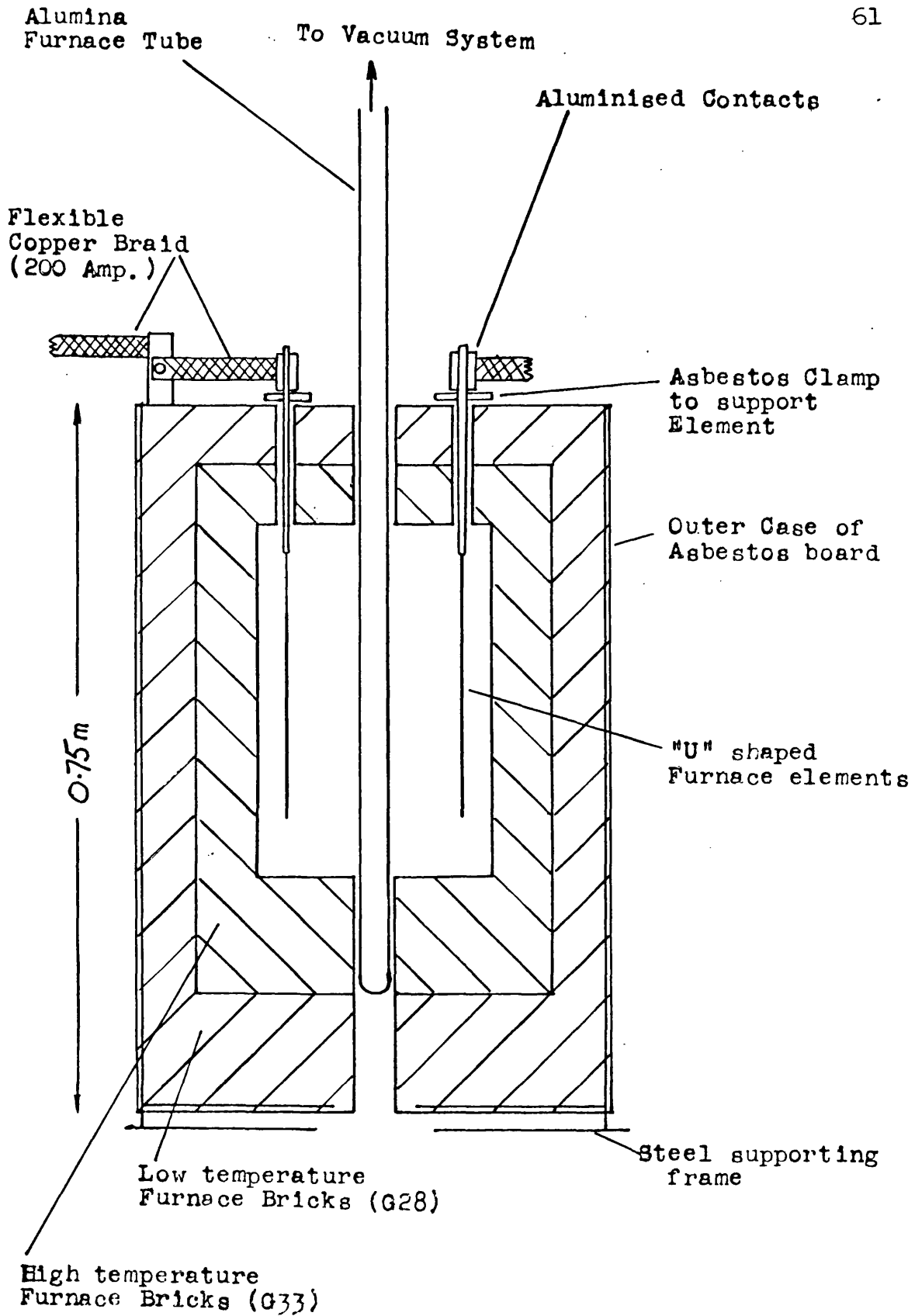


Figure 4-1 The Furnace

University.

The principles of the design are the same as those employed in the construction of the muffle furnace for the thermoelectric power apparatus; identical furnace bricks were used together with the same grade of alumina cement. The heating, however, was supplied by 'U'-shaped Super Kanthal elements (supplied by Hall and Pickles Ltd.). These hung free in the furnace, supported clear of the brickwork by clamps of asbestos affixed to their upper (cool) ends. The use of these elements enabled experiment temperatures of up to 1650°C to be achieved. The annular gap between the furnace tube and the outer furnace bricks was plugged with ceramic fibre to prevent air convection currents passing through the furnace since these would have caused loss of heat and temperature fluctuations.

The four heating elements were connected in series and supplied with electric power of up to 7.2 kilowatts at 190 Amps derived from the mains by a transformer unit, the circuit diagram of which is given in figure 4-2. The power to the furnace was adjusted by means of the variable auto-transformer to achieve the desired furnace temperature. Manual control gave adequate stability: the temperature was allowed to drift at a rate of about 10°C/hour during each individual measurement, the temperature being constant to within 2°C for any one measurement. The sample temperature was determined using a Platinum versus

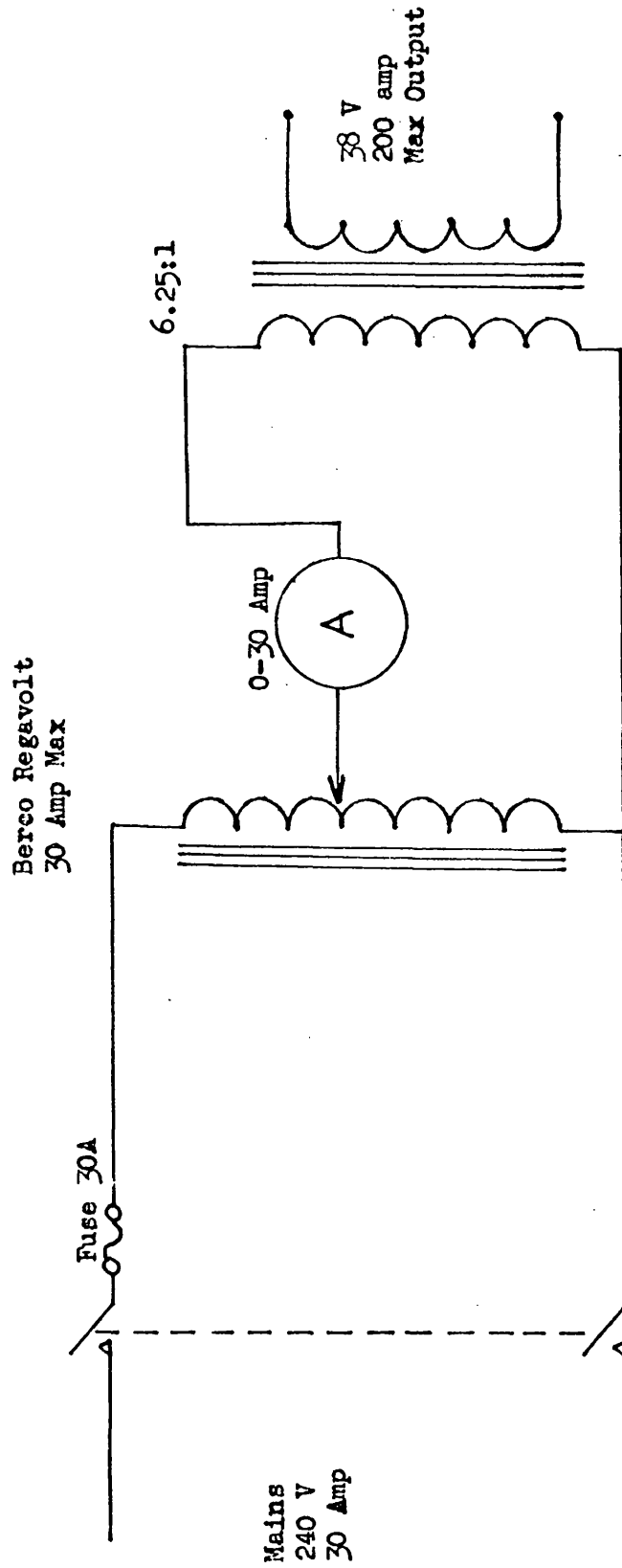


Figure 4-2 The Transformer Unit

Platinum/13% Rhodium thermocouple with the junction a few millimetres above the liquid surface as shown in figures 4-3 and 4-4. The thermocouple wires and associated alumina insulators were surrounded by a single closed end alumina sheath to protect the wires from contamination by sample or other vapour.

The furnace was mounted on an electrically operated lifting device which enabled the furnace to be moved with precision vertically with respect to the sample and furnace tube as required during the experiment. The device was particularly useful during the filling of the probe.

iii) The Specimen.

The arrangement of the various parts of the apparatus, apart from the furnace, is shown in figures 4-3 and 4-4.

The probe was made from an alumina four bore insulator of 4 mm. diameter, the lower end fashioned in the manner shown in figure 4-5 using a diamond impregnated grinding wheel. Thus, with the probe positioned as shown in figure 4-4 and with liquid drawn up the four capillaries to meet the tungsten wires, the necessary four points of contact (A,B,C,D) with the bulk sample were provided. The capillaries leading to A and C were used to pass the primary current for the resistivity measurement while the leads for the measurement of the resulting potential

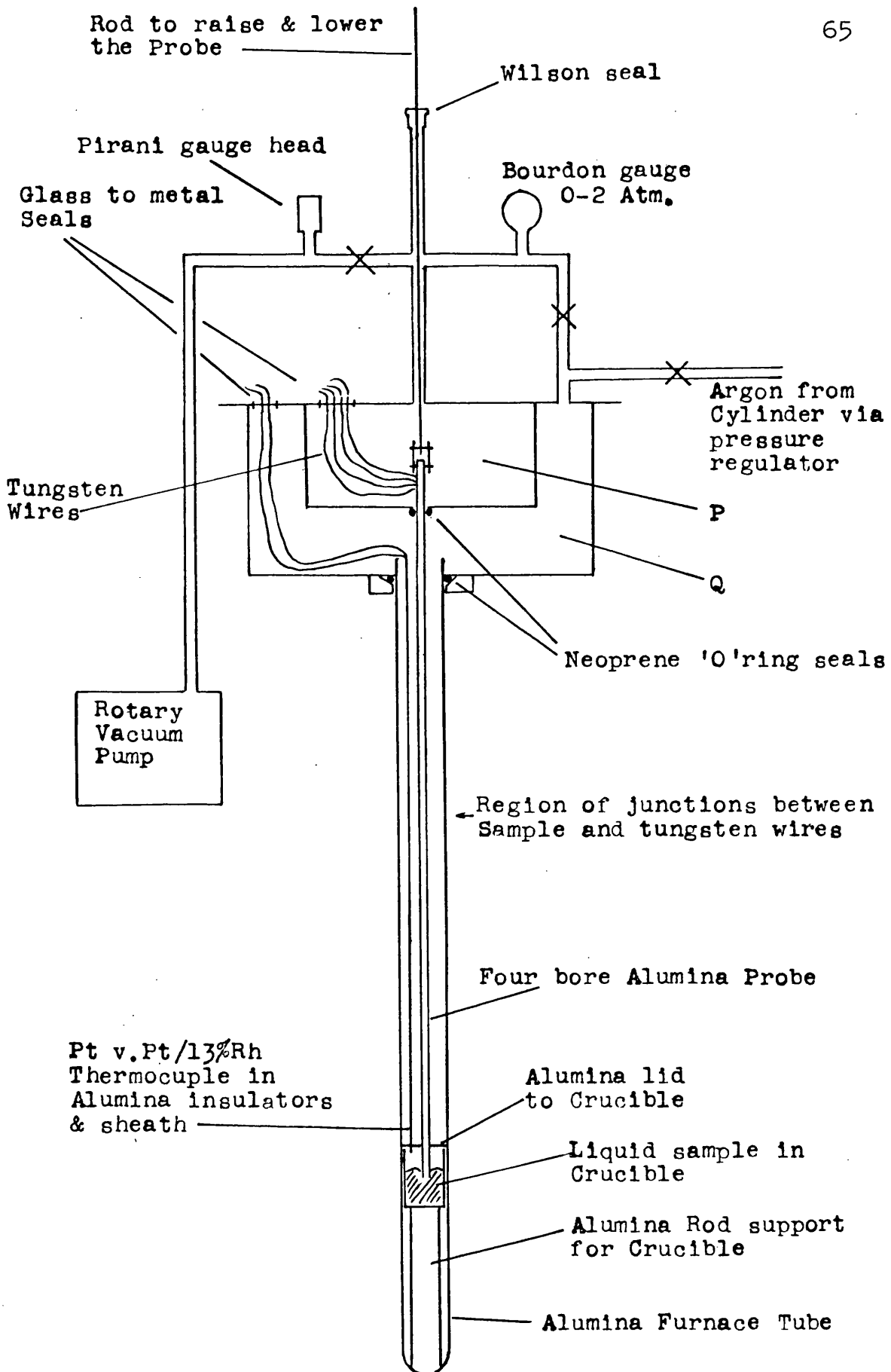


Figure 4-3. Vacuum System and Specimen Arrangement

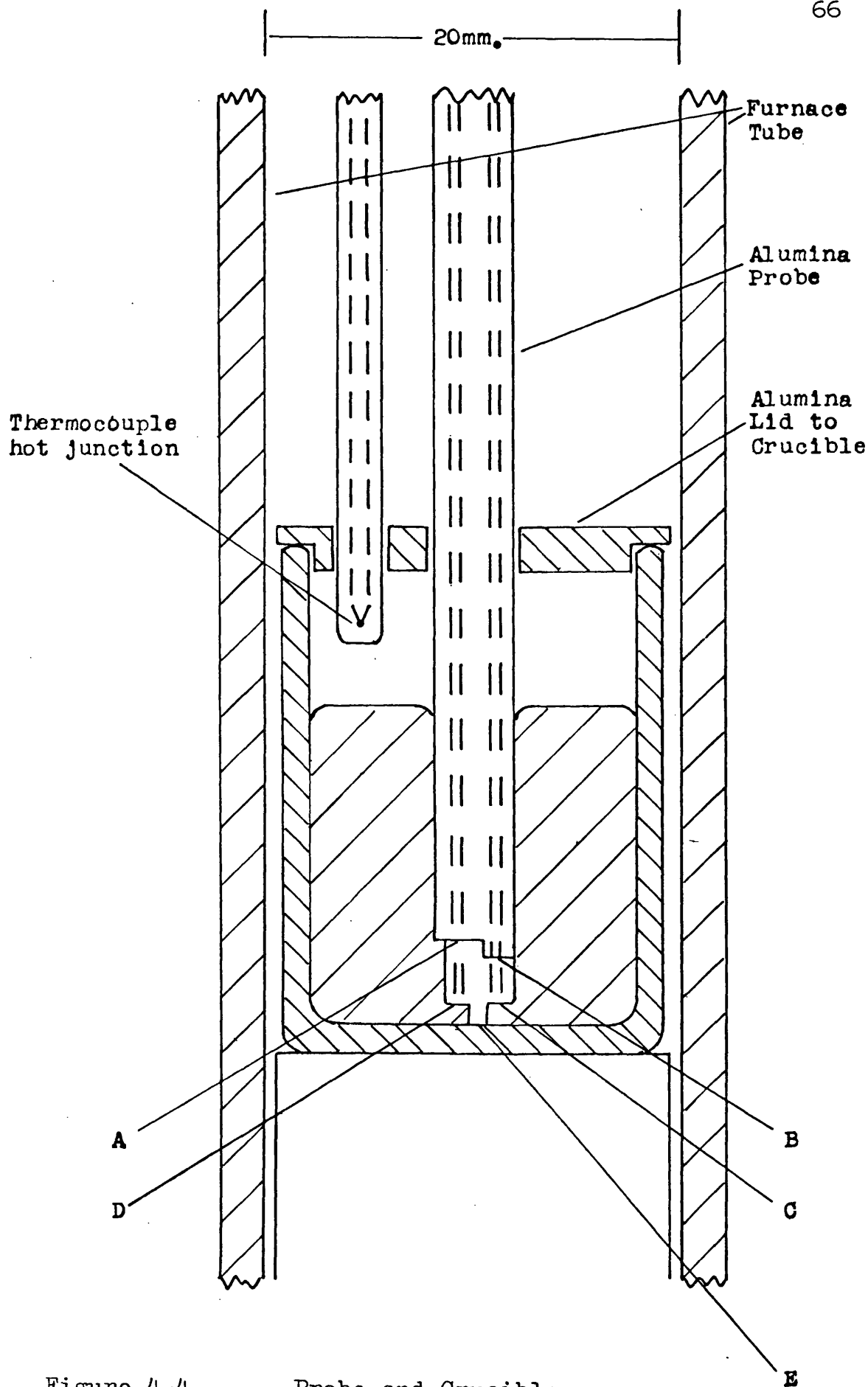


Figure 4-4 Probe and Crucible.

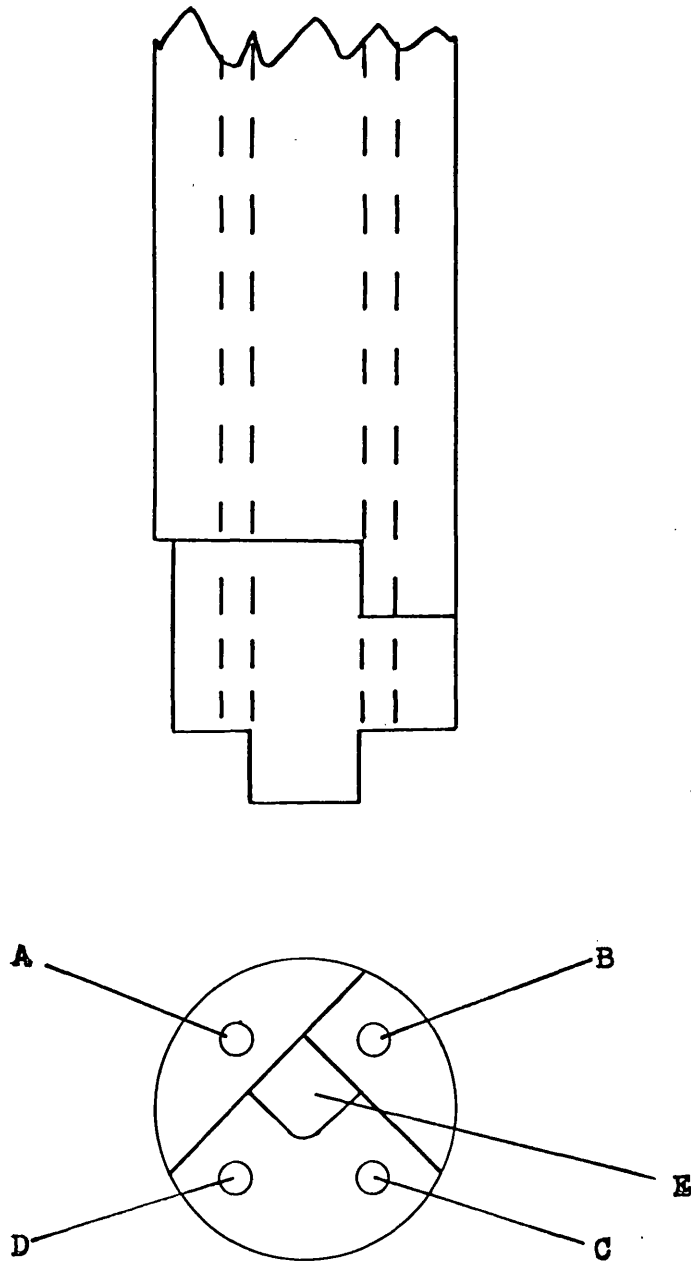


Figure 4-5 Detail of Probe End.

difference were in the capillaries ending at points B and D. The precise design of the end of the probe was arrived at after numerous trials using liquid mercury; the object was to find a geometry giving adequate signal output for reasonable primary currents but having a minimum sensitivity to small displacements of the probe with respect to the crucible. The peg E (figures 4-4 and 4-5) and the lid of the crucible were used to ensure reproducibility in the positioning of the probe in the crucible. The lid was a close fit to both the crucible and the probe. During several trials of this arrangement no variation was detectable between measurements taken before and after removal and replacement of the probe.

Before each high temperature experiment the probe to be used, together with its associated crucible, was calibrated by performing an experiment on doubly distilled mercury at room temperature (95.75×10^{-6} ohm.cm at 20°C). A correction was made to allow for thermal expansion occurring in a high temperature experiment and for this purpose the coefficient of linear expansion of alumina was taken as 8×10^{-6} per $^{\circ}\text{C}$. The probe and crucible were then mounted in the apparatus with the probe raised as far as possible and solid pieces of sample placed in the crucible.

The procedure for filling the probe was then as follows:

- (1) The apparatus was evacuated to

0.02 torr and repeatedly filled with argon and re-evacuated to remove air and water vapour.

(2) The apparatus was then filled with argon to a pressure of 1 atmosphere.

(3) The temperature of the sample was raised at a rate of approximately 250°C per hour as indicated by the thermocouple shown in figures 4-3 and 4-4.

(4) Just before the melting of the sample, the apparatus was evacuated to guard against the inclusion of gas bubbles in the liquid.

(5) An indicated temperature of at least 40°C above the melting temperature of the sample was maintained for not less than thirty minutes to ensure that the sample was molten.

(6) The probe was then slowly lowered into the liquid to the position shown in figure 4-4.

(7) Argon was then introduced into chamber Q only (figure 4-3), the differential pressure thus forced liquid metal up the capillaries of the probe to meet the tungsten wires. Contact with the tungsten occurred in a region (approximately 18cm. above the base of the crucible) where the ambient temperature was well below the melting point of the sample. Thus, that portion of the sample in the region of overlap with the tungsten soon solidified.

The freezing of the overlap region prevented continuous corrosion of the tungsten and also stopped the migration of dissolved tungsten from this region down to the sensitive region at the lower end of the probe. The length of overlap was approximately 1 centimetre.

A pressure of about 1 atmosphere of argon was maintained in chamber Q (figure 4-3) during the course of the measurements to ensure stability of the liquid in the capillaries and crucible. For each sample a test for the presence of significant bubbles in the liquid was performed by observing the potential difference as a function of system pressure, any variation indicating the presence of a cavity and that the measurement was unreliable.

iv) Measurement Circuitry.

The measurement was performed using a current step technique. The use of a method requiring the passage of a continuous current through the specimen was not practicable due to the effects of Peltier heating at the tungsten - sample junctions. By the Peltier effect, the current crossing the junctions in the current leads caused the heating of one junction and cooling of the other. The temperature variations so introduced in this region of the probe affected the junctions in the leads for the measurement of the potential difference and so gave rise to spurious thermoelectric e.m.f.s. Since the Peltier effect is

a reversible phenomenon these spurious e.m.f.s could not be cancelled out by the normal procedure of primary current reversal. However, the temperatures of the junctions in the potential leads change in a gradual manner due to the finite thermal capacity of the junctions and the non-infinite thermal conductivity of the alumina probe. Thus if a current step of the form shown in figure 4-6(a) is applied to the sample, the voltage across the potential difference leads is of the form shown in figure 4-6(b). The voltage change at the instant t' is not affected by the spurious thermoelectric effects mentioned. In the method employed, this voltage change was noted by monitoring the voltage for a few seconds before and after the instant t' .

The measurement circuitry employed is shown in figure 4-7. As in the thermoelectric power apparatus described in Chapter 3, the digital voltmeter (with an accuracy of ± 1 microvolt) samples the voltage at its input every 0.1 second and this information is passed to the Wang desk calculator for storage and analysis.

The primary current was supplied by the constant current power supply unit (Coutant LA400.2). This particular unit was chosen from those available for its good response to sudden loading. With the apparatus shown in figure 4-7, there was no detectable difference between the output current 0.2 seconds

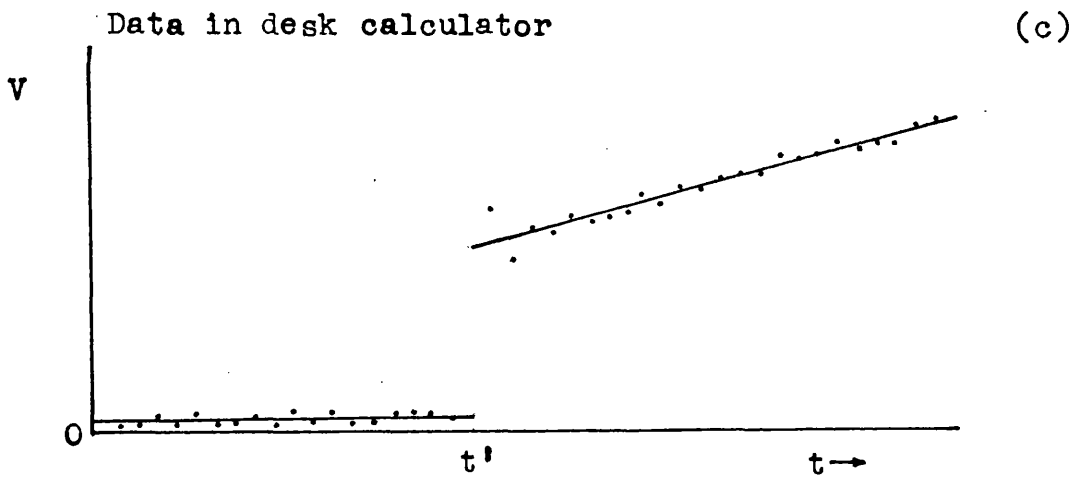
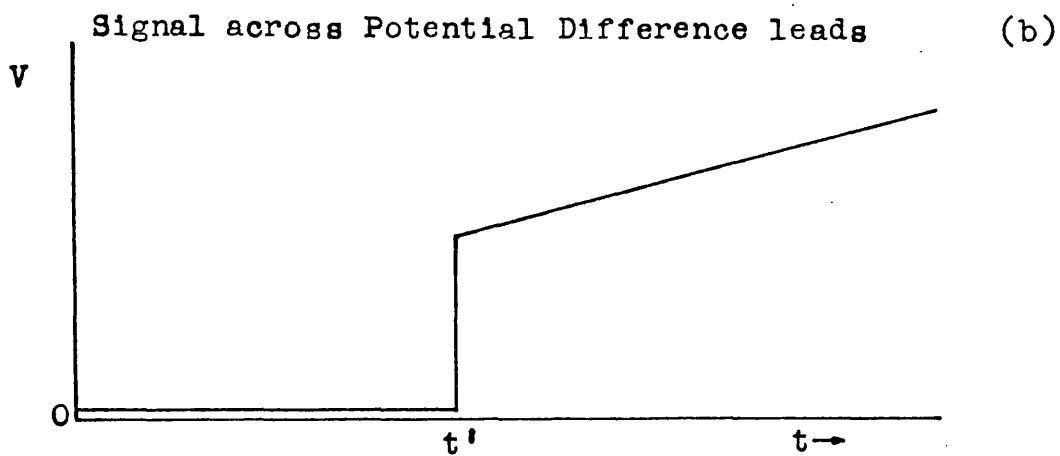
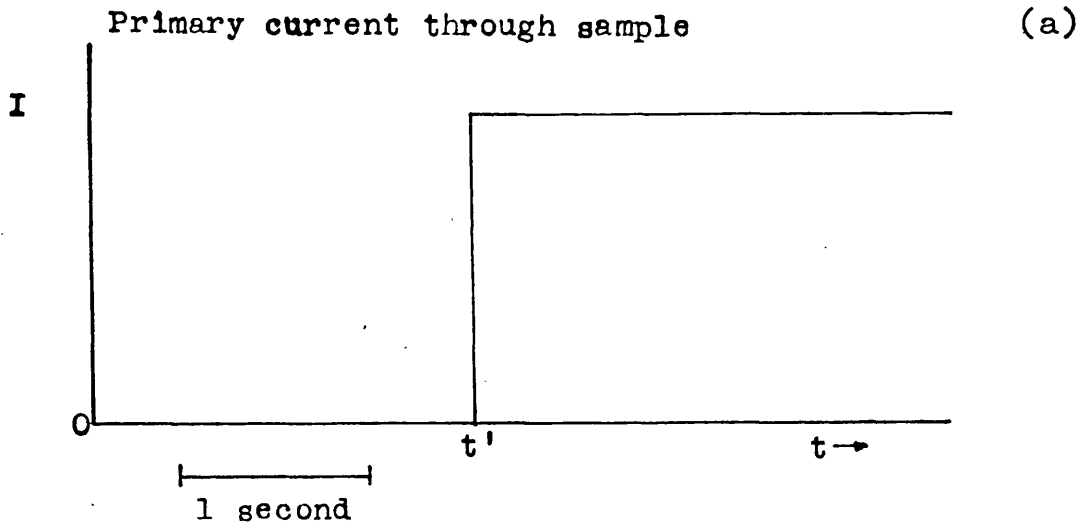


Figure 4-6

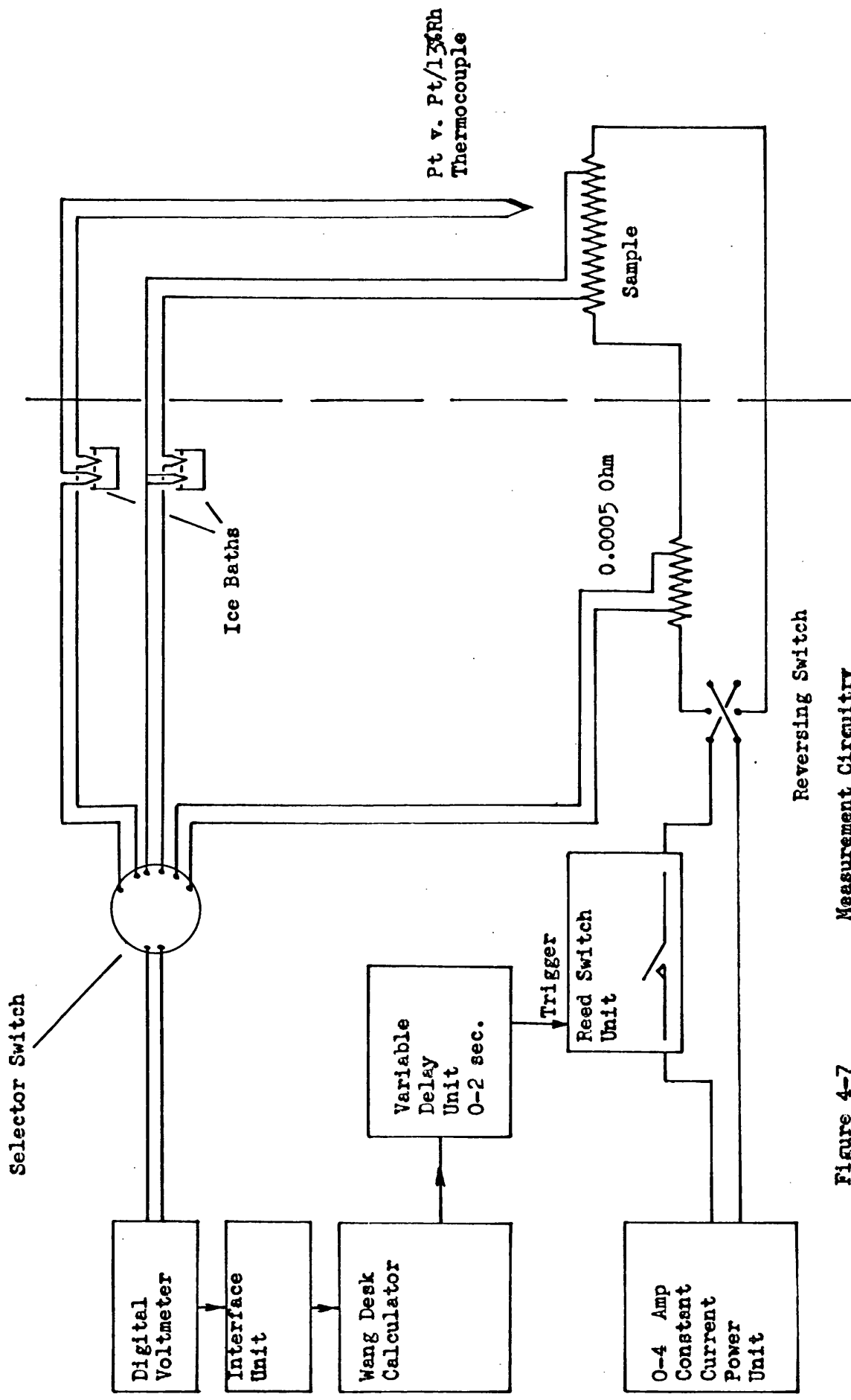


Figure 4-7 Measurement Circuitry

after the circuit was completed and the steady state current level. The reproducibility of the output current was such that there was no detectable variation between successive completions of the primary current circuit.

When readings were to be taken, the signal from the potential difference leads to the sample was selected by means of the switch shown (figure 4-7). Upon a command from the operator, the desk calculator commenced the acquisition of the information from the digital voltmeter and sent a trigger pulse to the electronic delay unit. After a delay of about two seconds, the trigger pulse caused the switch unit to complete the primary current circuit. Thus the points before and after time t' shown in figure 4-6(c) were stored in the desk calculator. The first two points after the instant t' were unreliable due to the imperfect transient response of the digital voltmeter and the current supply unit. The calculator was programmed to fit two straight lines by the method of least squares to the two portions of the graph as shown in figure 4-6(c) neglecting the first three points after time t' and thus to calculate the voltage change at the instant t' . After a reading, the primary current circuit was broken manually at the switch unit and the unit reset for another measurement.

This procedure was repeated with the current reversed by means of the switch shown in order to allow for spurious e.m.f.s other than those mentioned

above. The measurement of the primary current was straightforward using the digital voltmeter and shunt. Typically, currents of between one and two amperes were used giving voltages of the order of $100\mu\text{V}$ across the potential difference leads to the sample.

Before each measurement the apparatus was allowed to stabilize for at least ten minutes, a temperature change of 2°C in this period being the maximum tolerated. The temperature was noted immediately before and after each measurement and the mean of the two values used to determine the necessary correction for the thermal expansion of the probe and cell.

v) Errors.

The error inherent in this method of measurement of resistivity is difficult to quantify but is estimated at 3 per cent. The primary contributions to the error are possible movement and distortion of the probe and cell at high temperature and uncertainty in the determination of the voltage step as described above. This latter contribution is due both to the scatter in the points of figure 4-6(c) and the uncertainty in the time t' (this is not greater than ± 0.1 second).

Although the apparatus was designed for liquid state experiments and so not particularly suited to determining accurately the resistivity of solid metals, an experiment was performed at high temperature on pure solid palladium. The results obtained were

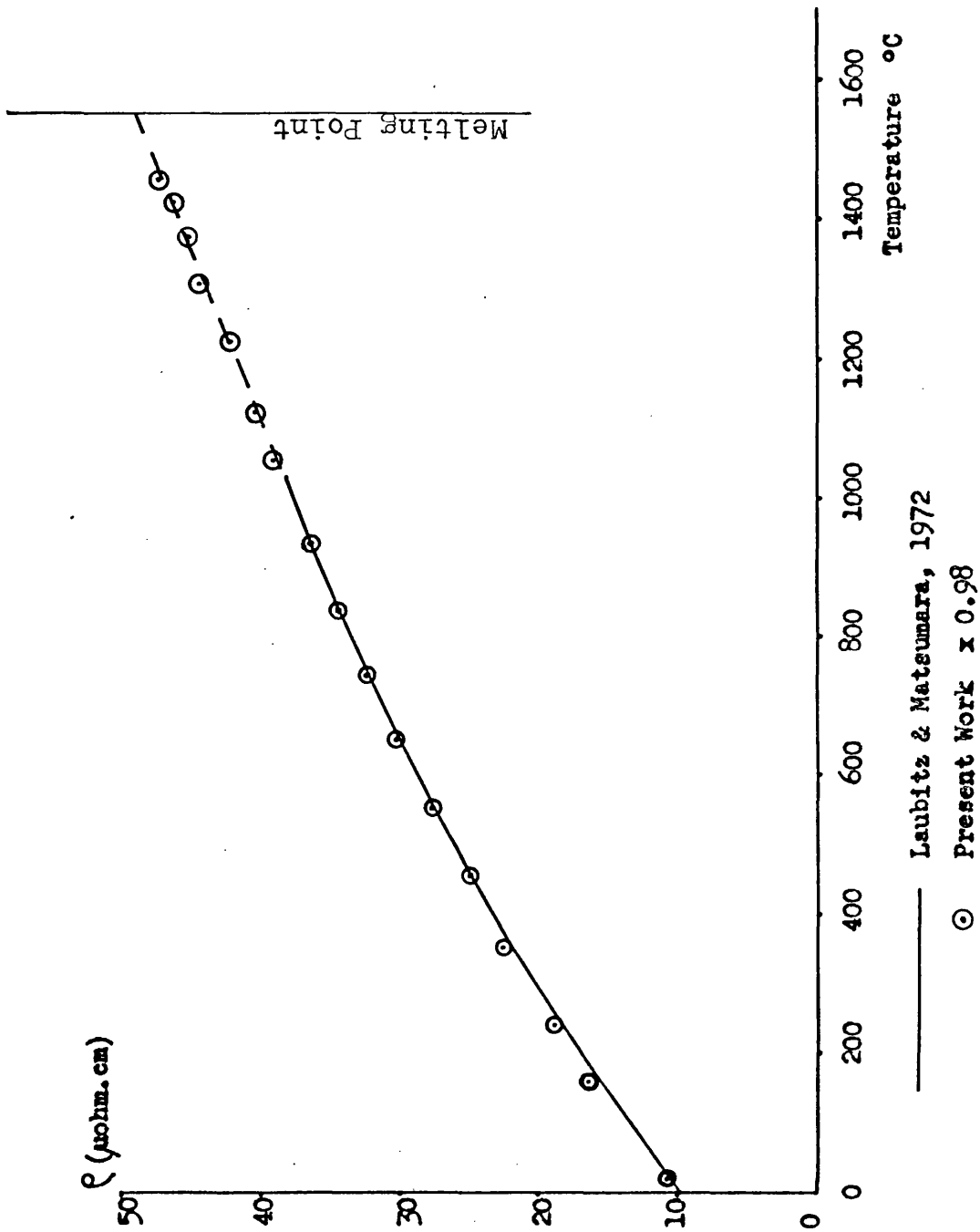


Figure 4-8 Resistivity of Solid Palladium (ρ).

2 per cent above the most recent data (Laubitz and Matsumara, 1972). For the purpose of comparison, the results for this solid state experiment only were normalized by a multiplicative correction of 0.98 to the more accurate solid data. This comparison is shown in figure 4-8.

The sample materials used in the resistivity measurements were obtained from the same suppliers and in the same grades of purity as described in Chapter 3. After the experiments on each sample, the probe was broken to expose the region of overlap between the sample and fine tungsten wires. From examination of this region the contamination of the bulk sample was estimated as less than 0.01 atomic per cent in each case.

CHAPTER 5. EXPERIMENTAL RESULTS.i) Thermoelectric Power of Pure Transition Metals.

Thermoelectric power measurements have been performed on the liquid transition metals nickel, cobalt, iron and palladium in an attempt to confirm and extend the initial results of Howe and Enderby (1973). A few resistivity measurements were also made to provide some comparison with the work of various Russian authors whose results were obtained using an indirect eddy current technique.

The metals investigated, some of which have a general technological importance, were selected from the range of transition metals for their lower melting points (and thus greater experimental accessibility) and also because of the recent theoretical interest in and prediction of their electronic properties (Chapters 2 and 6).

Graphs of the Seebeck e.m.f. versus the temperature difference across the sample are shown in figures 5-1 to 5-7. The first experiments performed on the pure liquids (other than palladium) were rather inaccurate due to inexperience in the use of the apparatus and so were repeated. The experiments on palladium were delayed until sufficient expertise in the manipulation of the apparatus had been obtained.

The results for the pure metals are summarised in Table 5-A. The temperature given in column 3 is the mean temperature of the sample during the

Seebeck e.m.f.
Liquid Nickel v. Tungsten
at 1489°C

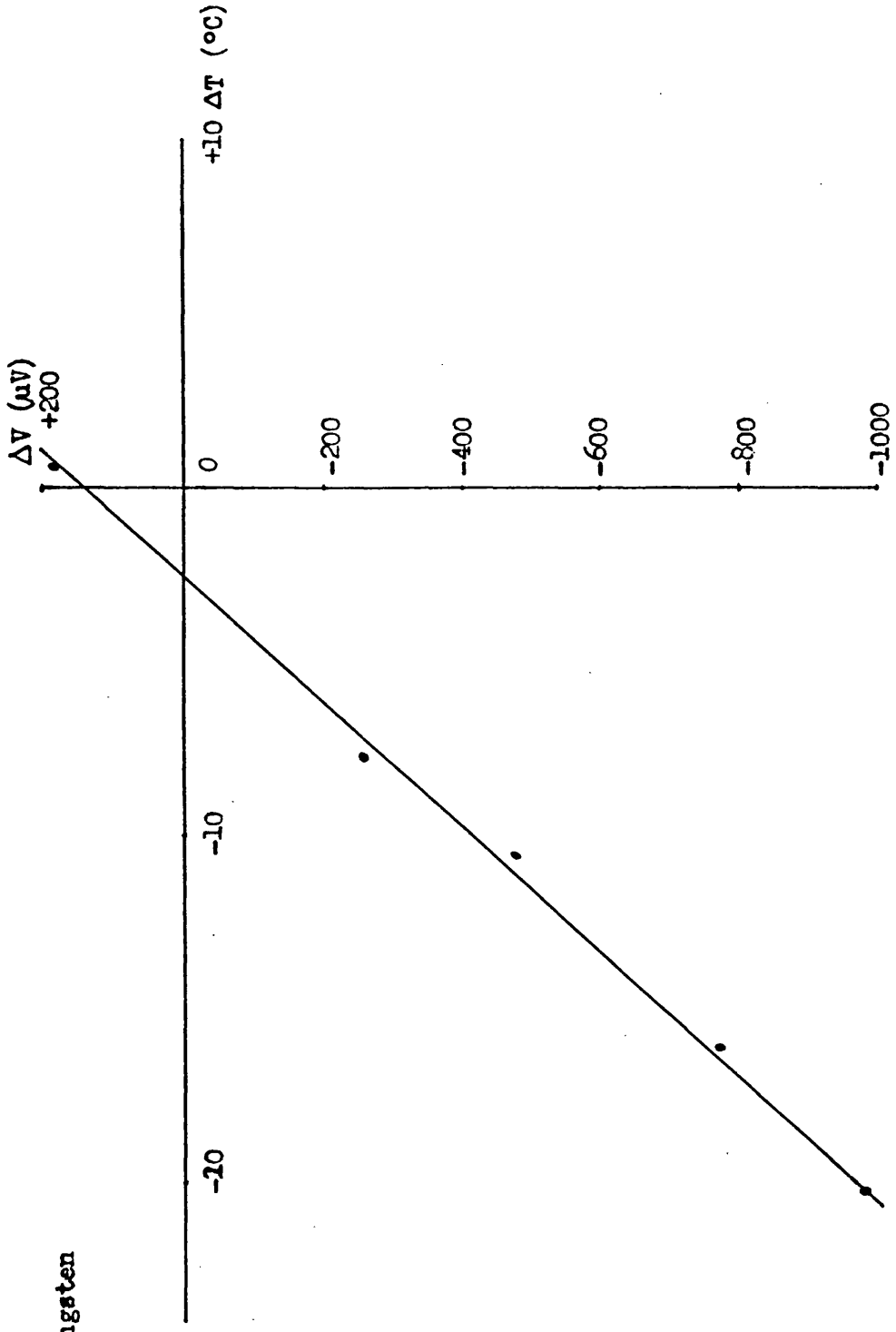


Figure 5-1

Seebeck e.m.f.
Solid Nickel v. Tungsten
at 1395°C

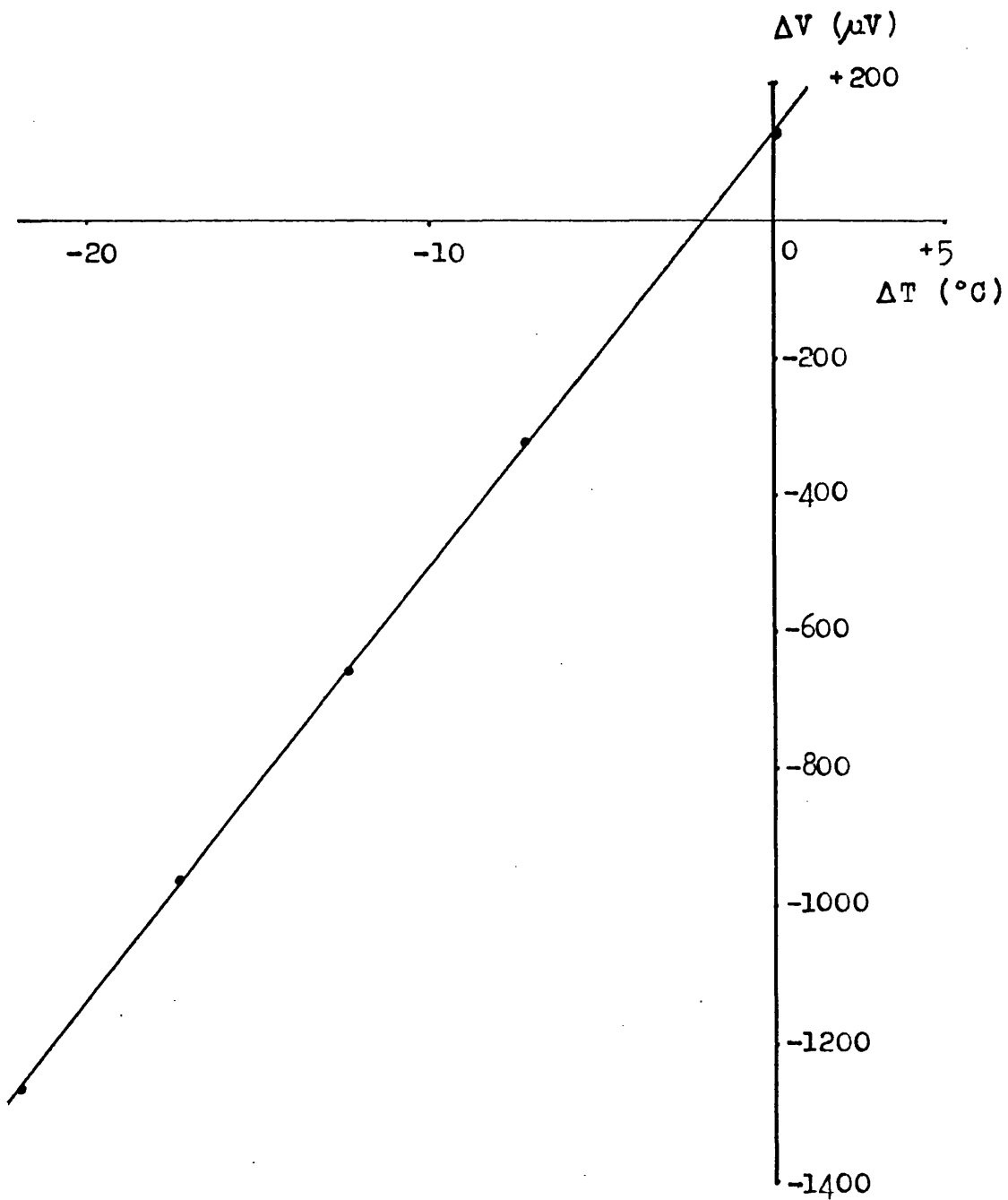


Figure 5-2

Seebeck e.m.f.
Liquid Cobalt v. Tungsten
at 1529°C

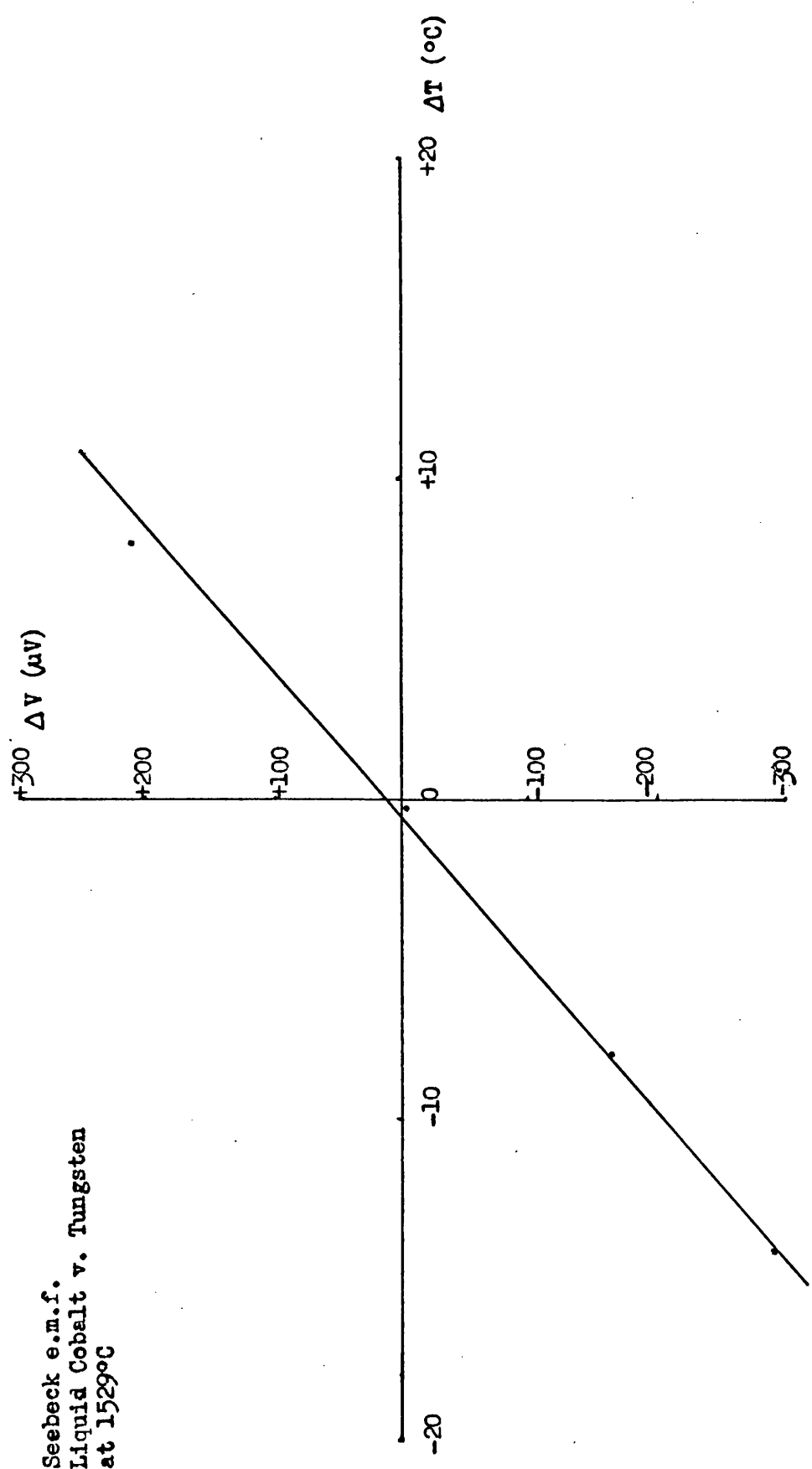


Figure 5-3

Seebeck e.m.f.
Solid Cobalt v. Tungsten
at 1435°C

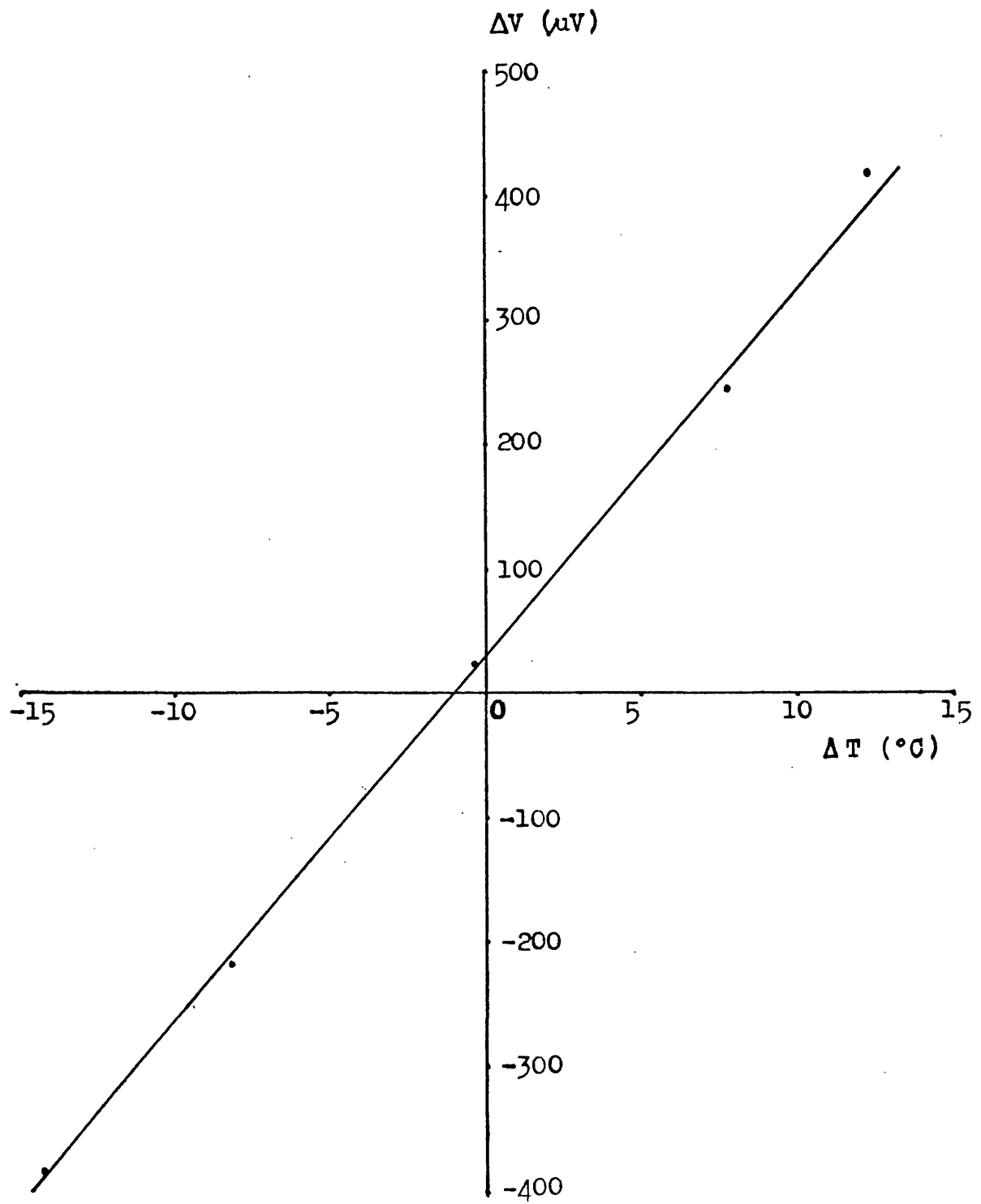


Figure 5-4

Seebeck e.m.f.
Liquid Iron v. Tungsten
at 1567°C

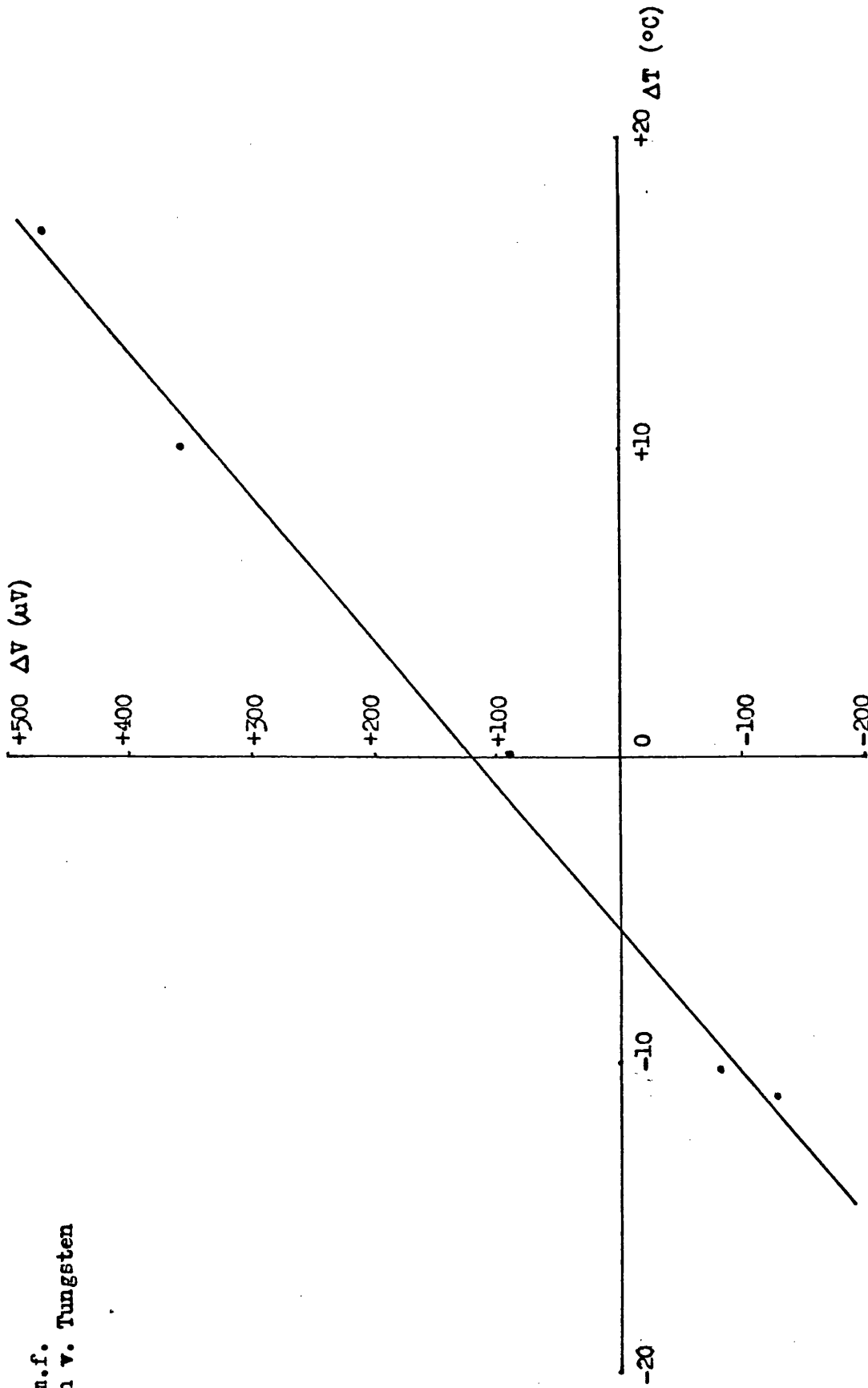


Figure 5-5

Seebeck e.m.f.
Solid Iron v. Tungsten
at 1480°C

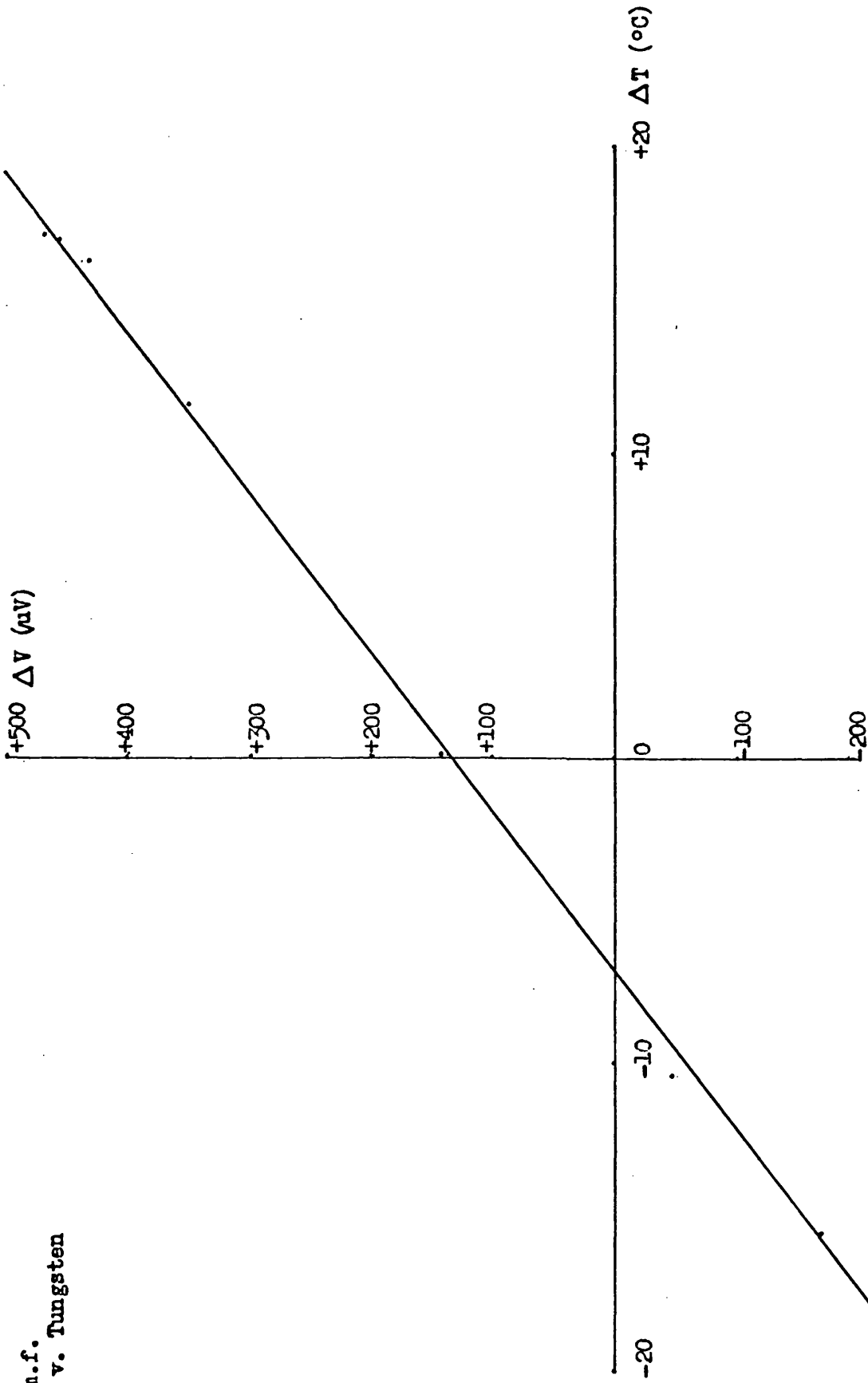


Figure 5-6

Seebeck e.m.f.
Liquid Palladium v. Tungsten
at 1581°C

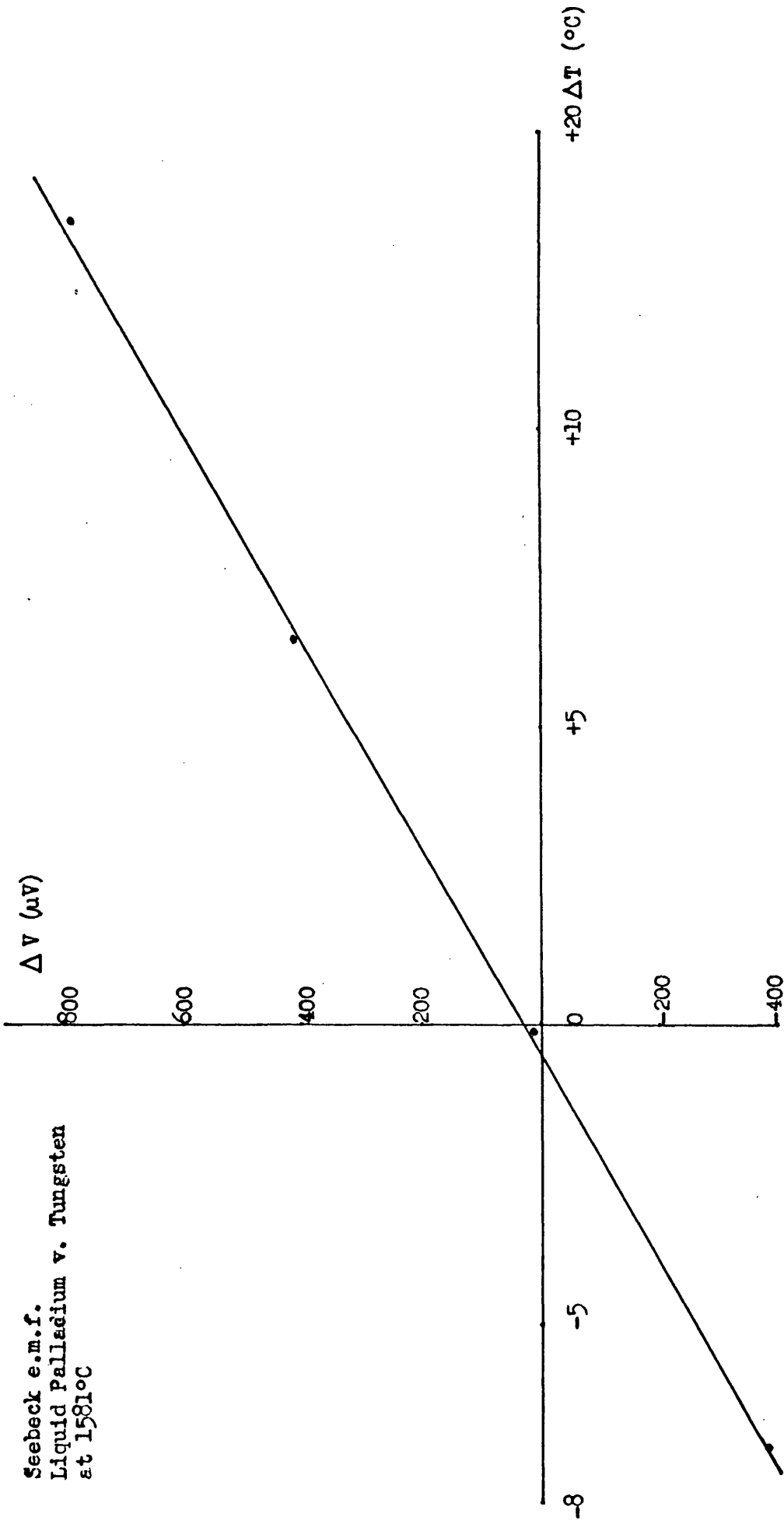


Figure 5-7

(1) Sample	(2) Melting Temperature (°C)	(3) Experiment Temperature (°C)	(4) Slope of e.m.f. v. temp. diff. graph ($\mu\text{V}/^\circ\text{C}$)	(5) Abs. Th. Power of Sample S ($\mu\text{V}/^\circ\text{C}$)	(6) Estimated Error in S ($\mu\text{V}/^\circ\text{C}$)	(7) Upper limit to Contamination level (atomic %)
Liquid Nickel	1453	1489	+55.6	-38	± 3	0.31
Solid Nickel	1453	1395	+62.8	-44	± 3	0.31
Liquid Cobalt	1492	1529	+21.8	-4	± 2	0.29
Solid Cobalt	1492	1435	+28.7	-10	± 2	0.29
Liquid Iron	1539	1567	+21.2	-4	± 2	0.41
Solid Iron	1539	1480	+19.1	-1	± 1	0.41
Liquid Palladium	1552	1581	+57.4	-41	± 3	0.2

TABLE 5-A.
Thermoelectric Power of Transition Metals.

course of the measurements. Column 6 gives the estimated error in the value of the absolute thermoelectric power from the sources (2) and (3) mentioned in Chapter 3(vii). Column 7 gives upper limits to the level of tungsten contamination present in the sample at the completion of the relevant measurements, determined in the manner described in Chapter 3(vii).

The results for pure transition metals are shown in figures 5-8 to 5-11 together with any available liquid data and some high temperature solid data for comparison. In the cases of nickel and cobalt there is agreement with the other data both in the liquid and solid states. For iron the situation is not clear as the errors are comparable with the small values of the absolute thermoelectric power. The consensus of values obtained at somewhat lower temperatures (Verdernikov, 1969) indicates that at least for γ iron, the results of Verdernikov are the more reliable. It is unlikely that the discrepancy between the results of Goetz and those of Verdernikov is due to errors in the values used for the reference materials since this discrepancy changes sign at the γ - δ phase transformation. It appears that the absolute thermoelectric power of iron becomes more negative on melting, but this is not certain.

Absolute Thermoelectric Power (S) of Nickel

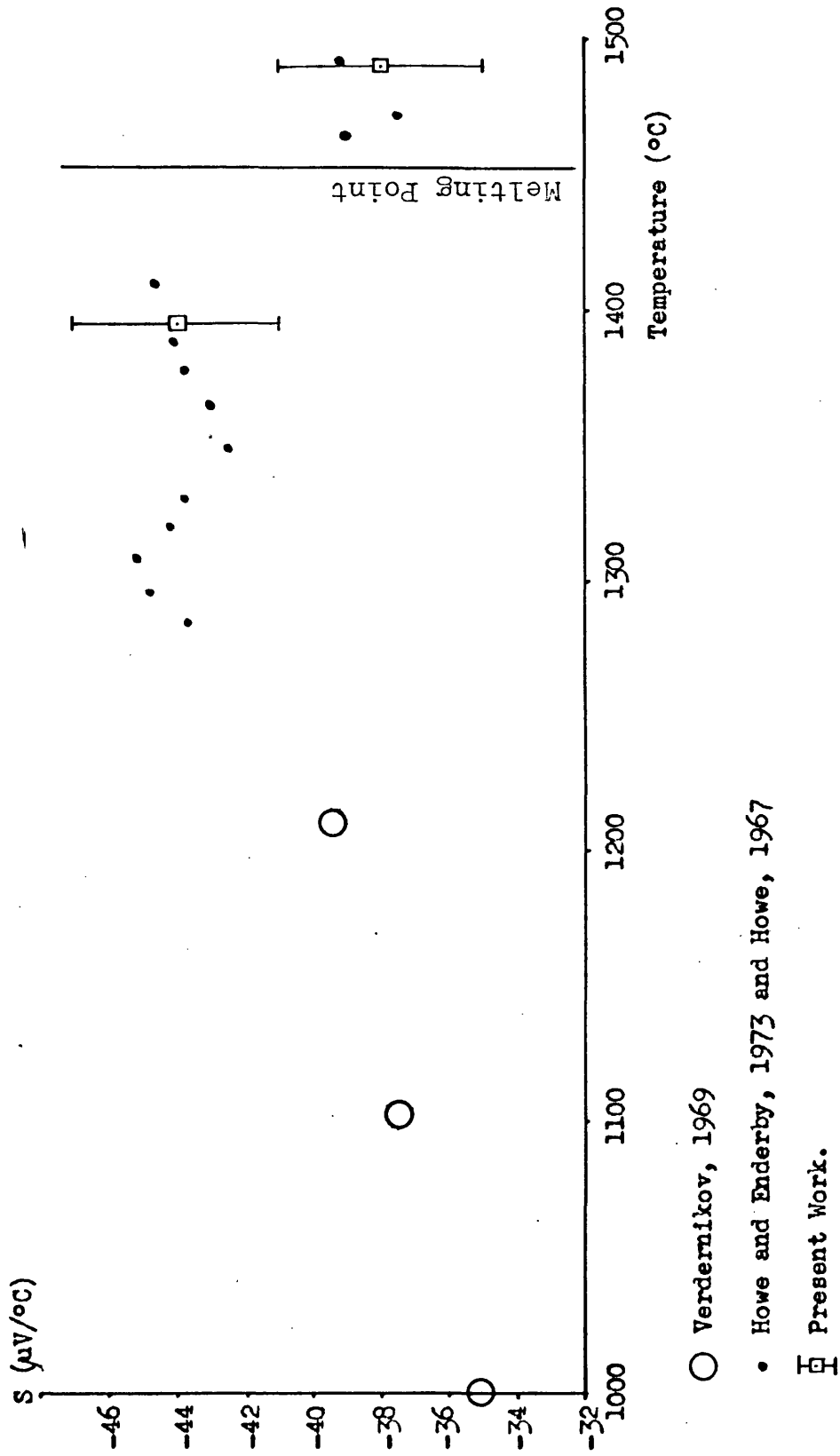
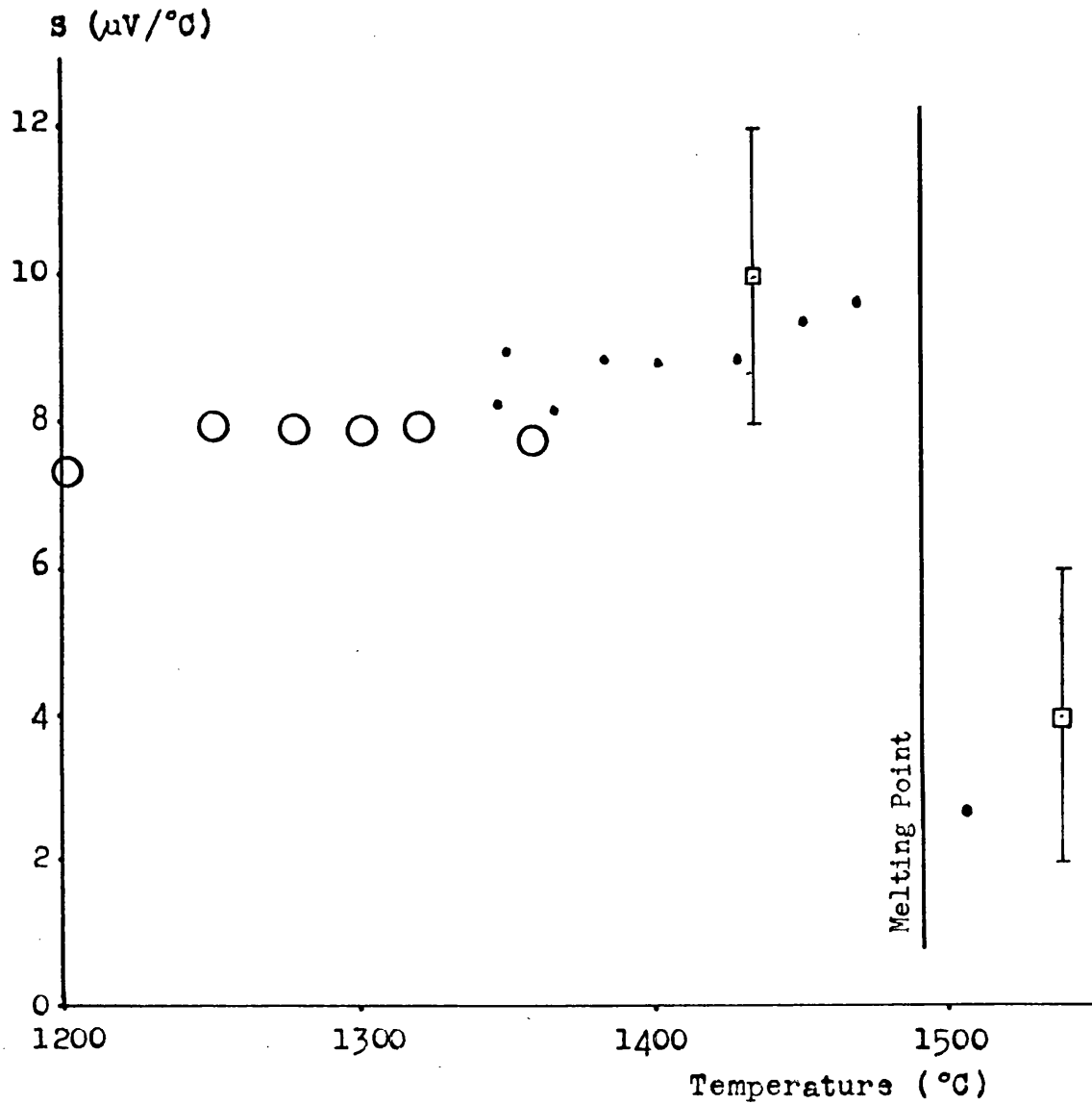


Figure 5-8



- Verdernikov, 1969
- Howe & Enderby, 1973
- Present Work.

Figure 5-9

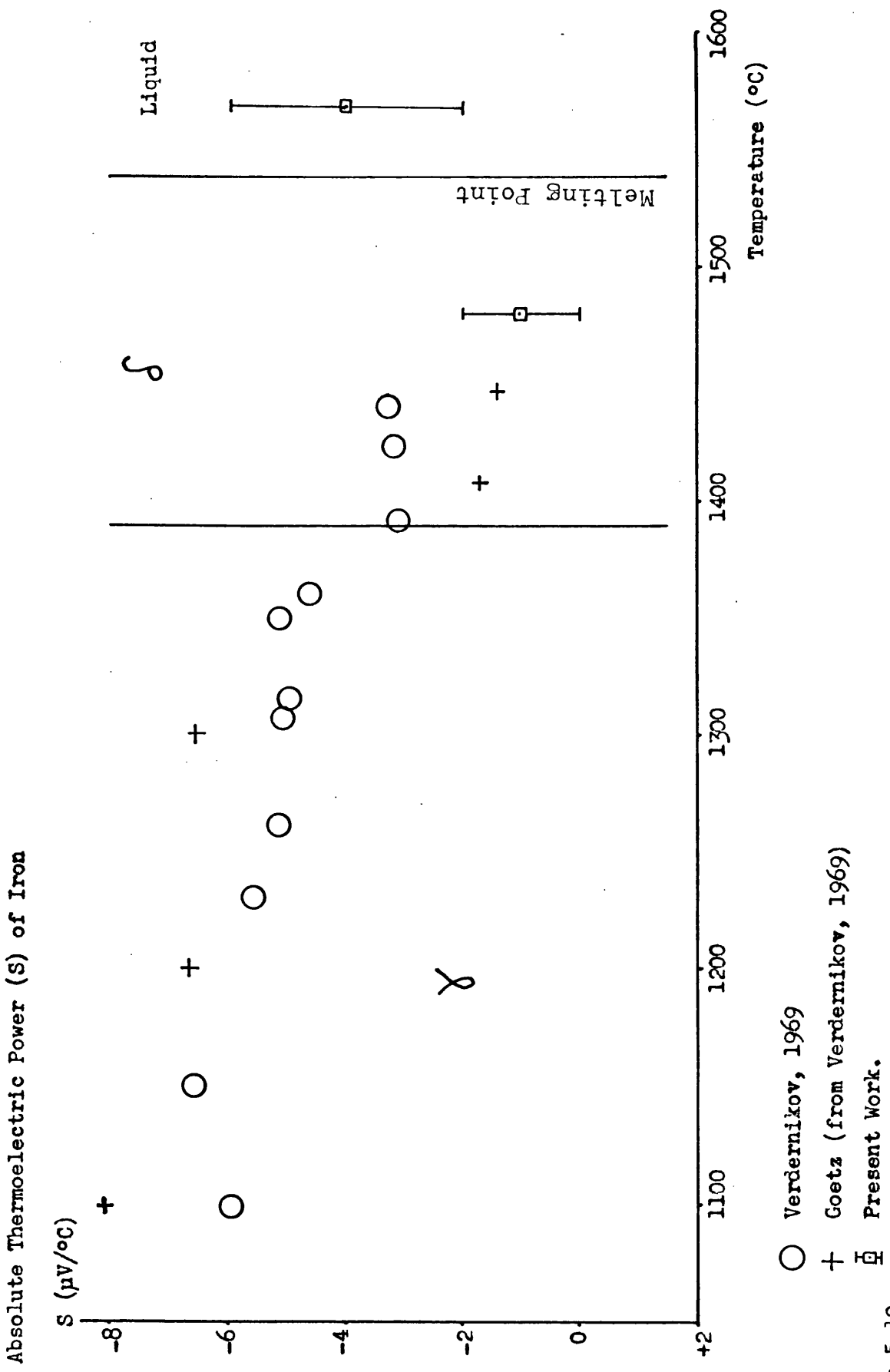


Figure 5-10

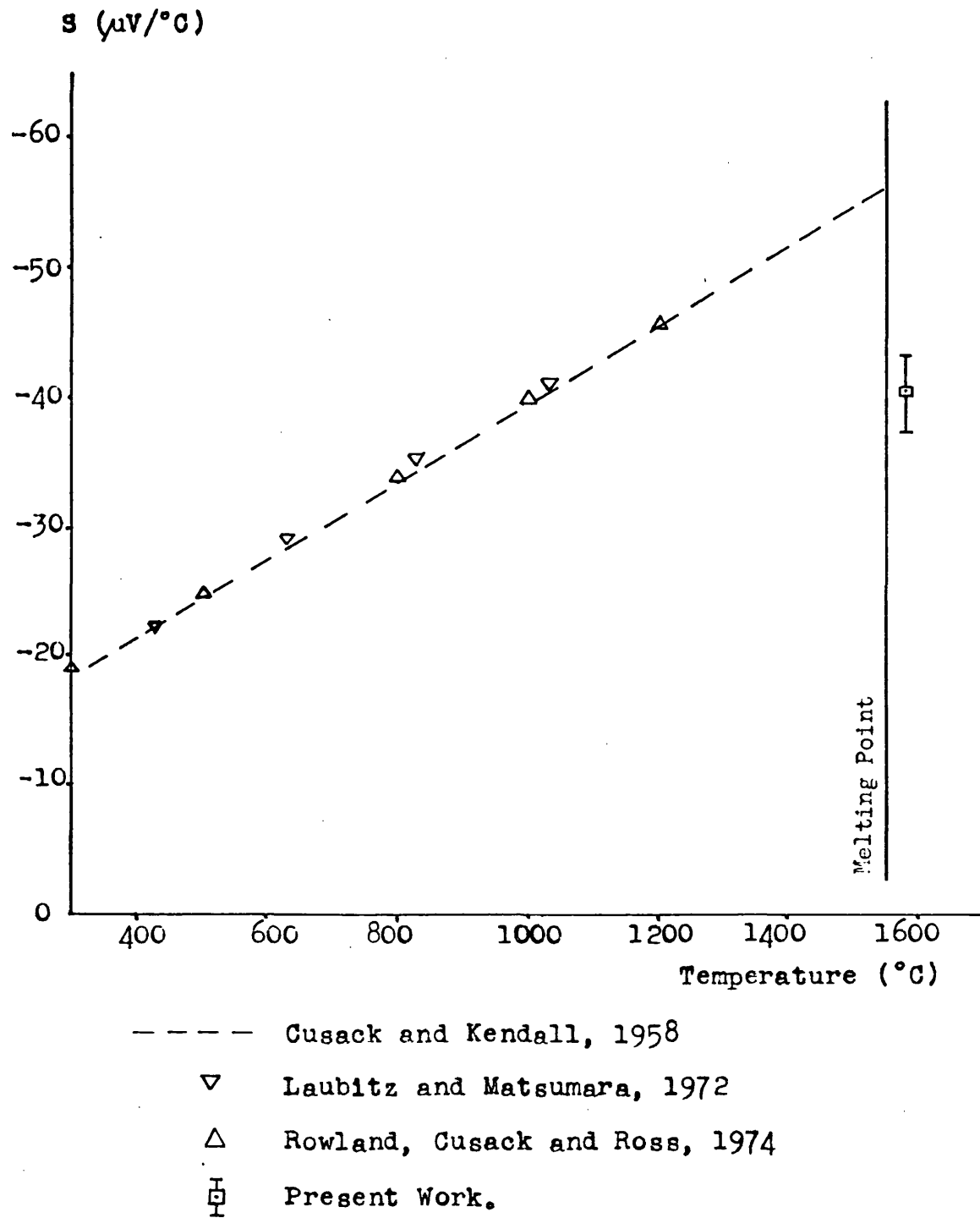
Thermoelectric Power (S) of Palladium

Figure 5-11

ii) Thermoelectric Power of Transition Metal Alloys.

The alloys investigated were made from elements adjacent to each other in the periodic table and which were known to have similar structure factors. The alloy phase diagrams indicate the formation of simple substitutional alloys. Thus, the concentration dependence of the electronic properties of these alloys should reflect primarily the variation in their electronic structure, whereas the direct effect of variation in their ionic distribution should produce a smaller contribution.

Nickel-cobalt in particular was examined in an attempt to provide a more quantitative test of the theories than is possible by considering the properties of the pure transition metals alone. Structure factors for nickel and cobalt are available from X-ray diffraction experiments (Waseda and Ohtani, 1974) and some resistivity values are available for these alloys. (Chapter 5(iii)).

A graph of the Seebeck e.m.f. measured for a nickel-cobalt alloy is given in figure 5-12 and the results for the nickel-cobalt series are summarised in Table 5-B. The composition of the alloy is given in column 1, the error in these values is less than ± 0.5 atomic per cent, the causes of error being the introduction of tungsten, and slight loss of sample by evaporation. The experiments were conducted at similar temperatures in order to allow direct comparison of values of

Seebeck e.m.f.
Liquid Ni₃₀Co₇₀ v. Tungsten
at 1532°C

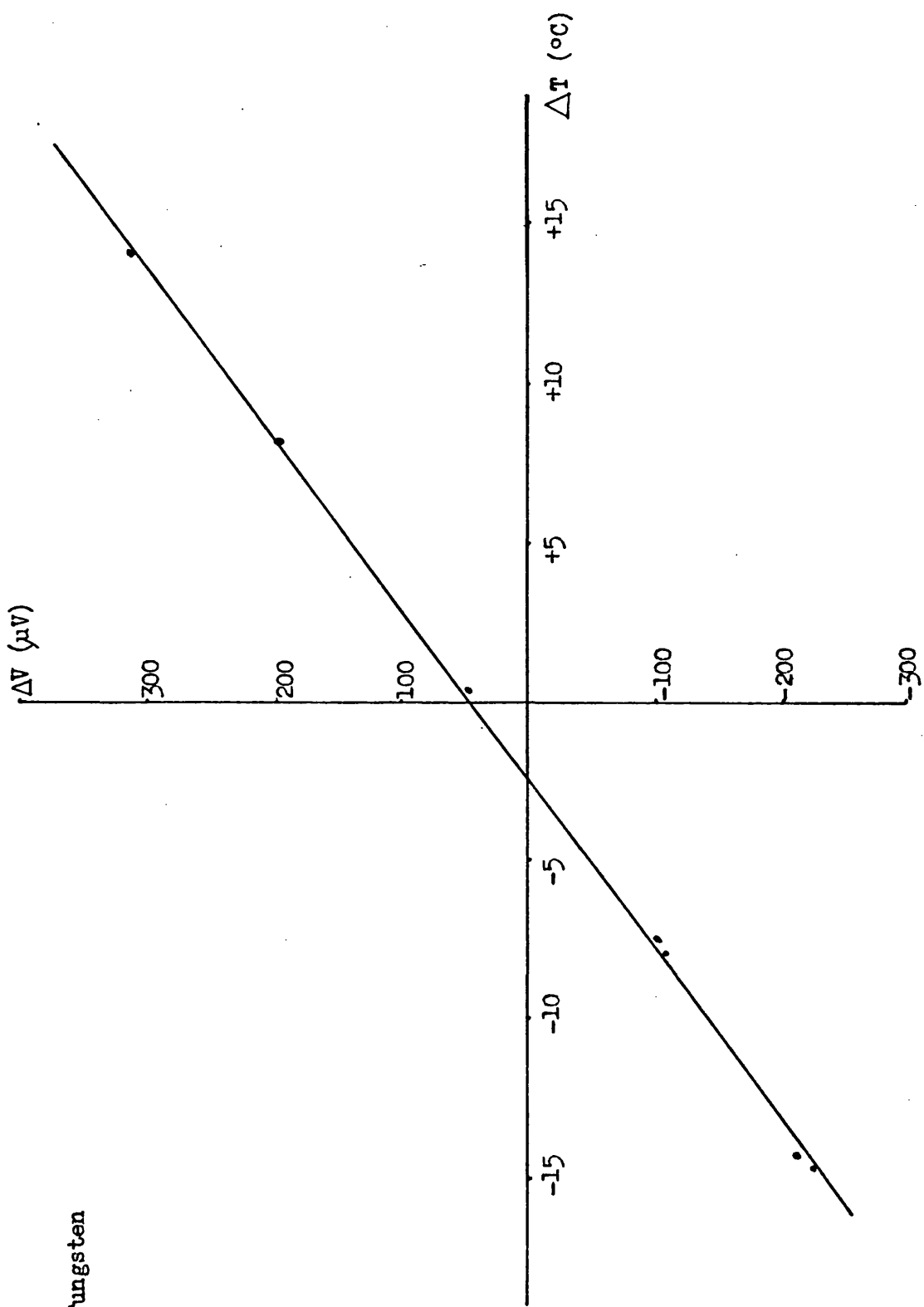


Figure 5-12

(1) Sample Composition (atomic %)	(2) Liquidus Temperature (°C)	(3) Experiment Temperature (°C)	(4) Slope of e.m.f. v. temp. diff. graph ($\mu\text{V}/^\circ\text{C}$)	(5) Abs. Th. Power of Sample S ($\mu\text{V}/^\circ\text{C}$)	(6) Estimated Error in S ($\mu\text{V}/^\circ\text{C}$)	(7) Upper limit to Contamination level (atomic %)
LIQUID						
Ni ₉₀ Co ₁₀	1460	1532	+34.0	-17	± 2	0.27
Ni ₇₈ Co ₂₂	1465	1532	+29.5	-12	± 2	0.35
Ni ₅₅ Co ₄₅	1470	1502	+21.6	-4	± 2	0.28
Ni ₃₀ Co ₇₀	1480	1532	+18.8	-1	± 1	0.27
SOLID						
Ni ₅₅ Co ₄₅	1470	1392	+25.9	-7	± 2	0.28

TABLE 5-B. Thermoelectric Power of Nickel - Cobalt Alloys.

the absolute thermoelectric power; the experiment with 45 atomic per cent cobalt was performed at a slightly lower temperature because of a temporary difficulty in the operation of one of the difference heaters. The liquidus temperature in column (2) was taken from the Phase diagram shown in figure 3-10. Explanation of other columns has been given above with reference to Table 5-A.

The variation in the absolute thermoelectric power of liquid nickel-cobalt alloys with composition is shown in figure 5-13, together with available values for solid alloys at high temperatures. It should be noted that for the solid data, the isotherms for which values are shown intersect the magnetic transformation line (Curie 'point') for the alloys. The compositions at which this occurs were determined from figure 3-10 and are shown in figure 5-13 by short vertical lines.

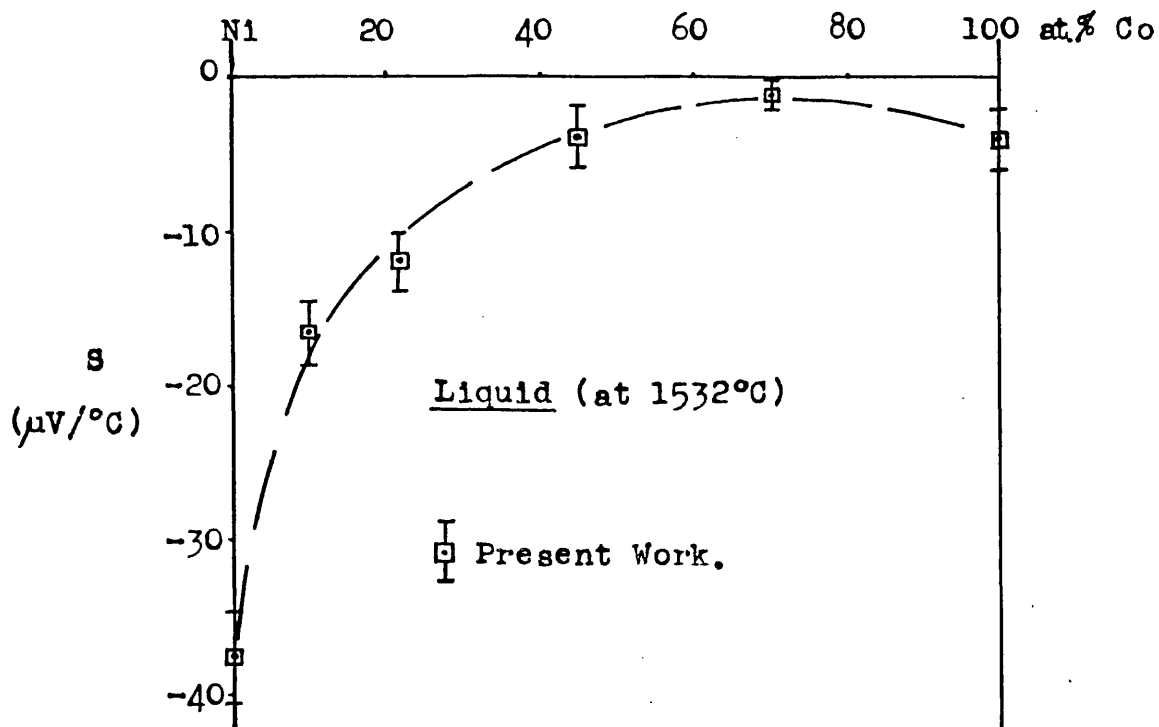
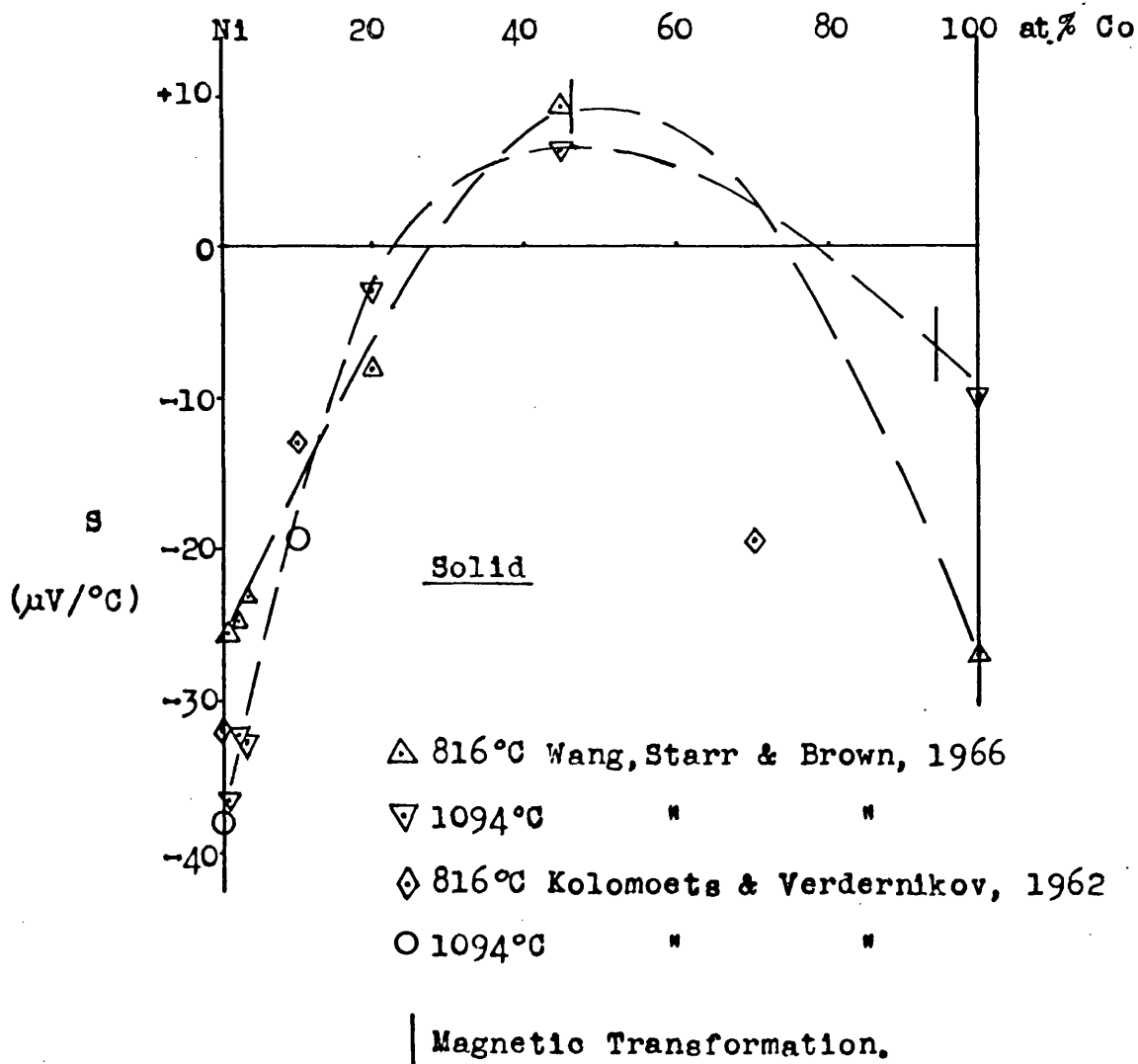


Figure 5-13 Thermoelectric Power (S) of Ni-Co Alloys.



A graph of the Seebeck e.m.f. for a silver-palladium alloy is given in figure 5-14 and the results for these alloys are summarised in Table 5-C. The error in composition is again less than ± 0.5 atomic per cent, the sources of error being the same as in the case of nickel-cobalt alloys.

For the silver-palladium alloys it is not practicable to perform all the experiments at the same temperature in the liquid because of the high vapour pressure of silver, its rapid increase with temperature and the particularly corrosive properties of silver vapour. Accordingly, the silver-palladium alloy experiments were performed at 80°C above the liquidus. This excess temperature provided a margin of safety to allow for possible errors in the phase diagram (figure 3-10) since accidental solidification of the sample could lead to crucible failure.

The absolute thermoelectric powers of the liquid silver-palladium alloys are plotted as a function of composition in figure 5-15. The value for pure liquid silver is that at 1040°C and is taken from the work of Ricker and Schaumann (1966) and from the work of Howe and Enderby (1967), the two values being in agreement. For comparison purposes, figure 5-16 shows the high temperature solid data of Rudinski (1956), values taken from the work of Geibel (1911) and the lower temperature data of Taylor and Coles (1956).

Seebeck e.m.f.
Liquid Pd₆₂Ag₃₈ v. Tungsten
at 1478°C

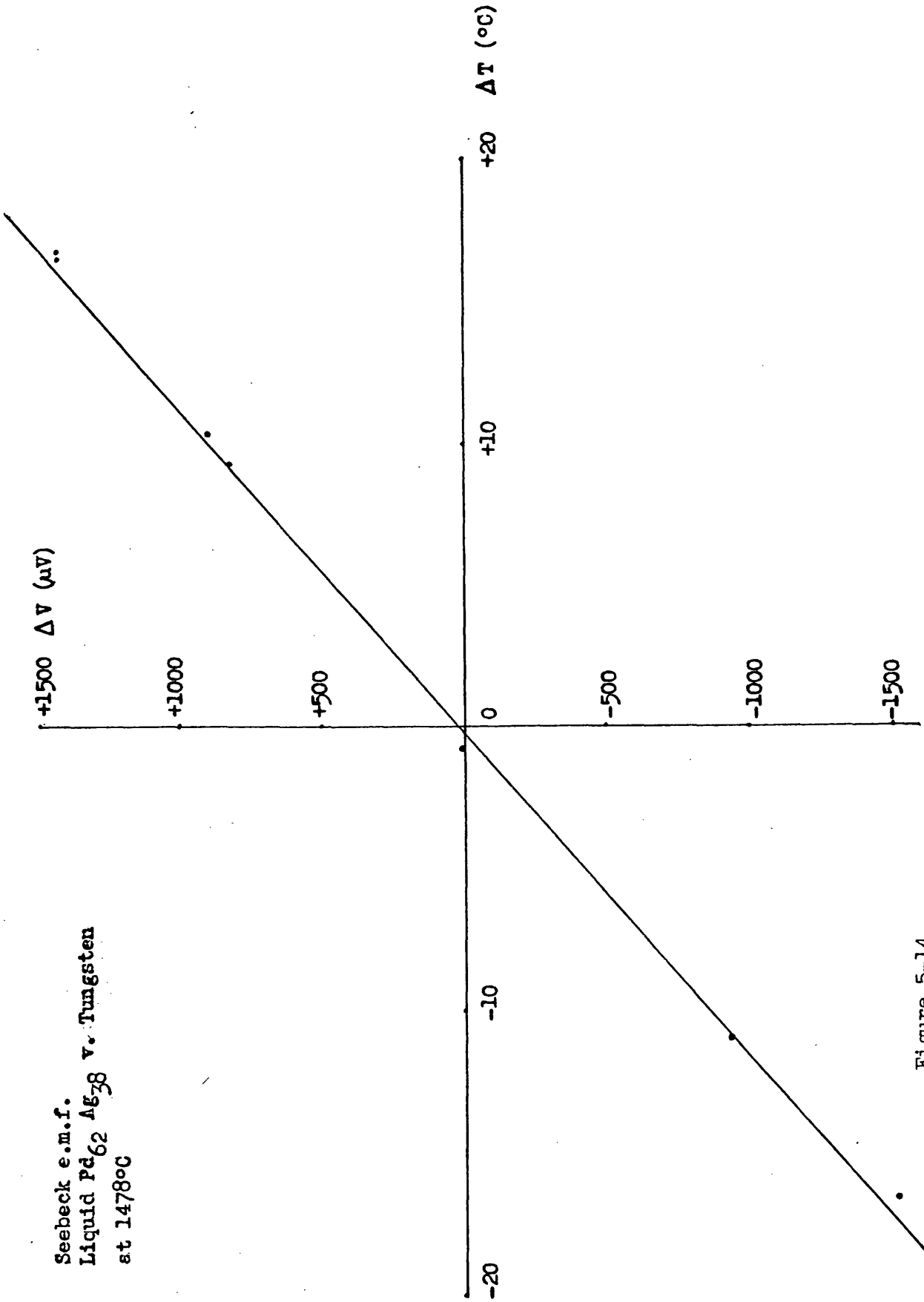


Figure 5-14

(1) Sample Composition (atomic %)	(2) Liquidus Temperature (°C)	(3) Experiment Temperature (°C)	(4) Slope of e.m.f. v. temp. diff. graph ($\mu\text{V}/^\circ\text{C}$)	(5) Abs. Th. Power of Sample S ($\mu\text{V}/^\circ\text{C}$)	(6) Estimated Error in S ($\mu\text{V}/^\circ\text{C}$)	(7) Upper limit to Contamination level (atomic %)
LIQUID						
Pd ₁₅ Ag ₈₅	1110	1193	+34.8	-15	± 2	0.17
Pd ₂₆ Ag ₇₄	1190	1278	+51.2	-32	± 3	0.29
Pd ₄₁ Ag ₅₉	1290	1378	+65.8	-47	± 5	0.46
Pd ₅₁ Ag ₄₉	1345	1428	+77.7	-59	± 4	0.26
Pd ₆₂ Ag ₃₈	1390	1478	+88.2	-70	± 4	0.14
Pd ₇₆ Ag ₂₄	1450	1528	+77.0	-60	± 3	0.17

TABLE 5-C. Thermoelectric Power of Silver - Palladium Alloys.

Thermoelectric Power (S) of Silver-Palladium Alloys.

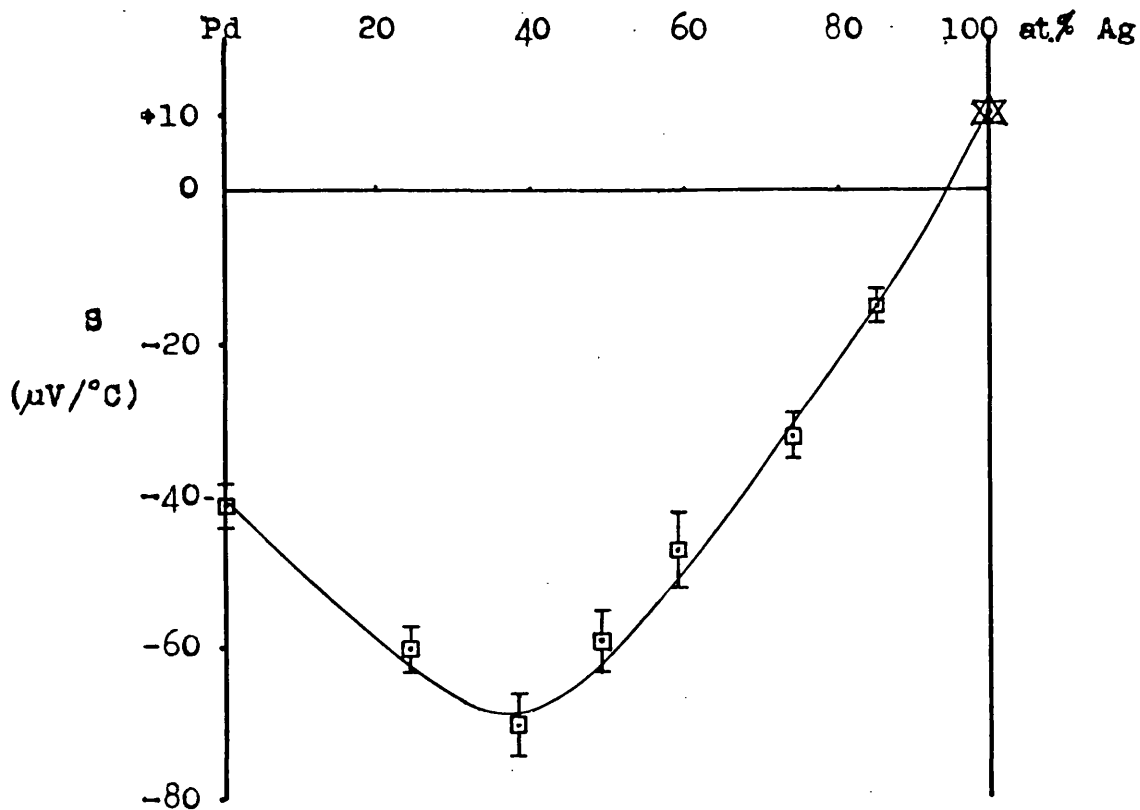
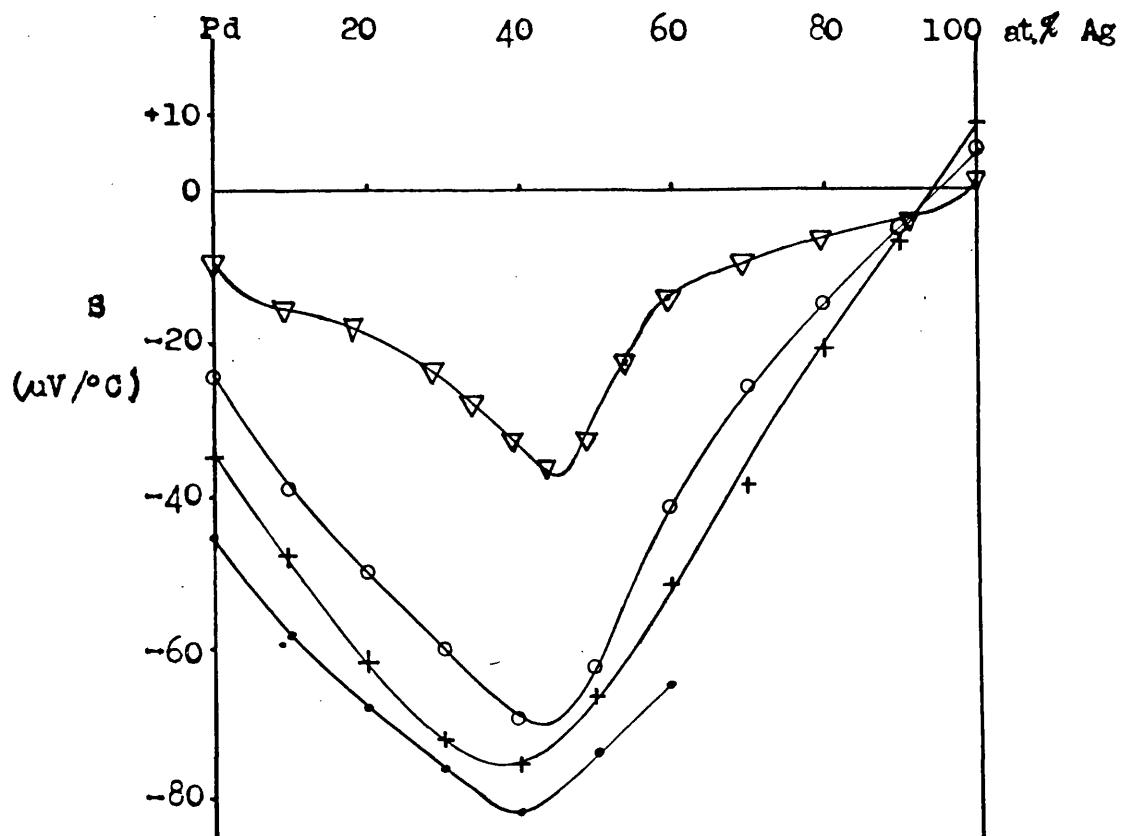
Liquid (at approx. 80°C above the Liquidus.) \square Present Work. \triangle Howe and Enderby, 1967 ∇ Ricker and Schaumann, 1966

Figure 5-15

Thermoelectric Power (S) of Silver-Palladium Alloys.

Solid

▽ 0°C Taylor and Coles, 1956

○ 500°C Rudinski, 1956

+ 850°C Geibel, 1911

• 1200°C Rudinski, 1956

Figure 5-16

iii) Resistivity.

The previously available data for the resistivity of some liquid transition metals and the appropriate high temperature solid data, together with the values obtained in this work, are given in Table 5-D. Recently Guntherodt, Hauser, Kunzi and Muller (1975) have reported experiments on the same metals and their data is also given. In view of the experimental difficulties involved in working at high temperatures the measure of agreement secured is satisfactory. The values reported by the Russian workers however, (with the exception of Regel and Mokrovsky (1953)) are consistently above both sets of data. For this there is no clear explanation though it is interesting to note that Regel and Mokrovsky (1953), Vertman and Samarin (1961), Dubinin, Esin and Vatolin (1969) and Vatolin, Esin and Dubinin (1967) used an indirect eddy current technique which involved measuring the torque on a specimen in a rotating magnetic field and which therefore may be subject to systematic errors of a different nature from those occurring in more direct experiments.

For the comparison described in Chapter 6, of the resonance approximation theory (Chapter 2) and experiment, it was necessary to know the resistivity of liquid nickel-cobalt alloys. For this purpose it was hoped to rely on the reported data of Vertman

Experimental Data for the Resistivity of Transition Metals.

Sample	Temp. (°C)	Resist- ivity. ($\mu\Omega$.cm)	Source
Ni Liquid:			
	1455	85 \pm 2	Present Work.
	1455	85	Regel & Mokrovsky, 1953
	1600	125	Dubinin, Esin & Vatolin, 1969
	1495	106	Vertman & Samarin, 1961
	1460	83	Guntherodt, Hauser, Kunzi, & Muller, 1975
Ni Solid:			
	1445	65	Regel et al, 1953
	*(1400)	56	Kierspe, Kohlhaas & Gonska, 1967
	1449	58	Guntherodt et al, 1975
Co Liquid:			
	1500	117 \pm 4	Present Work.
	1500	102	Regel et al, 1953
	1600	128	Dubinin et al, 1969
	1530	131	Vertman et al, 1961
	1505	116	Guntherodt et al, 1975
Co Solid:			
	1490	97	Regel et al, 1953
	*(1400)	104	Kierspe et al, 1967
	1493	98	Guntherodt et al, 1975
Pd Liquid:			
	1552	83 \pm 2	Present Work.
	1600	120	Vatolin, Esin & Dubinin, 1967
	1580	79	Guntherodt et al, 1975

TABLE 5-D.

cont.-

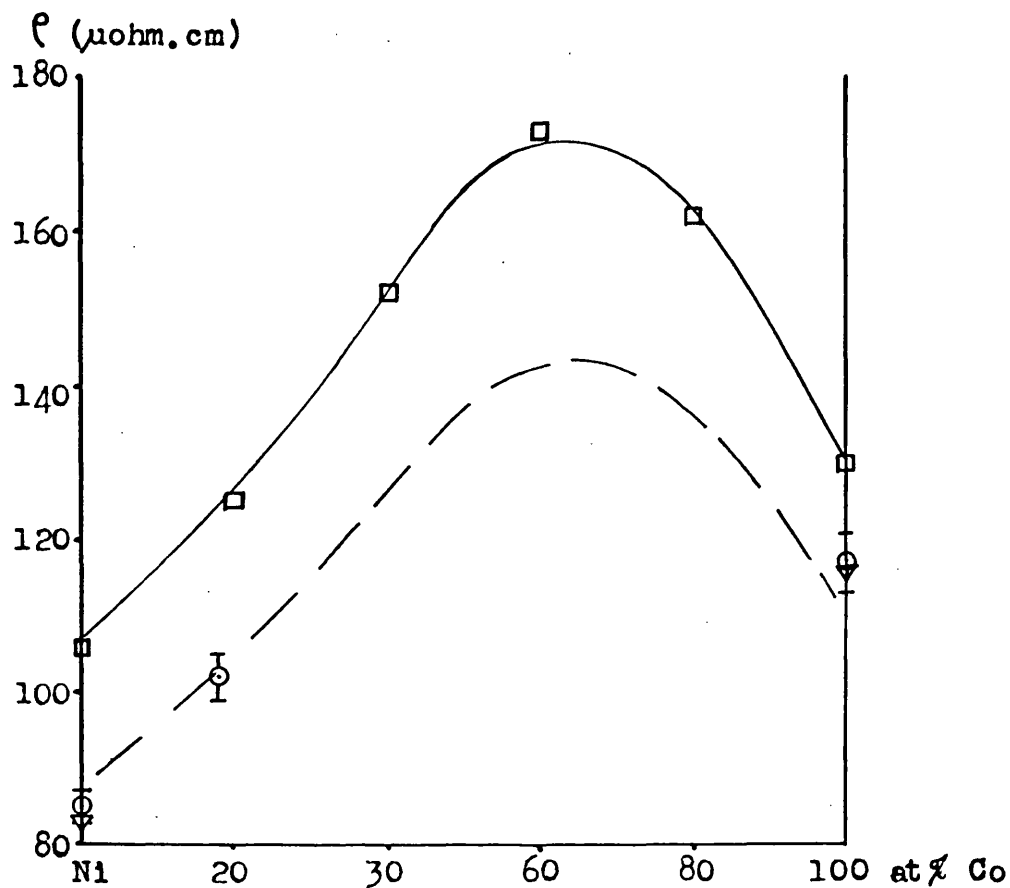
TABLE 5-D cont. - Experimental Resistivity Data.

Sample	Temp. (°C)	Resist- ivity. ($\mu\Omega$.cm)	Source
Pd Solid:			
	1485	44	Guntherodt et al, 1975
Fe Liquid:			
	1540	135 \pm 4	Present Work.
	1570	139	Powell, 1953
	1540	110	Regel et al, 1953
	1540	136	Guntherodt et al, 1975
Fe Solid:			
	1520	127	Powell, 1953
	1530	123	Regel et al, 1953
	*(1450)	127	Kierspe et al, 1967
	1522	128	Guntherodt et al, 1975

* For these cases the resistivity values were obtained by extrapolating the authors' data from the temperatures shown in brackets to just below the melting points.

Resistivity (ρ) of Liquid Nickel - Cobalt Alloys.

(at approx. 1500°C)



—, □ Vertman et al, 1961

○ Present Work.

▽ Guntherodt et al, 1975

— — — Vertman et al, 1961 - scaled by 0.83,
see text.

Present work, Alloy Data:

$\text{Ni}_{82} \text{Co}_{18}$ Resistivity = $102 \pm 3 \mu\text{ohm.cm}$ at 1480°C

Figure 5-17

Resistivity (ρ) of Silver-Palladium Alloys.

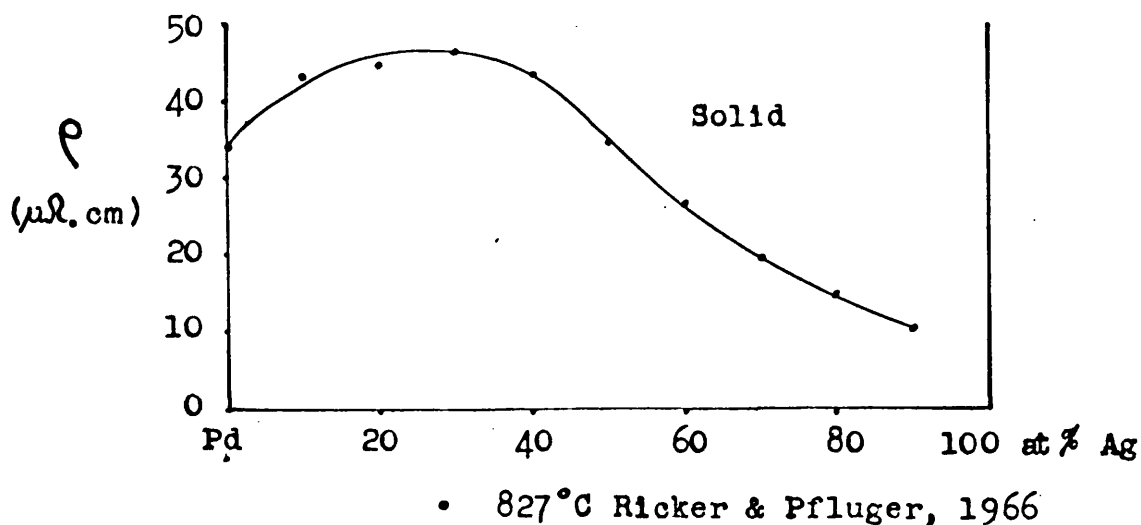
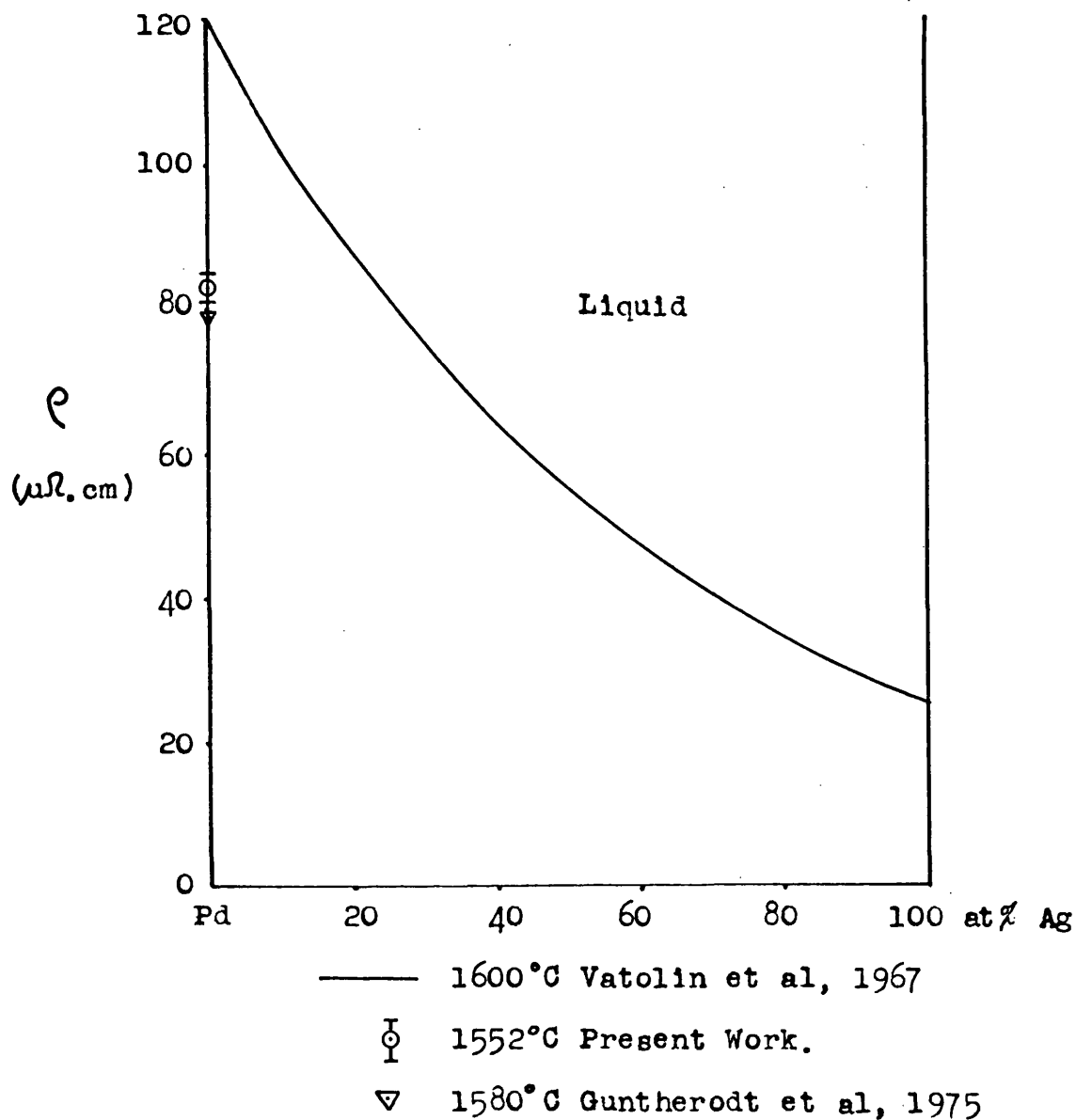


Figure 5-18

and Samarin (1961) but as stated their data for pure liquid nickel and cobalt were significantly different from the consensus of other experimental values. All their data were therefore normalised to these end points by means of a single multiplicative correction of 0.83. The data before and after this procedure are shown in figure 5-17 together with the result of a measurement performed on a nickel-cobalt alloy containing 18 atomic per cent cobalt to provide some check on the suitability of this scaling.

Figure 5-18 shows the available data for the resistivity of silver-palladium alloys in the liquid state and some data pertaining to the solid state at high temperature. Here it was found that the value for pure liquid palladium is in gross disagreement with our measurements and those reported by Guntherodt et al (1975) but the liquid alloy data are included as no other data are available.

CHAPTER 6. COMPARISON OF THEORETICAL AND EXPERIMENTAL
VALUES OF RESISTIVITY AND THERMOELECTRIC
POWER.

i) Pure Metals.

The situation concerning calculations of the resistivity and thermoelectric power of pure liquid transition metals has been mentioned in Chapter 2. The results of the reported theoretical calculations generally do not disagree with experiment; the calculations of Brown (1973) correctly predicted the magnitudes of the resistivity and thermoelectric power of liquid palladium. The thermoelectric power of liquid iron is however, small in magnitude and does not have the large negative value predicted by the first application of a resonance type approximation to liquid transition metals (Evans et al, 1971). Table 6-A summarises the values obtained in recent calculations, together with some of the relevant physical parameters used. In these calculations the dependence of the predicted values on the input parameters (some of which are not well known) is evident. It is this sensitivity which renders close comparison of theory and experiment dubious. For this reason a suitable binary TT alloy was investigated and the theory is now extended to cover this case.

ii) Transition Metal - Transition Metal Alloys.

The comparison between theory and experiment

Calculations of the Resistivity (ρ) and Thermoelectric Power (S) of Liquid Transition Metals.

<u>Results.</u>		<u>Input Parameters.</u>		<u>Reference.</u>
S	ρ	k_F	Z_{eff}	a(q)
($\mu V/^\circ C$)	($\mu\Omega cm$)	\AA^{-1}		
Iron				
-4	135			Present Experimental Work.
-48	372	1.66		A Evans, Greenwood & Lloyd, 1971
-43	276	1.72	2	A Evans et al, 1971
	196		1	A Dreirach, Evans, Guntherodt & Kunzi, 1972
Nickel				
-38	85			Present Experimental Work.
-38	227	1.61		B Evans et al, 1971
-33	106	1.76	2	B Evans et al, 1971
	78		1	C Dreirach et al, 1972
-53	27.2		.46	D Brown, 1973
-53	56.3		.46	C Brown, 1973
Palladium				
-41	83			Present Experimental Work.
-78	41.6		.36	D Brown, 1973
-74	62		.36	E Brown, 1973

a(q) indicates the source of the structure factor used:

A Waseda & Suzuki, 1970

B The experimental structure factor for Iron (A) was used.

C Waseda, Suzuki, Tamaki & Takeuchi, 1970

D A Hard Sphere model with packing fraction = 0.45 was used.

E The experimental structure factor for Nickel (C) was used.

TABLE 6-A.

described here for nickel-cobalt alloys is similar to that developed by Howe and Enderby (1967) in that the thermoelectric power of the liquid alloy is predicted in terms of the resistivity of the liquid alloy and the resistivities and thermoelectric powers of the pure components in the liquid state. Howe and Enderby considered liquid 'equal valency' alloys of normal metals (that is, metals that are not rare earth, transition, or actinide metals) in terms of the Faber-Ziman theory (Faber and Ziman, 1965), and assumed that the scattering potentials were local and sufficiently weak to render the free electron approximations valid. For TT alloys in the resonance scattering approximation however, the scattering is described in terms of partial wave analysis and is dominated by the back scattering contribution of the d-wave phase shift (Chapter 2 (ii)). In this case the resistivity of the liquid alloy may also be predicted in terms of the resistivities of the alloy constituents in the liquid state. The comparison does however, require the Fermi energy, the atomic volume and the partial structure factors to be substantially independent of the alloy composition. These requirements are apparently met for liquid nickel-cobalt; the liquid densities of the constituents differ by less than 1.3 per cent (Allen, 1972) and their structure factors are similar (Waseda and Ohtani, 1974). As mentioned in Chapter 2 the Fermi energies

and wave vectors for transition metals are not well known but the close similarity of nickel and cobalt - as indicated by their atomic weights, their atomic electronic configurations (Phillips and Williams, 1965) and the alloy phase diagram (Hansen, 1958) as well as estimates of the Fermi wave vectors for the solid metals (Heine, 1967) - implies that the conditions for the application of such a method may reasonably be considered as fulfilled.

The theory of the resonance type approximation was given in Chapter 2 and led to an approximate expression (equation 2.5) for the resistivity of a pure liquid transition metal. The first step is to generalise this to include the case of liquid TT alloys.

The resistivity must be expressed as:

$$\rho = \frac{12\pi m^2}{e^2 k^3 k_F^2} \int_0^1 x^3 \langle T \rangle dx \quad 6.1$$

$$\begin{aligned} \text{where } \langle T \rangle = & c |t_A|^2 \left[1-c + ca_{AA}(q) \right] \\ & + (1-c) |t_B|^2 \left[c + (1-c)a_{BB}(q) \right] \\ & + c(1-c)(t_A^* t_B + t_A t_B^*) (a_{AB}(q) - 1) \quad 6.2 \end{aligned}$$

Here c is the concentration of atoms of type A,

t_A is the t matrix for scattering from

an atom of type A,

t_B is the t matrix for scattering from

an atom of type B

and a_{AA} , a_{AB} and a_{BB} are the three partial

structure factors of the alloy.

This is similar in form to the case of alloys of simple metals mentioned in Chapter 1.

By analogy with the case of pure liquid transition metals (Chapter 2):-

$$|t_A|^2 = \frac{50\pi^2 \chi^6}{m^3 E \Omega^2} \sin^2 \eta_2^A (P_2(\cos\theta))^2 \quad 6.3$$

$$|t_B|^2 = \frac{50\pi^2 \chi^6}{m^3 E \Omega^2} \sin^2 \eta_2^B (P_2(\cos\theta))^2$$

Where η_2^A now represents the d-wave phase shift for scattering from an atom of type A and η_2^B represents that for scattering from an atom of type B.

and:

$$t_A^* t_B = \frac{50\pi^2 \chi^6}{m^3 E \Omega^2} \sin \eta_2^A \sin \eta_2^B (P_2(\cos\theta))^2 \exp(i(\eta_2^B - \eta_2^A))$$

$$t_A t_B^* = \frac{50\pi^2 \chi^6}{m^3 E \Omega^2} \sin \eta_2^A \sin \eta_2^B (P_2(\cos\theta))^2 \exp(i(\eta_2^A - \eta_2^B))$$

There is thus an implicit assumption that the t matrix for scattering from an ion does not vary with the composition of the alloy. This is in keeping with the use of a single site resonant scattering model when the Fermi energy is assumed not to vary with alloy composition. It should however be noted that at low concentrations of ions of type A in a host of type B the large mean separation of type A ions may significantly change the t matrix for those ions from its value in pure liquid A, and vice versa.

As for the pure transition metal case, the integrals can readily be approximately calculated and this gives for the resistivity of the liquid TT alloy:

$$\rho_{\text{alloy}} = D \left[\begin{aligned} &c \sin^2 \eta_2^A (1-c + c\bar{a}) \\ &+ (1-c) \sin^2 \eta_2^B (c + (1-c)\bar{a}) \\ &+ 2c(1-c) \sin \eta_2^A \sin \eta_2^B \cos(\eta_2^A - \eta_2^B) (\bar{a} - 1) \end{aligned} \right] \quad 6.4$$

$$\text{Where } D = \frac{30\pi^3 k^3}{mE_F k_F^2 \Omega e^2}$$

and $\bar{a} = a(q)$ at $q = 2k_F$ (In this substitutional model we assume $a_{AA} = a_{AB} = a_{BB} = a$ as described in Chapter 1 for simple metal liquid alloys.).

Using equation 6.4 and the two appropriate versions of equation 2.5, the resistivity of the alloy is expressed in terms of the resistivities (ρ_A and ρ_B) of the two pure liquid components. Since the latter quantities are known from experiment the resistivity of the alloy may be predicted. It is given by:

$$\rho_{\text{alloy}} = L'c^2 + M'c + N' \quad 6.5$$

Where:

$$L' = (1-\sqrt{a})(\rho_A + \rho_B - 2G)$$

$$M' = (\sqrt{a})(\rho_A + \rho_B) - 2\rho_B + 2(1-\sqrt{a})G$$

$$N' = \rho_B$$

With:

$$G = \sqrt{\rho_A \rho_B \left(1 - \frac{\rho_A}{Da}\right) \left(1 - \frac{\rho_B}{Da}\right)} + \frac{\rho_A \rho_B}{Da}$$

Furthermore, the thermoelectric power of the alloy may be predicted from knowledge of the thermoelectric powers (S_A and S_B) of the pure liquid constituents, the resistivities of the pure liquid constituents, and the resistivity of the liquid alloy (ρ_{alloy}) - all quantities which may be experimentally observed. The approximate expression for the thermoelectric power of the alloy (S_{alloy}) is derived from equation 6.4 using equation 1.7 :

$$S_{\text{alloy}} = J \left[(U'c^2 + V'c + W') / \epsilon_{\text{alloy}} - 2/E_F \right] \quad 6.6$$

Where:

$$J = \frac{\pi^2 k_B^2 T}{3|e|}$$

and:

$$U' = \frac{2m}{\hbar^2 k_F} (\gamma \bar{a}) \left[\frac{d a(q)}{dq} \right]_{q=2k_F} (\epsilon_A + \epsilon_B - 2G) \\ + (1-\gamma \bar{a}) (\epsilon_A^{Y_A} + \epsilon_B^{Y_B} - 2K')$$

$$V' = \frac{4m}{\hbar^2 k_F} (\gamma \bar{a}) \left[\frac{d a(q)}{dq} \right]_{q=2k_F} (G - \epsilon_B) \\ + (\gamma \bar{a}) (\epsilon_A^{Y_A} + \epsilon_B^{Y_B}) + 2(1-\gamma \bar{a})K' - 2\epsilon_B^{Y_B}$$

$$W' = \frac{2m}{\hbar^2 k_F} (\gamma \bar{a}) \left[\frac{d a(q)}{dq} \right]_{q=2k_F} \epsilon_B + \epsilon_B^{Y_B}$$

contd.

With

$$K' = c_{A Y_A} \left[\frac{\sqrt{\frac{e_B}{D\bar{a}}} \sqrt{1 - \frac{e_B}{D\bar{a}}}}{2\sqrt{\frac{e_A}{D\bar{a}}} \sqrt{1 - \frac{e_A}{D\bar{a}}}} \left(1 - 2\frac{e_A}{D\bar{a}}\right) + \frac{e_B}{D\bar{a}} \right]$$

$$+ c_{B Y_B} \left[\frac{\sqrt{\frac{e_A}{D\bar{a}}} \sqrt{1 - \frac{e_A}{D\bar{a}}}}{2\sqrt{\frac{e_B}{D\bar{a}}} \sqrt{1 - \frac{e_B}{D\bar{a}}}} \left(1 - 2\frac{e_B}{D\bar{a}}\right) + \frac{e_A}{D\bar{a}} \right]$$

$$Y_A = \frac{S_A}{J} + \frac{2}{E_F} - \frac{2m}{\hbar^2 k_F \bar{a}} \left[\frac{d a(q)}{dq} \right]_{q=2k_F}$$

$$Y_B = \frac{S_B}{J} + \frac{2}{E_F} - \frac{2m}{\hbar^2 k_F \bar{a}} \left[\frac{d a(q)}{dq} \right]_{q=2k_F}$$

Such calculations of the resistivity and thermoelectric power of liquid nickel-cobalt alloys have been performed, in which use was made of experimentally derived data for ρ_{alloy} in equation 6.6. Results are given in figure 6-1 together with some experimental data for comparison (Chapter 5).

Before performing the calculations it was necessary to determine suitable values of the Fermi energy (E_F) and wave vector (k_F) for substitution in equations 6.5 and 6.6. In these calculations however, the extreme sensitivity to the choice of E_F mentioned in Chapters 2(ii) and 6(i) concerning first principles calculations did not occur. This was because in the present work the magnitude of the d-wave phase shift at the Fermi energy for a type A ion, say, was evaluated directly from the experimental resistivity of pure liquid A; not - using a calculated value of the Fermi energy - from a theoretical expression for the d-wave phase shift which would be a rapidly varying function of energy near a d-wave resonance.

The structure factor used to determine \bar{a} and $\left[\frac{d}{dq} a(q) \right]_{q=2k_F}$ was an average of the structure factors for pure liquid nickel (at 1500°C) and pure liquid cobalt (at 1550°C) obtained from X-ray diffraction experiments (Waseda et al, 1974). Similarly, the density of the alloy was taken

Resistivity (ρ) and Thermoelectric Power (S) of Liquid Nickel-Cobalt Alloys

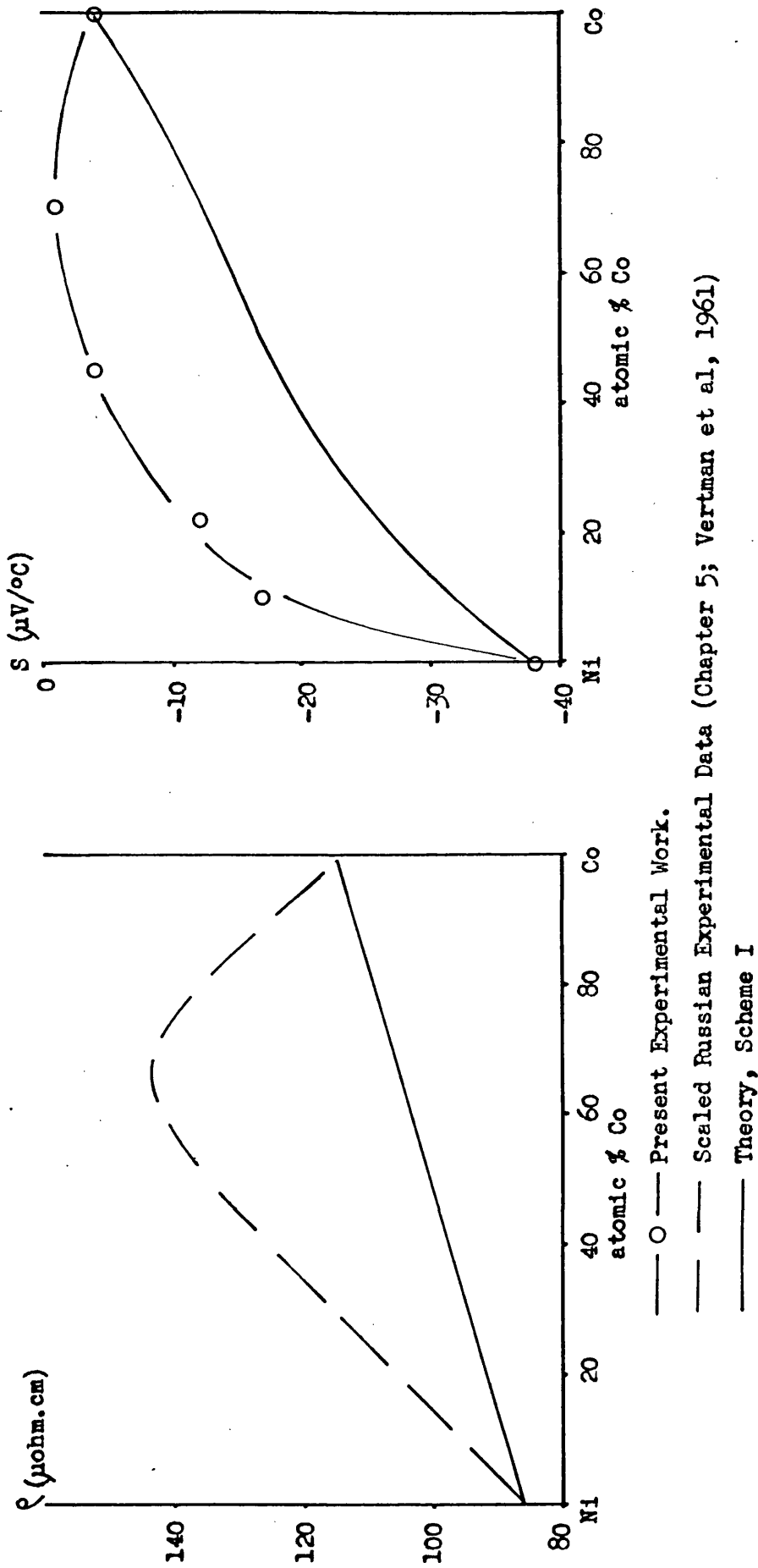


Figure 6-1(a)

Resistivity (ρ) and Thermoelectric Power (S) of Liquid Nickel-Cobalt Alloys

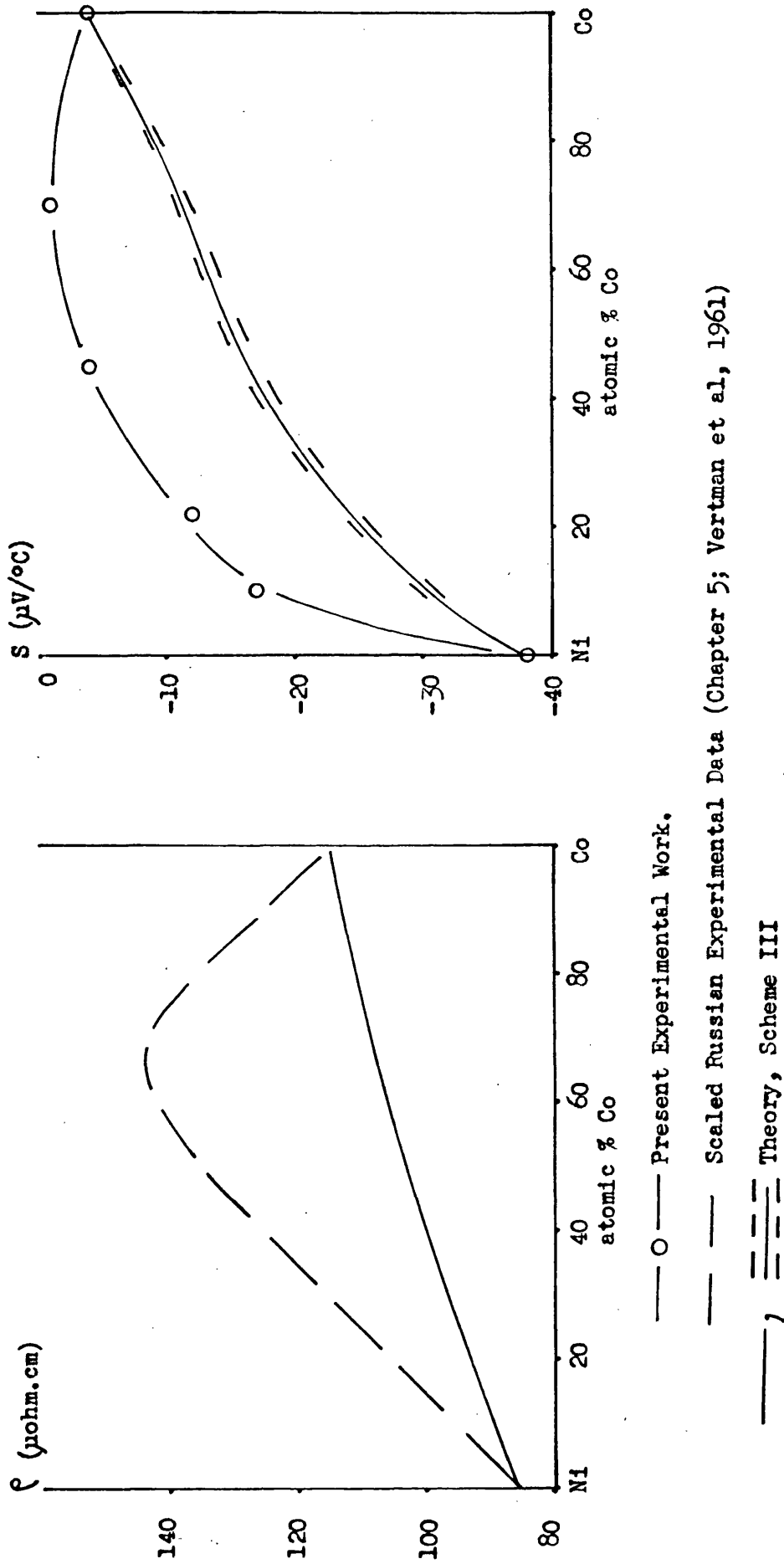


Figure 6-1(b)

Resistivity (ρ) and Thermoelectric Power (S) of Liquid Nickel-Cobalt Alloys

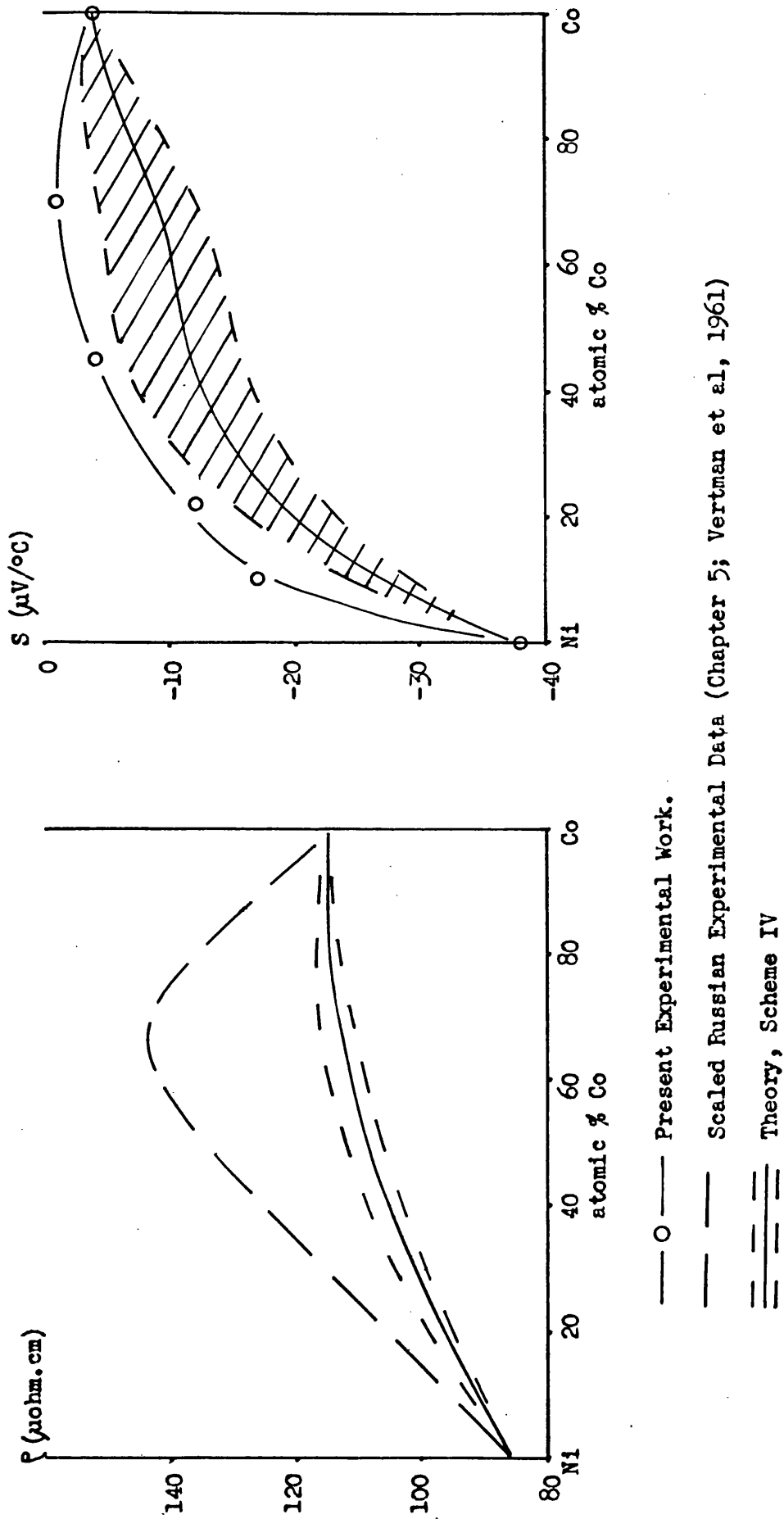


Figure 6-1(c)

as the average of the densities of pure liquid nickel and cobalt at the same temperatures.

The schemes employed in the calculations were as follows:

Scheme I.

The effective valence Z_{eff} was chosen as unity as indicated by Dreirach et al (1972) for nickel and the Fermi wave vector calculated using equation 2.8. The Fermi energy was varied by ± 0.02 Rydberg from the free electron value appropriate to the above value of k_F , in order to allow for uncertainties in the position of the band with respect to the 'muffin tin zero'. To allow for its experimental error the structure factor evaluated at $q=2k_F$ was allowed to vary by ± 0.02 subject to the constraint that it should not be less than the limiting value at long wavelength. Similarly $\left[\frac{d}{dq} a(q) \right]_{q=2k_F}$ was varied by ± 10 per cent. The predicted values of the resistivity and thermoelectric power are shown in figure 6-1(a) the range of predicted values lying within the thickness of the lines.

Scheme II.

Scheme I was followed except that the Fermi energy was fixed at 0.62 Rydberg and

an effective electronic mass of 0.81 m used in accordance with the values obtained by Dreirach et al (1972) for nickel.

The results are virtually indistinguishable from those of Scheme I.

Scheme III.

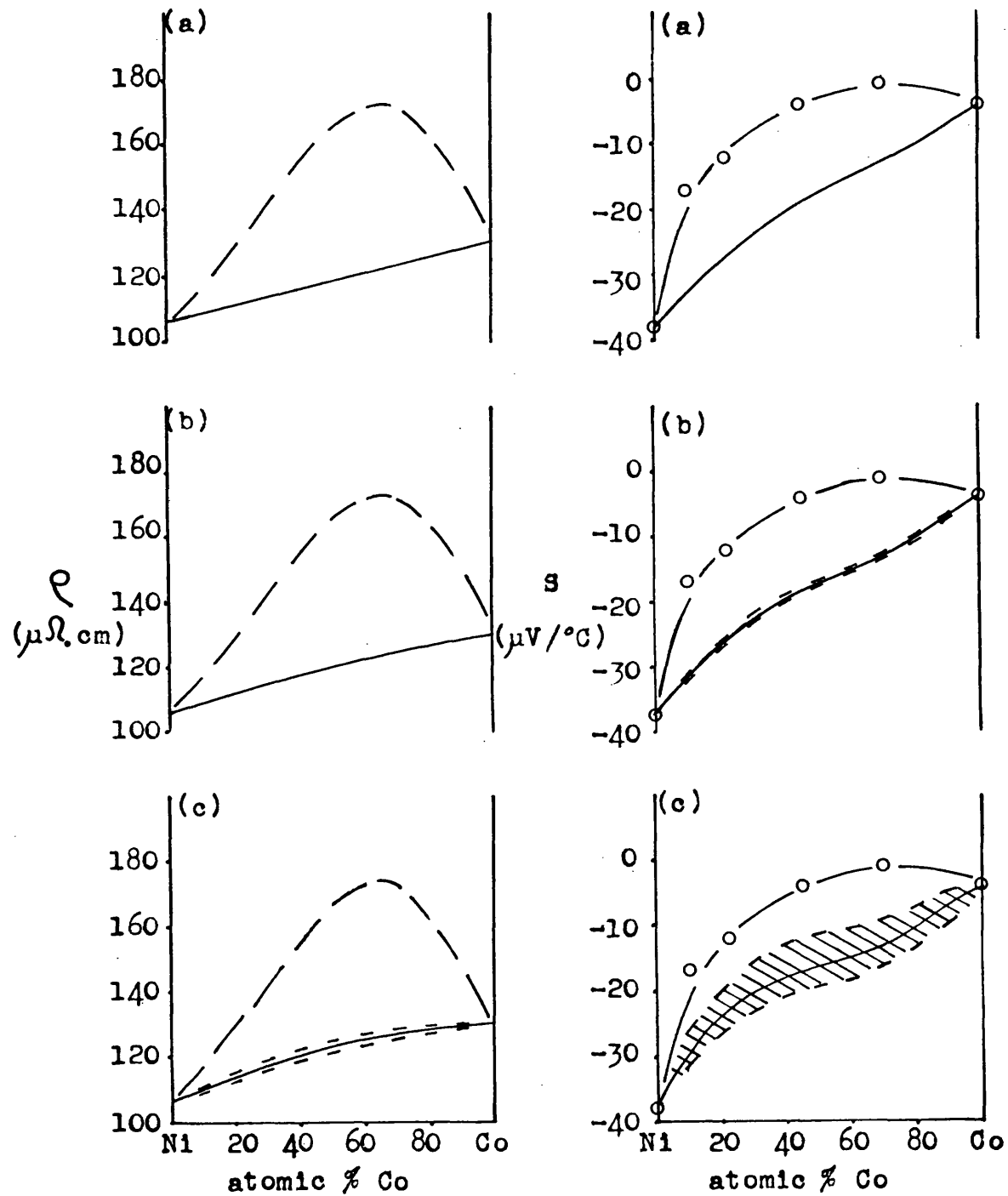
Scheme I was followed but with Z_{eff} set to 0.46 as suggested by Brown (1973). The results (figure 6-1(b)) are similar in form to those of Scheme I. The band for the theoretical values of the thermoelectric power indicating the range of predicted values.

Scheme IV.

This was again similar to Scheme I but this time with Z_{eff} chosen arbitrarily as 0.2. The results are shown in figure 6-1(c) and are clearly sensitive to the input parameters but some appreciable curvature is now evident in the theoretical curves for the resistivity and thermoelectric power.

In all the above schemes the scaled experimental resistivities (Chapter 5(iii)) were used in the prediction of the thermoelectric power of the alloy and for comparison with the predicted resistivity. For completeness the Schemes I, III and IV were repeated (and numbered V, VI and VII respectively) using the raw experimental data. The results,

Resistivity (ρ) and Thermoelectric Power (S) of Liquid
Nickel-Cobalt Alloys



—○— Present Experimental Work.

— — — Unscaled Russian Experimental Data

(Chapter 5; Vertman et al, 1961)

—, —, — Theory. a - Scheme V, b - Scheme VI,

c - Scheme VII.

Figure 6-2

shown in figure 6-2, do not differ in form from those of figure 6-1.

The above calculations, apart from the case of the very low value of the effective valence, are insensitive to the choice of input parameters and indicate that for nickel-cobalt alloys the resonant scattering model described does not account for the magnitude of the observed variation of resistivity and thermoelectric power with alloy concentration. It does appear however, that if very low (and possibly unphysical) values of the effective valence are assumed, the theory may be able to account qualitatively for the variation of the thermoelectric power and perhaps resistivity with alloy composition. However, due to the possible difference mentioned above between values of the t matrix for an ion in a pure liquid metal and for a similar ion in an alloy with a low concentration of that type of ion, the comparison of theory and experiment should be restricted to the approximate range $0.25 < c < 0.75$, where the substantial overlap between like ions should eliminate this effect (Mott, 1972).

iii) Silver-Palladium.

A similar direct comparison of the theory and experiment can not be made for liquid silver-palladium since for pure liquid silver the effect of the s -wave phase shift can by no means be neglected

as insignificant in comparison with that of the d-wave phase shift. In fact, at the Fermi energy the term $\sin^2\eta_0$ is of the order of 0.03 and the term $\sin^2\eta_2$ is approximately 0.01 while $\sin^2\eta_1$ is of the order of 0.0001 (Dreirach et al, 1972). Thus for pure liquid silver, equation 2.5 is incorrect and equation 2.7 can only be reduced to:

$$\rho = \frac{24\pi^3 k_F^3}{mE_F k_F^2 \Omega e^2} \left[25\sin^2\eta_2 \int_0^1 a(q) [P_2(\cos\theta)]^2 x^3 dx \right. \\ \left. + \sin^2\eta_0 \int_0^1 a(q) x^3 dx \right. \\ \left. + 10\sin\eta_0 \sin\eta_2 \cos(\eta_2 - \eta_0) \int_0^1 a(q) P_2(\cos\theta) x^3 dx \right] \quad 6.7$$

This renders inapplicable the method of comparison described above (Section ii).

The change in the atomic volume of approximately 10 per cent across the phase diagram (Allen, 1972) is also not insignificant and the effective valence may vary with alloy composition. The valence of silver is unity and it has been suggested as a result of de Haas-van Alphen experiments (Vuillemin et al, 1965) that a value of 0.36 is appropriate to palladium (Brown, 1973) but more recently values of the order of one have been obtained from theoretical calculations and x-ray diffraction data (Brown, 1976).

Experimentally, as figure 6-3 shows, there is a striking similarity between the thermoelectric powers of liquid and high temperature solid silver-palladium alloys, which indicates that there may be a common theoretical explanation of the variation of the thermoelectric powers with alloy concentration. This points towards an s-d scattering model of the type proposed by Mott being an adequate explanation, since it can (Chapter 2) predict the form of the observed thermoelectric power of the solid alloy and the predictions of such a model should not be very sensitive to melting, as they are not, at high temperature, significantly dependent on the structure factors of the alloy (Mott, 1972). On the other hand it must be remembered (i) that the thermoelectric power measurements for the liquid alloys were not obtained at constant temperature but at temperatures approximately 80°C above the liquidus and (ii) that unlike the thermoelectric powers there is little similarity between the reported resistivities of liquid and solid silver-palladium alloys. As shown in figure 6-4 the values for the resistivity of the liquid reported by Vatolin et al (1967) do not show the maximum at 30 atomic per cent silver found in the solid state at 827°C by Ricker and Pfluger (1966). Some doubt must however attach to the reported liquid resistivities since the reported value for pure liquid palladium ($120\mu\text{ohm.cm}$) is far in excess of the

Thermoelectric Power (S) of Silver-Palladium Alloys.

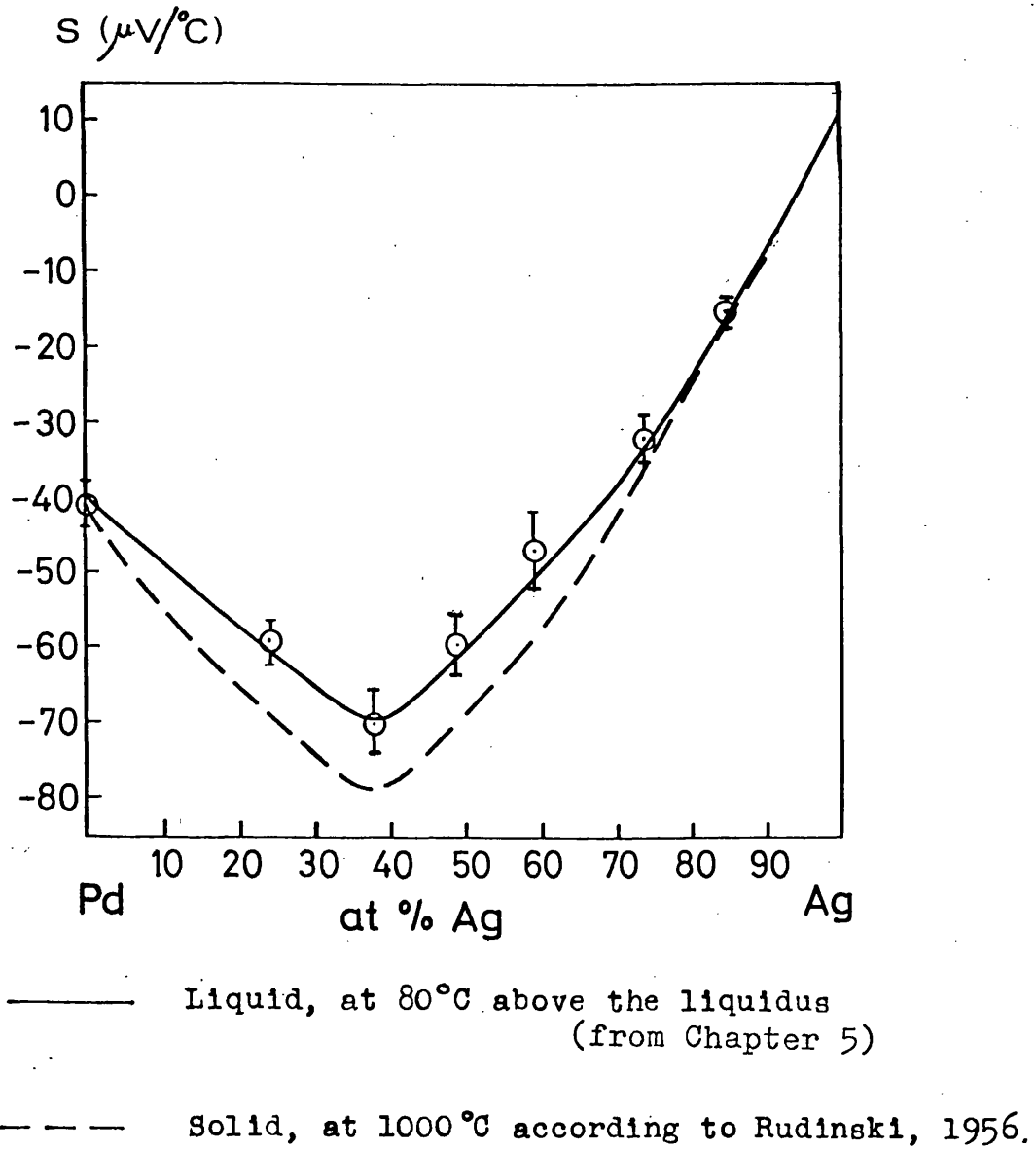


Figure 6-3

Resistivity (ρ) of Silver-Palladium Alloys.

- Liquid, at 1600°C according to Vatolin et al, 1967
- - - " " " " " scaled by 0.69
- - - Solid, at 827°C according to Ricker & Pfluger, 1966

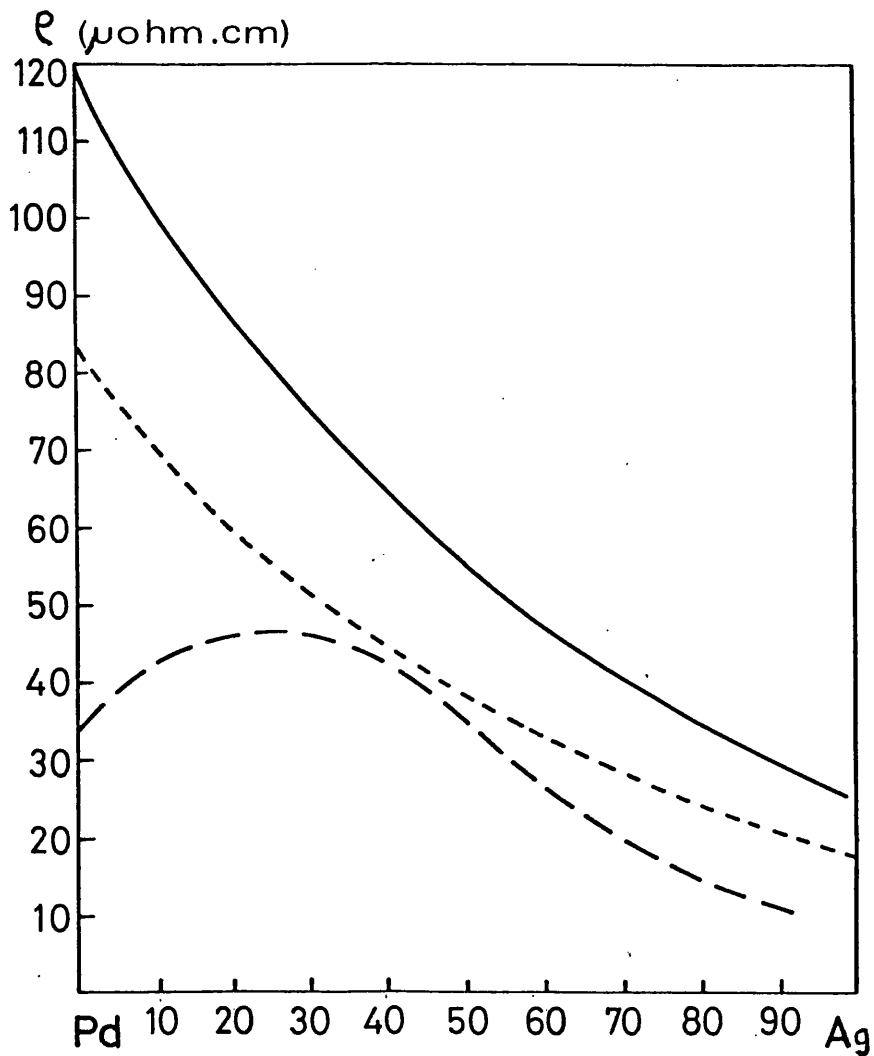


Figure 6-4

value ($\approx 80 \mu\text{ohm.cm}$) reported in this thesis and recently confirmed by Guntherodt et al (1975). For comparison purposes the data of Vatolin et al (1967) are shown in figure 6-4 both as published and scaled by a factor of 0.69 .

CHAPTER 7.

CONCLUSION.

As described in previous Chapters apparatus has been developed to perform resistivity and thermoelectric power measurements on liquid transition metals and their alloys. Satisfactory operation at the necessarily high temperatures, containment of the corrosive and volatile samples and the provision of electrical contacts to the sample were achieved by suitable use of high purity refractory ceramics and metals, together with the application of rapid data acquisition techniques. Due to the relatively large dimensional variations inherent in the ceramic castings presently available, and the difficulty of performing workshop operations on the refractory materials, the functional parts of both apparatuses are rather large. This gives rise to large and expensive sample requirements and also means that large furnaces are needed. The use of large furnaces causes long heating and cooling periods, but this difficulty was reduced somewhat by the use of automatic programmable temperature control. With increased experience in the use of these refractory materials it is likely that smaller and more convenient apparatuses could be developed to improve the rate of data acquisition. In particular for the thermoelectric power apparatus direct rapid vertical dipping of tungsten rods into the two ends of the sample pipe boat might significantly improve

the positional accuracy of the sample-tungsten contact point. This should allow an overall reduction in size, but would however require a specially constructed furnace tube or the use of an enveloping vacuum chamber.

With the exception of two of the Russian schools referred to in Chapter 5, there is satisfactory agreement (considering the experimental difficulties encountered at such high temperatures) between the measurements on pure transition metals given in this thesis and other values previously reported (Chapter 5). The resistivity of pure liquid palladium was, however, found to be significantly below the previously available value, in general accord with the predictions of Brown (1973). Nevertheless, the change in resistivity upon melting is still much larger for palladium than for the other transition metals discussed. The decrease observed in this quantity in traversing the first long period of the periodic table from iron to nickel may be due in part to a reduction in the d electron contribution to the conductivity. This is possible since this contribution is presumed to be less sensitive to melting and, as shown by ten Bosch et al (1975), will decrease as the (model) d band changes from being half filled to filled.

The level of agreement shown in Table 6-A between experiment and the resonant scattering approximation would, by itself, tend to indicate that such a model is not too far removed from a realistic physical

picture. A similar model was used with success (Ratti and Jain, 1973) to account for the variation in the resistivity and thermoelectric power of liquid caesium under pressure and this adds support; nevertheless, the arguments of Mott (1972) have force.

Provided the assumption of a substitutional model is indeed suitable, the calculations of Chapter 6 show that the predictions of the resonance approximation do not agree with experiment for liquid nickel-cobalt alloys, implying that this theory, in its present form, is inapplicable to pure liquid nickel or cobalt as claimed by Mott (1972). This failure, together with the relative success of Dreirach et al (1972) in obtaining qualitative agreement between experiment and the predictions of their resonant scattering theory applied to liquid transition metal — non-transition metal alloys supports the argument advanced by Mott that such a theory is only applicable to alloys of transition metals containing a significant concentration (approximately 25 atomic % or more) of a non-transition metal.

The arbitrary assumption of a very low effective valence, whilst perhaps enabling the resonance approximation to remain consistent with experiment for liquid nickel-cobalt alloys as shown in Chapter 6, does imply a long mean free path for the conduction electrons which is unlikely if conditions of resonant scattering obtain.

For liquid silver-palladium the similarity of the solid and liquid thermoelectric power (but not resistivity) data give some support to the ideas advanced by Mott (1972) but, as was indicated in Chapter 6, for this alloy a comparison similar to that used for nickel-cobalt alloys can not be made between the resonance approximation and experiment. As for the nickel-cobalt case, the experimental resistivity of pure liquid palladium can be used in conjunction with equation 2.5 to fix effectively the d-wave phase shift for scattering from palladium ions. A similar procedure can not be followed for silver using equation 6.7 since there are two unknowns the s-wave and d-wave phase shifts (η_0^{Ag} and η_2^{Ag}). Nevertheless, silver-palladium is a useful alloy system; the similarity between the thermoelectric powers of the liquid and solid alloys coupled with the disparity between the resistivities in the liquid and solid states make the alloy worthy of further investigation. In particular, more reliable experimental data for the resistivity of the liquid alloy are now required to clarify the experimental situation.

The use of liquid transition metal — transition metal alloys provides a convenient test for theories of liquid transition metals and liquid nickel-cobalt is particularly suitable due to the marked similarity of the two constituents. In order to facilitate

accurate comparison of future theories with experiment it would be useful to have available the three partial structure factors for the liquid alloy. These could be obtained from neutron diffraction experiments by isotopic enrichment and substitution of the nickel, although there would be some experimental difficulty due to the high absorption coefficient of cobalt. Similarly the partial structure factors for liquid silver-palladium alloys could be determined by neutron diffraction experiments using isotopic enrichment of the silver but the high absorption coefficient of silver would cause some difficulty.

It would also be useful, particularly in the development of fully quantitative theories along the lines proposed by Mott, to have experimental evidence of the electronic band structure of liquid transition metal alloys such as liquid silver-palladium and nickel-cobalt. This data could be obtained from a series of ultra-violet photoemission experiments on these alloys.

REFERENCES

- Allen, B.C., 1972, *Physics and Chemistry of Liquid Metals*,
Ed. S.Z. Beer (New York: Marcel Dekker)
- Beeman, W.W., and Friedman, H., 1939, *Phys. Rev.*, 56, 392
- Bradley, C.C., 1962, *Phil. Mag.*, 7, 1337
- Bradley, C.C., Faber, T.E., Wilson, E.G., and Ziman, J.M.,
1962, *Phil. Mag.*, 7, 865
- Brown, J.S., 1973, *J. Phys. F*, 3, 1003
- Brown, J.S., 1976, to be published
- Callen, H.B., 1948, *Phys. Rev.*, 73, 1349
- Cohen, M.H., and Heine, V., 1961, *Phys. Rev.*, 122, 1821
- Coles, B.R., and Taylor, J.C., 1962, *Proc. Roy Soc.*,
A267, 139
- Cubiotti, G., Donato, E., Giuliano, E.S., Ruggeri, R.,
and Stancanelli, A., 1975, *J. Phys. F*, 5,
L129
- Cusack, N.E., and Kendall, P.W., 1958, *Proc. Phys. Soc.*,
72, 898
- Dreirach, O., 1971, *J. Phys. F*, 1, L40
- Dreirach, O., Evans, R. Guntherodt, H-J., and Kunzi, H-U.,
1972, *J. Phys. F*, 2, 709
- Drude, P., 1900, *Ann. Physik*, 1, 566
- Dubinín, E.L., Esin, O.A., and Vatolin, N.A., 1969,
Russ. J. Phys. Chem., 43, 1463 (English
Translation)
- Dugdale, J.S., and Guénault, A.M., 1966, *Phil. Mag.*, 13,
503
- Egelstaff, P.A., 1967, *An Introduction to the Liquid
State* (London: Academic Press)
- Evans, R., 1970, *J. Phys. C*, 3, *Metal Phys. Suppl. No. 2*,
S137
- Evans, R., Greenwood, D.A., Lloyd, P., and Ziman, J.M.,
1969, *Phys. Lett.*, 30A, 313
- Evans, R., Greenwood, D.A. and Lloyd, P., 1971, *Phys.
Lett.*, 35A, 57

- Faber, T.E., 1972, An Introduction to the Theory of Liquid Metals (Cambridge: University Press)
- Faber, T.E., and Ziman, J.M., 1965, Phil. Mag., 11, 153
- Friedel, J., 1969, The Physics of Metals, 1. Electrons, Ed. J.M. Ziman (Cambridge: University Press)
- Friedman, H., and Beeman, W.W., 1940, Phys. Rev., 58, 400
- Geibel, W., 1911, Z. anorg. Chem., 70, 240
- Greenfield, A.J., 1966, Phys. Rev. Lett., 16, 6
- Guntherodt, H-J., Hauser, E., Kunzi, H-U., and Muller, R., 1975, Phys. Lett., 54A, 291
- Hansen, M., 1958, Constitution of Binary Alloys (New York: McGraw-Hill)
- Heine, V., 1967, Phys. Rev., 153, 673
- Howe, R.A., 1967, Ph.D. Thesis, University of Sheffield
- Howe, R.A., and Enderby, J.E., 1967, Phil. Mag., 16, 467
- Howe, R.A., and Enderby, J.E., 1973, J. Phys. F, 3, L12
- Kierspe, W., Kohlhaas, R., and Gonska, H., 1967, Z. angew. Phys., 24, 28
- Kimura, H., and Shimizu, M., 1964, J. Phys. Soc. Japan, 19, 1632
- Kolomoets, N.V., and Verdernikov, M.V., 1962, Soviet Phys. Solid State, 3, 1996
- Lander, J.J., 1948, Phys. Rev., 74, 479
- Laubitz, M.J., and Matsumara, T., 1972, Canadian J. Phys., 50, 196
- Mott, N.F., 1972, Phil. Mag., 26, 1249
- Mott, N.F., and Jones, H., 1936, Theory of the Properties of Metals and Alloys (Oxford: Clarendon Press)
- Norris, C., and Myers, H.P., 1971, J. Phys. F, 1, 62
- Phillips, C.S.G., and Williams, R.J.P., 1965, Inorganic Chemistry (Oxford: Clarendon Press)
- Powell, R.W., 1953, Phil. Mag., 44, 772
- Ratti, V.K., and Evans, R., 1973, J. Phys. F, 3, L238
- Ratti, V.K., and Jain, A., 1973, J. Phys. F, 3, L69

- Regel, A.R., and Mokrovsky, H.P., 1953, Zh. Tekh. Fiz., 28, 2121
- Ricker, T., and Pflugger, E., 1966, Z. Metalk., 57, 39
- Ricker, T., and Schaumann, G., 1966, Phys. Kond. Mat., 5, 31
- Rowland, T., Cusack, N.E., and Ross, R.G., 1974, J. Phys. F, 4, 2189
- Rudinski, A.A., 1956, Thermoelectric Properties of the Noble Metals and their Alloys (Washington: A.E.C.-tr-3724)
- Schiff, L.I., 1955, Quantum Mechanics (New York: McGraw-Hill)
- Skinner, H.B.W., and Johnston, J.E., 1937, Proc. Roy. Soc., 161, 420
- Stocks, G.M., Williams, R.W., and Faulkner, J.S., 1973, J. Phys. F, 3, 1688
- Sundstrom, L.J., 1965, Phil. Mag., 11, 657
- Taylor, J.C., and Coles, B.R., 1956, Phys. Rev., 102, 27
- ten Bosch, A., and Bennemann, K.H., 1975, J. Phys. F, 5, 1333
- Van Zytveld, J.B., Enderby, J.E., and Collings, E.W., 1972, J. Phys. F, 2, 73
- Van Zytveld, J.B., Enderby, J.E., and Collings, E.W., 1973, J. Phys. F, 3, 1819
- Vatolin, N.A., Esin, O.A., and Dubinin, E.L., 1967, Russ. J. Phys. Chem., 41, 971 (English Translation)
- Verdernikov, M.V., 1969, Advances in Physics, 18, 337
- Vertman, A.A., and Samarin, A.M., 1961, Izv. Akad. Nauk USSR, Met. i Topl., 2, 83
- Vuillemin, J.J., and Priestley, M.G., 1965, Phys. Rev., Lett., 14, 307
- Wang, T.P., Starr, C.D., and Brown, N., 1966, Acta. Met., 14, 649
- Waseda, Y., and Ohtani, M., 1974, Phys. Stat. Sol.(b), 62, 535
- Wilson, J.R., 1965, Metall. Rev., 10, 381

- Wingfield, B.F., and Enderby, J.E., 1968, Phys. Lett.,
27A, 704
- Wiser, N., 1966, Phys. Rev., 143, 393
- Wood, J.H., 1962, Phys. Rev., 126, 517
- Ziman, J.M., 1960, Electrons and Phonons (Oxford:
Clarendon Press)
- Ziman, J.M., 1961, Phil. Mag., 6, 1013
- Ziman, J.M., 1964, Adv. Phys., 13, 89
- Ziman, J.M., 1967, Adv. Phys., 16, 551
- Ziman, J.M., 1967b, Proc. Phys. Soc., 91, 701
- Ziman, J.M., 1972, Principles of the Theory of Solids
(Cambridge: University Press)

LETTER TO THE EDITOR

The resistivity and thermoelectric power of solid and liquid palladium

B C Dupree, J B Van Zytveld† and J E Enderby

Department of Physics, University of Leicester, Leicester LE1 7RH

Received 12 August 1975

Abstract. The resistivity ρ of palladium has been investigated on both sides of the melting point, and the thermoelectric power S has been measured in the liquid phase. The values for ρ and S in the liquid are respectively $83 \pm 2 \mu\Omega \text{ cm}$ and $-41 \pm 3 \mu\text{V deg}^{-1}$, which are in general accord with the theoretical predictions of Brown (1973). An interesting feature is the comparatively large value of $\Delta\rho/\rho_{\text{solid}}$ across the melting point. Two possible contributions to this effect are identified.

Interest in the electronic properties of the liquid transition metals has been active and growing in recent years (cf ten Bosch and Benneman 1975, Evans *et al* 1973, Mott 1972). There are quite severe experimental problems in handling these reactive high-temperature liquids, with the result that most of this recent work has been of a theoretical nature. In the present letter, we report the first measured data on the thermopower S of pure liquid Pd, together with results for the electrical resistivity ρ and the change in electrical resistivity at the melting point $\Delta\rho$. A single resistivity measurement on liquid Pd at 1600 °C has been reported by Dubinin *et al* (1969).

For both measurements the samples were held in high-grade alumina crucibles. The thermopower of liquid Pd was measured using rapid data acquisition by means of a short-term dipping technique. The dipping of the W counter-electrode introduced a total of less than 0.2 at% W impurity into the sample; this level of impurity made no measurable difference to the experimental results. The experimental method does not enable data to be taken in the solid for the same specimen, but fortunately the extensive solid-state results of Rowland *et al* (1974) and Laubitz and Matsumura (1972) are in excellent agreement. The data of Cusack and Kendall (1958) were used for the absolute thermoelectric power of W.

The resistivity measurements were made on a liquid sample held in a cylindrical cell whose constant was determined by reference to doubly distilled mercury at room temperature. Contact to each sample was made by drawing the liquid up into the four capillaries of a specially designed alumina probe. In this probe the sample liquid contacted W leads, where the region of overlap was immediately frozen. This permitted contamination-free measurements of resistivity to be made over long periods of time. The impurity introduced in this process was less than 0.01 at%. A standard

† Permanent address: Physics Department, Calvin College, Grand Rapids, Michigan, USA.

four-probe DC technique was used. A complete description of both measurement techniques will appear elsewhere.

The sample material, obtained from Johnson Matthey, had a nominal initial purity of 99.9%. Typical batch purities reported by the manufacturer for this material were 99.95%.

We display our experimental results in figure 1 and table 1, and compare these results with theoretical predictions in table 2. Figure 1 also shows other available data where appropriate. We have also measured ρ for solid Pd, since the available

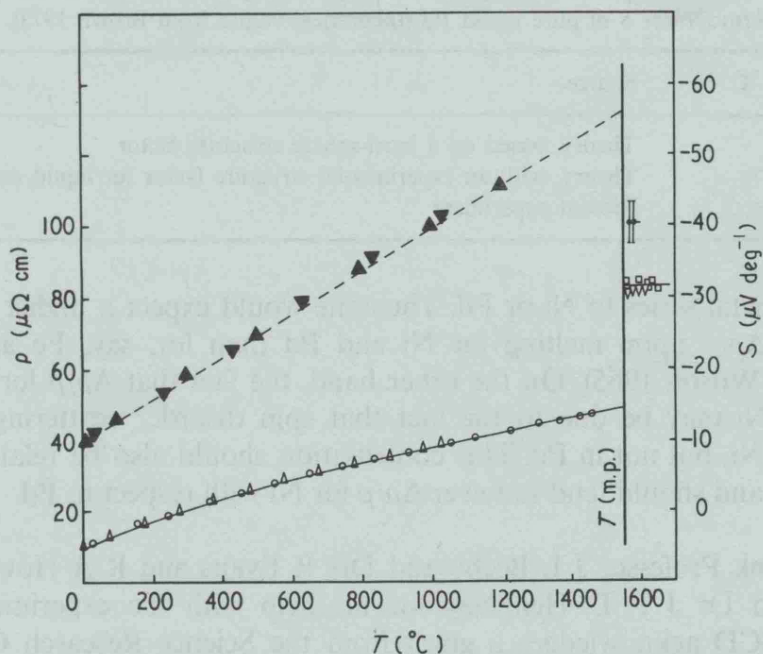


Figure 1. The thermopower S (full symbols) and electrical resistivity ρ (open symbols) of pure Pd from room temperature to above its melting point: \blacktriangle Rowland *et al* 1974; \blacktriangledown , \triangle Laubitz and Matsumura 1972; --- Cusack and Kendall 1958; \bullet , \square , ∇ present results; \circ present results, normalized to Laubitz and Matsumura 1972 (see text).

data do not extend above 1027 °C. Our estimate of the accuracy of our sample dimensions for this measurement is $\pm 2\%$. We therefore normalized our solid data to those of Laubitz and Matsumura (1972) by applying a multiplicative correction of 0.98.

We see that the thermopower of liquid Pd is large and negative; in this property it is similar to liquid Ni (Howe and Enderby 1973), and follows theoretical predictions (see Evans *et al* 1973, Brown 1973). The magnitude of the liquid resistivity is also very nearly equal to that of Ni (Wilson 1965), and the calculated values of Brown (1973) fall reasonably close, especially when an experimental structure factor is used (albeit that of Ni). The temperature dependence of resistivity $d\rho/dT$ is very small, and is consistent with the predictions of both Mott (1972) and Evans *et al* (1973).

The change in ρ upon melting, $\Delta\rho/\rho$, is considerably larger than that for any other transition metal studied to date, and is nearly as large as that for Cu. Two points should be considered in analysing this unusual behaviour. As shown by ten Bosch and Bennemann (1975), the d contribution to the conductivity, presumed to be less sensitive to melting than that of the s band, should reach a maximum when the d band is half-filled, and should have dropped considerably in going through

Table 1. Experimental data for resistivity ρ and thermopower S of pure Pd at its melting temperature (1552 °C).

Resistivity	Thermopower (liquid data at 1581 °C)
$\rho = 83 \pm 2 \mu\Omega \text{ cm}$	$S = -41 \pm 3 \mu\text{V } ^\circ\text{C}^{-1}$
$d\rho/dT = 0.00 \pm 0.02 \mu\Omega \text{ cm } ^\circ\text{C}^{-1}$	$(S_L - S_s)/S_s = -0.28 \pm 0.09$
$(\rho_L - \rho_s)/\rho_s = 0.70 \pm 0.05$	

Table 2. Comparison between theoretical and experimental results for resistivity ρ and thermopower S of pure liquid Pd (theoretical values from Brown 1973).

ρ ($\mu\Omega \text{ cm}$)	S ($\mu\text{V } ^\circ\text{C}^{-1}$)	Source
42	-78	Theory, based on a hard-sphere structure factor
62	-74	Theory, with an experimental structure factor for liquid nickel
83 ± 2	-41 ± 3	Present experiment

the transition metal series to Ni or Pd. Thus one would expect a higher conductivity and a greater $\Delta\rho/\rho$ upon melting for Ni and Pd than for, say, Fe and Co. This is as observed (Wilson 1965). On the other hand, the fact that $\Delta\rho/\rho$ for Pd is about twice that for Ni may be due to the fact that spin disorder scattering contributes significantly in Ni, but not in Pd. This contribution should also be relatively insensitive to melting, and should tend to lower $\Delta\rho/\rho$ for Ni with respect to Pd.

We wish to thank Professor J L Beeby and Drs R Evans and R A Howe for helpful discussions, and Dr J P D Hennessy for his help with the experimental aspects of this work. BCD acknowledges a grant from the Science Research Council; and JBVZ wishes to thank the Physics Department, University of Leicester, for its hospitality, and the Science Research Council for a Senior Research Fellowship supporting his visit.

References

- ten Bosch A and Bennemann K H 1975 *J. Phys. F: Metal Phys.* **5** 1333-41
 Brown J S 1973 *J. Phys. F: Metal Phys.* **3** 1003-7
 Cusack N E and Kendall P W 1958 *Proc. Phys. Soc.* **72** 898-901
 Dubinin E L, Esin O A and Vatolin N A 1969 *Russ. J. Phys. Chem.* **43** 1463-5 (Engl. trans.)
 Evans R, Gyorffy B L, Szabo N and Ziman J M 1973 *Proc. 2nd Int. Conf. on the Properties of Liquid Metals* ed S Takeuchi (London: Taylor and Francis) pp 319-31
 Howe R A and Enderby J E 1973 *J. Phys. F: Metal Phys.* **3** L12-4
 Laubitz M J and Matsumura T 1972 *Can. J. Phys.* **50** 196-205
 Mott N F 1972 *Phil. Mag.* **26** 1249-61
 Rowland T, Cusack N E and Ross R G 1974 *J. Phys. F: Metal Phys.* **4** 2189-202
 Wilson J R 1965 *Metall. Rev.* **10** 381-590



ABSTRACT

Apparatus has been developed to perform measurements of the thermoelectric power and resistivity of liquid metals at high temperatures of the order of 1500°C . Measurements have been performed on the transition metals, iron, cobalt, nickel and palladium in the liquid state, together with some measurements on these metals in the solid state and on liquid alloys of nickel with cobalt and palladium with silver. In most cases the results obtained are in agreement with other experimental data, where available.

If use is made of a single site resonant scattering model (the only theory for liquid transition metals for which a number of quantitative calculations of resistivity and thermoelectric power have been reported), approximate expressions can be derived which give the resistivity of liquid nickel - cobalt

alloys in terms of the resistivities of the pure components. It is also possible to express the thermoelectric power of the alloy in terms of the thermoelectric powers and resistivities of the pure components and the resistivity of the alloy. The predictions of these expressions have been compared with the experimental data; the comparison indicates that the theory does not account for the observed transport properties of liquid nickel-cobalt alloys. The conclusion is therefore drawn that by implication the theory is not applicable, in its present form, to pure liquid transition metals.